T.C.
YEDİTEPE UNIVERSITY
INSTITUTE OF HEALTH SCIENCES
ORAL AND MAXILLOFACIAL SURGERY PROGRAM

INVESTIGATION OF THE EFFECTS OF HESPERIDIN APPLICATION ON BONE HEALING AFTER TOOTH EXTRACTION IN RATS

DOCTOR OF PHILOSOPY THESIS

Engin Emre SELÇUK, DDS

İstanbul-2025

T.C.
YEDİTEPE UNIVERSITY
INSTITUTE OF HEALTH SCIENCES
ORAL AND MAXILLOFACIAL SURGERY PROGRAM

INVESTIGATION OF THE EFFECTS OF HESPERIDIN APPLICATION ON BONE HEALING AFTER TOOTH EXTRACTION IN RATS

DOCTOR OF PHILOSOPY THESIS

Engin Emre SELÇUK, DDS

SUPERVISOR
Dr. Volkan Çağrı DAĞAŞAN

İstanbul-2025

THESIS APPROVAL FORM

Institute : Yeditepe University Institute of Health Sciences
Programme : Oral and Maxillofacial Surgery
Title of the Thesis : Investigation of the Effects of Hesperidin Application on Bone Healing After Tooth Extraction in Rats
Owner of the Thesis : Engin Emre SELÇUK, DDS
Examination Date : 14/04/2025

This study was approved as a Master/Doctorate Thesis in regard to content and quality by the Jury.

Title	Name-Surname (Institution)
Chair of the Jury:	Prof. Dr. Ceyda Özçakır Tomruk Yeditepe University, Faculty of Dentistry
Supervisor:	Dr.Volkan Çağrı DAĞAŞAN Yeditepe University, Faculty of Dentistry
Member/Examiner:	Assoc. Prof. Dr.Berkem Atalay İstanbul University-Oral and Dental Health Program
Member/Examiner:	Assoc. Prof. Dr.Ezgi Hacıhasanoğlu Yeditepe University,Faculty of medicine
Member/Examiner:	Assoc. Prof. Dr.Gül Merve Yalçın Ülker Okan University, Faculty of Dentistry

APPROVAL

This thesis has been deemed by the jury in accordance with the relevant articles of Yeditepe University Graduate Education and Examinations Regulation and has been approved by Administrative Board of Institute with decision dated ..... and numbered .....

(Signature)

Prof. Dr. Burcu Gemici Başol

Director of Institute of Health Sciences

DECLARATION

I declare that this thesis is my own work, and I have not engaged in any unethical behavior at any stage, from planning to writing. I affirm that all information in the thesis has been obtained following academic and ethical standards. I acknowledge and reference all information and interpretations not obtained through the in the bibliography. I further declare that I have not violated any patent or copyright during the thesis research and writing.

14 / 04/ 2025

Engin Emre SELÇUK, DDS

ACKNOWLEDGEMENTS

Firstly, I would like to express my heartfelt gratitude to my esteemed advisor, Dr. Volkan Çağrı Dağaşan, for his invaluable clinical and academic contributions throughout my doctoral journey. His unwavering support and guidance during the preparation of my thesis have been truly invaluable.

I extend my sincere thanks to the Head of our Department, Prof. Dr. Ceyda Özçakır Tomruk, for her patience and warm demeanor in answering all my questions. I am deeply grateful for the extensive academic and clinical knowledge I gained from her throughout my doctoral education.

I would also like to express my heartfelt gratitude to my professors, Assoc. Prof. Dr. Ahmet Hamdi Arslan, Assoc. Dr. Çağrı Burdurlu, Assoc. Dr. Ediz Deniz, Prof. Dr. Fatih Cabbar and Prof. Dr. Nurhan Güler. Their knowledge and experience have been an inspiration to me since the very first day I embarked on my journey in dentistry. Their unwavering support in every matter and at all times, combined with their ability to make me feel like part of a family rather than just a student, is something I deeply cherish and appreciate.

I would like to thank my wife Kevser Selçuk, who has been here since the first day I met her, the owner of this thesis, the love of my life.

I am also deeply grateful to all my juniors in the maxillofacial surgery department for their constant encouragement and solidarity throughout this period.

Finally, I would like to express my deepest gratitude to my family who have always stood by me throughout my life, believed in me and helped me come this far and my closest friends, and all my loved ones for their unwavering support throughout my doctoral education. Together, we have navigated both the good and challenging times, and I am truly fortunate to have them in my life.

Engin Emre SELÇUK, DDS

TABLE OF CONTENTS

THESIS APPROVAL FORM ii
DECLARATION iii
ACKNOWLEDGEMENTS iv
TABLE OF CONTENTS v
LIST OF TABLES vii
LIST OF FIGURES viii
LIST OF GRAPHICS x
LIST OF SYMBOLS AND ABBREVIATIONS xi
ABSTRACT xii
ÖZET xiii
1. INTRODUCTION AND PURPOSE 1
2. GENERAL INFORMATIONS 3
2.1. General Characterıstıcs of the Bone Area 3
2.2. Bone Cells 4
2.2.1. Osteoprogenitor cells 4
2.2.2. Osteoblasts 5
2.2.3. Osteocytes 6
2.2.4. Osteoclasts 7
2.2.5. Cells lining the bone surface 8
2.3. Periosteum and Endosteum 8
2.4. Bone Types 9
2.4.1. Primary bone tissue (woven bone) 9
2.4.2. Secondary bone tissue (lamellar bone) 9
2.5. Bone Formation and Development 10
2.5.1. Intramembranous bone formation (direct ossification) 10
2.5.2. Endochondral bone formation 11
2.6. Bone Growth and Remodeling 11
2.7. Healing of Bone Tissue 12
2.7.1. Inflammatory stage 12
2.7.2. Repair phase 13
2.7.3. Remodeling phase 13
2.8. Alveolar Bone 13

2.9. Healing of Tooth Extraction Wound 15
2.10. Antioxidants 19
2.11. Hesperidin 19
2.11.1. Antioxidant activity of hesperidin 21
2.11.2. Effect of hesperidin on inflammation 22
2.11.3. Effect of hesperidin on pain management 22
2.11.4. Effect of hesperidin on bone health 22
2.11.5. Effect of hesperidin on infections 23
2.11.6. Human studies on hesperidin 24
2.11.7. Synergystic effect of hesperidin 25
2.11.8. Safety of hesperidin 27
2.11.9. Bioavailibility and absorption of hesperidin 28
2.11.10. Cellular mechanisms of action of hesperidin 29
2.12. Absorbable Hemostatic (Gelatin) Sponge (HS) 31
3. MATERIALS AND METHOD 34
3.1. Preparation, Dosage and Route of Administration of Hesperidin 36
3.2. Tooth extraction method 41
3.3. Histological Evaluation 46
3.4. Statistical Evaluation 47
4. FINDINGS 48
4.1. Histological Findings 48
4.1.1. Histological findings of the sacrificed groups on day 28 48
4.1.2. Histological findings of the sacrificed groups on day 56 52
4.1.3. Statistical evaluation of histological findings 58
5. DISCUSSION 65
6. CONCLUSION 76
7. REFERENCES 78
8. CURRICULUM VITAE 91

LIST OF TABLES

Table 2.1. Synergistic interactions between hesperidin/hesperetin and specific natural compounds.(94-98) 26
Table 2.2. Synergistic interactions between hesperidin/hesperetin and specific pharmaceuticals .(73,74,99-103)..... 26
Table 2.3. Protective effects of hesperidin and diosmetin against the toxicity of selected compounds and drugs..(104-106)..... 27
Table 2.4. Influence of hesperidin on bioavailability of selected drugs..(93,108-110) . 28

Table 3.1. Scoring of histological findings 47

Table 4.1. Histological findings of the sacrificed groups on day 28..... 48
Table 4.2. Histological findings of the sacrificed groups on day 56..... 52
Table 4.3. İnflammation..... 58
Table 4.4. Epitelization 60
Table 4.5. Dunn's multiple comparison test 60
Table 4.6. Connective tissue 61
Table 4.7. New bone formation..... 63

LIST OF FIGURES

Figure 2.1. Possible differentiation fates of mesenchymal stem cells..(28)..... 5
Figure 2.2. H&E images after 4weeks. IM, implant site; TB, trabecular bone; BM, bone marrow; CT, connective tissue; OCY, osteocytes; OB, osteoblast lining cells; OCL, osteoclast; RBC, red blood cell; L, lymphocytes; CHO, chondrocytes; F, fibroblasts.(30) 6
Figure 2.3. Comparison of H&E sections of peri-implant tissue in different groups at two-time points. Magnification, × 200.(30)..... 7
Figure 2.4. Histological H&E images of OCL, osteoclast.(30)..... 8
Figure 2.5. Chemical formulation of hesperidin .(68) 20
Figure 2.6. Chemical structure of hesperidin (hesperetin-7-*O*-rutinoside).(89) 24
Figure 2.7. Hesperetin-7-glucoside.(89)..... 24
Figure 2.8. Glucosyl Hesperidin.(89) 25
Figure 2.9. Hesperidin Methyl Chalcone.(89) 25
Figure 2.10. Commercially used version of Absorbable haemostatic gelatin sponge ... 32

Figure 3.1. Commercial form of Hesperidin (Sigma-Aldrich H5254 Hesperidin ≥80%) and liquid form prepared in a magnetic stirrer..... 36
Figure 3.2. Weighing powdered hesperidin..... 37
Figure 3.3. Prepared and labeled falcon tubes 38
Figure 3.4. After mixing Hesperidin with CMC (carboxymethyl cellulose) and placing it in falcon tubes, labeling and sequential preparation for 28 days 39
Figure 3.5. Falcon tubes prepared to be vortexed one per day and containing hesperidin and its solution ready to be placed in the refrigerator 40
Figure 3.6. Preperated Hesperidin solutions before putting +4 C refrigerator 40
Figure 3.7. Ketamine hydrochloride (10% Ketasol, Richter Farma, Germany) and xylazine hydrochloride (2% Rompun, Bayer, Germany) 41
Figure 3.8. Image of an anesthetized rat before tooth extraction..... 42
Figure 3.9. Extraction wound and extracted tooth after extraction of lower left first molars..... 42
Figure 3.10. Image of the extracted tooth before fixation with formalin..... 43

Figure 3.11. Rats that have been anesthetized and have had their teeth extracted are placed in cages after the procedure. 43
Figure 3.12. Identity forms prepared for rats before they were placed in cages 44
Figure 3.13. A place where experimental animals are kept for the required periods of time and where humidity, temperature and other ideal conditions are provided. 44
Figure 3.14. Mice sacrificed in a closed box with isoflurane 45
Figure 3.15. The state of a rat that has been sacrificed and its mandible removed and placed in a 10% formalin container 45

Figure 4.1. Fibrous connective tissue areas (star) on day 28 of Spongestan 49
Figure 4.2. Areas of bone formation on day 28 of Sponges (star) 49
Figure 4.3. Local hesperidin 28th day fibrous connective tissue areas (star) 50
Figure 4.4. Local hesperidin 28th day focal bone formation areas (star) 50
Figure 4.5. Local hesperidin gavage 28th day fibrous connective tissue area (star) 51
Figure 4.6. Focal bone formation areas on day 28 of local hesperidin gavage 51
Figure 4.7. Control day 28 widespread inflammatory cells 52
Figure 4.8. Spongostan epithelialization areas on day 56 (star) 53
Figure 4.9. Areas of bone formation on day 56 of Sponges (star) 53
Figure 4.10. Local hesperidin 56th day fibrous connective tissue areas (star) 54
Figure 4.11. Local hesperidin mild inflammation areas on day 56 54
Figure 4.12. Local hesperidin 56th day bone formation areas 55
Figure 4.13. Local hesperidin gavage 56th day epithelialization area (star) 55
Figure 4.14. Areas of new bone formation (star) on day 56 of local hesperidin gavage 56
Figure 4.15. Control 56th day epithelialization area (star) 57
Figure 4.16. Control 56th day fibrous connective tissue areas-MTC (star) 57
Figure 4.17. Control 56th day necrosis areas 57
Figure 4.18. Control, 56th day, new bone formation areas (star) 58

LIST OF GRAPHICS

Graph 4.1. İnflammation 59
Graph 4.2. Epitelization..... 61
Graph 4.3. Connective tissue..... 62
Graph 4.4. New bone formation..... 64

LIST OF SYMBOLS AND ABBREVIATIONS

COX-2	Cyclooxygenase-2
HS	Hemostatic Sponge
HSP	Hesperidin
IL-11	interleukin-11
IL-6	interleukin-6
iNOS	Inducible Nitric Oxide Synthase
M-CSF	Macrophage-Colony Stimulating Factor
NO	Nitric Oxide
OVX	Ovariectomized mice
SGLT1	Sodium-glucose linked transporter 1
TNF	Tumor Necrotizing Factor

ABSTRACT

Selçuk, E.E. Investigation of the effects of hesperidin application on bone healing after tooth extraction in rats. Yeditepe University, Health Sciences Institute Oral and Maxillofacial Surgery Program, PhD Thesis, Istanbul, 2025.

Objective: The aim of this study was to investigate histopathologically and histochemically the effects of local and systemic hesperidin (HSP) application on extraction socket healing in rats that underwent experimental tooth extraction.

Materials and Methods: A total of 48 male Sprague Dawley rats were assigned to four groups (n=12): Control, Spongostan, Spongostan + local hesperidin, and local + systemic hesperidin. Following extraction of the lower left first molars, each group was split into two subgroups (n=6). Systemic hesperidin (100 mg/kg) was administered via gavage from day one. Half of the animals were sacrificed on day 28 and the others on day 56. Left mandibles were collected for histopathological and statistical analysis.

Results: The obtained data were evaluated histochemically and statistically. A significant difference was found only in the 56th day epithelialization scores between the groups. More bone formation was observed in the local hesperidin+gavage and control groups compared to other groups. Significant decrease in inflammation in all groups except the local hesperidin group; A significant increase in epithelialization was observed. No significant difference was detected between groups in terms of connective tissue.

Conclusion: In conclusion,histochemical analysis results revealed,long term inflammation,epithelization and new bone formation levels are negatively effected in local hesperidin group.Whereas local hesperidin+gavage group showed parallel results with control and spongestan group in short term.This study showed;hesperidin's systemic administration by gavage can enhance healing in both soft and hard tissue whereas local application tends to slows down healing.More research is needed to reach a definitive conclusion.

Keywords: Antioxidant, tooth extraction, hesperidin, healing, gavage.

ÖZET

Selçuk, E. E. Sıçanlarda diş çekimi sonrası hesperidin uygulamasının kemik iyileşmesi üzerine etkilerinin araştırılması. Yeditepe Üniversitesi, Sağlık Bilimleri Enstitüsü, Ağız Diş Çene Cerrahisi Doktora Tezi, İstanbul, 2025.

Amaç: Deneysel olarak diş çekimi yapılan sıçanlarda lokal ve sistemik hesperidin (HSP) uygulamasının çekim soket iyileşmesi üzerine etkilerini histopatolojik ve histokimyasal olarak incelemektir.

Gereç ve Yöntem: Çalışmada 48 adet Sprague Dawley cinsi erkek sıçan kullanıldı. Denekler 12 sıçandan oluşan 4 ana gruba ayrıldı: Kontrol, spongestan, şpongestan+lokal HSP, lokal hesperidin+sistemik HSP grubu. Sistemik HSP gruplarına deney süresince gavaj yoluyla uygun dozda HSP uygulaması yapıldı. Deneyin 1'inci günü, tüm sıçanların alt sol 1. büyük azı dişleri çekildikten sonra her ana grup 6'şar denekten oluşan 2 alt gruba ayrıldı. Gavaj yoluyla verilen HSP deneyin 1.gününden itibaren 100 mg/kg uygulanmaya başlandı. Her gruptan 6 denek toplam 24 denek 28. günde kalanı 56. günde sakrifiye edildi. Deneklerin sol mandibulaları çıkartılıp histopatolojik incelemeye alındı.

Bulgular: Elde edilen veriler histokimyasal ve istatistiksel olarak değerlendirildi. Gruplar arasında sadece 56. gün epitelizasyon skorlarında anlamlı fark bulundu. Lokal hesperidin+gavaj ve kontrol gruplarında diğer gruplara kıyasla daha fazla kemik oluşumu görüldü. İnflamasyonda lokal hesperidin grubu dışında tüm gruplarda anlamlı düşüş; epitelizasyonda ise anlamlı artış gözlendi. Bağ dokusu açısından gruplar arası anlamlı fark saptanmadı.

Sonuçlar: Histokimyasal analiz sonuçlarında, uzun vadeli inflamasyon, epitelizasyon ve yeni kemik oluşumu seviyelerinin lokal hesperidin grubunda negatif etkilendiği ortaya çıktı. Lokal hesperidin+gavaj grubu ise kısa vadede kontrol ve spongestan grubuyla paralel sonuçlar gösterdi. Bu çalışma; hesperidin'in gavaj yoluyla sistemik uygulanmasının hem yumuşak hem de sert dokuda iyileşmeyi artırabileceğini, lokal uygulamanın ise iyileşmeyi yavaşlatma eğiliminde olduğunu gösterdi. Kesin bir sonuca ulaşmak için daha fazla araştırmaya ihtiyaç var.

Anahtar Kelimeler: Antioksidan, diş çekimi, hesperidin, iyileşme, gavaj.

1. INTRODUCTION AND PURPOSE

Tooth extraction is a prevalent surgical procedure within the fields of oral, dental, and maxillofacial surgery (1). The healing process of a tooth extraction wound parallels that of a fracture, exhibiting comparable stages. The stages include the formation of a hematoma in the extraction cavity, organization of the clot, epithelialization of the wound surface, formation of woven bone in the connective tissue of the extraction cavity, replacement of woven bone with trabecular bone, and remodeling of the alveolus (2). The healing process is typically uneventful; however, it may be impaired or delayed in patients who are immunosuppressed, have immune diseases, diabetes, or metabolic bone disorders. Healing is influenced by several critical factors, including the use of specific medications, the presence of infection, the extraction site, the patient's age and health status, and smoking habits (3,4).

The relationship between bone formation and resorption is regulated by the interplay of various factors within the microenvironment, including bone cells, cytokines, hormones, growth factors, transcription factors, ions, and extracellular matrix proteins (5,6). In bone tissue, specialized cells, including osteoblasts and osteoclasts, are responsible for the secretion and resorption of the bone matrix, respectively (5,6). Bone metabolism is influenced by various factors, including age and the organism's pathophysiological conditions. Bone loss associated with aging results from an imbalance between osteoblast and osteoclast activities (7,8). Hormonal changes and metabolic disorders can speed up the resorption process, leading to bone diseases such as osteoporosis, which is characterized by diminished bone mass (9). Metabolic disorders and autoimmune diseases, including rheumatoid arthritis, are frequently linked to inflammatory responses (10). Bone turnover is consequently affected by various biological conditions.

Although native biological mechanisms facilitate tissue healing, therapeutic interventions are often required to enhance bone tissue regeneration. Various therapies have been suggested to enhance the regeneration of extensive injuries and to improve the biomechanical properties of newly formed bone, including the use of bone grafts, biomaterials growth factors photobiomodulation or ultrasound strategies and cell-based therapies (11-15).

Additionally, the age and pathophysiological conditions of the organism may accelerate bone loss, prompting the investigation of alternative therapeutic strategies to reduce bone loss or promote bone neoformation. The utilization of natural phytochemical agents is emphasized as a promising therapeutic approach, given their numerous beneficial biological properties. Nutritional phytochemicals found in fruits, vegetables, and cereals, including flavonoid polyphenolic compounds, have been shown to enhance bone mineral density through various mechanisms, while also positively influencing bone homeostasis and health (8,16).

Flavonoids, beyond their nutritional benefits, may be utilized in polymer production and serve as stabilizing agents for biopolyesters like polylactide (PLA) and polyhydroxyalkanoate (PHA), which are extensively employed in tissue engineering for membranes and scaffolds (17,18).

This study examined the effects of systemic and local applications of hesperidin on healing following tooth extraction, utilizing spongestan for local application.

2. GENERAL INFORMATIONS

2.1. General Characterıstıcs of the Bone Area

Bone tissue, which comprises the primary constituent of the skeletal system, is a specialized form of connective tissue. The structure is composed of intercellular tissue, also known as extracellular matrix, which transports cells and contains embedded fibers. This extracellular matrix undergoes calcification, distinguishing it from other connective tissues (19).

Bones are dense tissues that provide structural support to the body, facilitate movement in conjunction with the attached muscles, safeguard the brain, spinal cord, and internal organs, contain bone marrow which produces blood cells, and serve as storage for essential minerals such as calcium, phosphorus, sodium, and magnesium that are vital for various bodily functions (19,20). The constituents of bone tissue include osteoprogenitor cells, osteoblasts, osteocytes, bone-lining cells, and osteoclasts. The bone matrix is composed of 30% organic and 70% inorganic components (21). Type I collagen is the primary structural component of the organic fraction, making up around 90% of it. Furthermore, it includes a reduced quantity of Type V collagen and minimal quantities of Type III, XI, and XIII collagen. The matrix additionally include glycosaminoglycans, proteoglycans, glycoproteins including osteocalcin, osteopontin, and osteonectin, diverse sialoproteins, growth factors, and cytokines. Osteonectin functions as an adhesive that connects collagen and hydroxyapatite crystals, whereas osteopontin serves to attach cells to the matrix. Osteocalcin protein is responsible for sequestering calcium from the bloodstream and activating osteoclasts (22,23). The inorganic component of the matrix consists primarily of crystal salts, such as Calcium Hydroxyapatite and Calcium Phosphate, predominantly in the form of hydroxyapatite (24). Body bones are categorized as long and flat bones based on their shapes, and they are further classified as compact bone and cancellous bone based on their histological characteristics. Compact bone is denser than spongy bone, however spongy bone has a porous structure characterized by the presence of bone marrow cavities and trabeculae. Cancellous bone has little resistance to mechanical forces, rendering it susceptible to fractures with relative ease (25). Flat bones have both their inner and exterior surfaces made up of compact bone, while long bones only have compact bone on their outer surfaces. Compact bone is responsible for

providing mechanical support. The spongiosa bone, situated in the core of the bone, is accountable for carrying out metabolic functions (26).

2.2. Bone Cells

2.2.1. Osteoprogenitor cells

Precursor cells capable of undergoing mitosis and differentiating into osteoblasts, they are derived from mesenchymal cells found in the bone marrow. These cells have a flat and spindle-like structure, with oval-shaped nuclei and pale cytoplasm that is mildly basophilic and acidophilic. Their endoplasmic reticulum is highly developed. Osteoprogenitor cells are located within the inner layer of the periosteum, Haversian canals, and endosteum. The osteoprogenitor cells found in the inner layer of the periosteum are referred to as periosteal cells, whereas the osteoprogenitor cells that line the inner layer of the bone marrow, Havers and Volkmann canals are known as endosteal cells (22,23,25,27). During the process of fracture healing and bone growth, osteoprogenitor cells that are in an active state undergo a transformation into osteoblasts and release bone matrix (22).

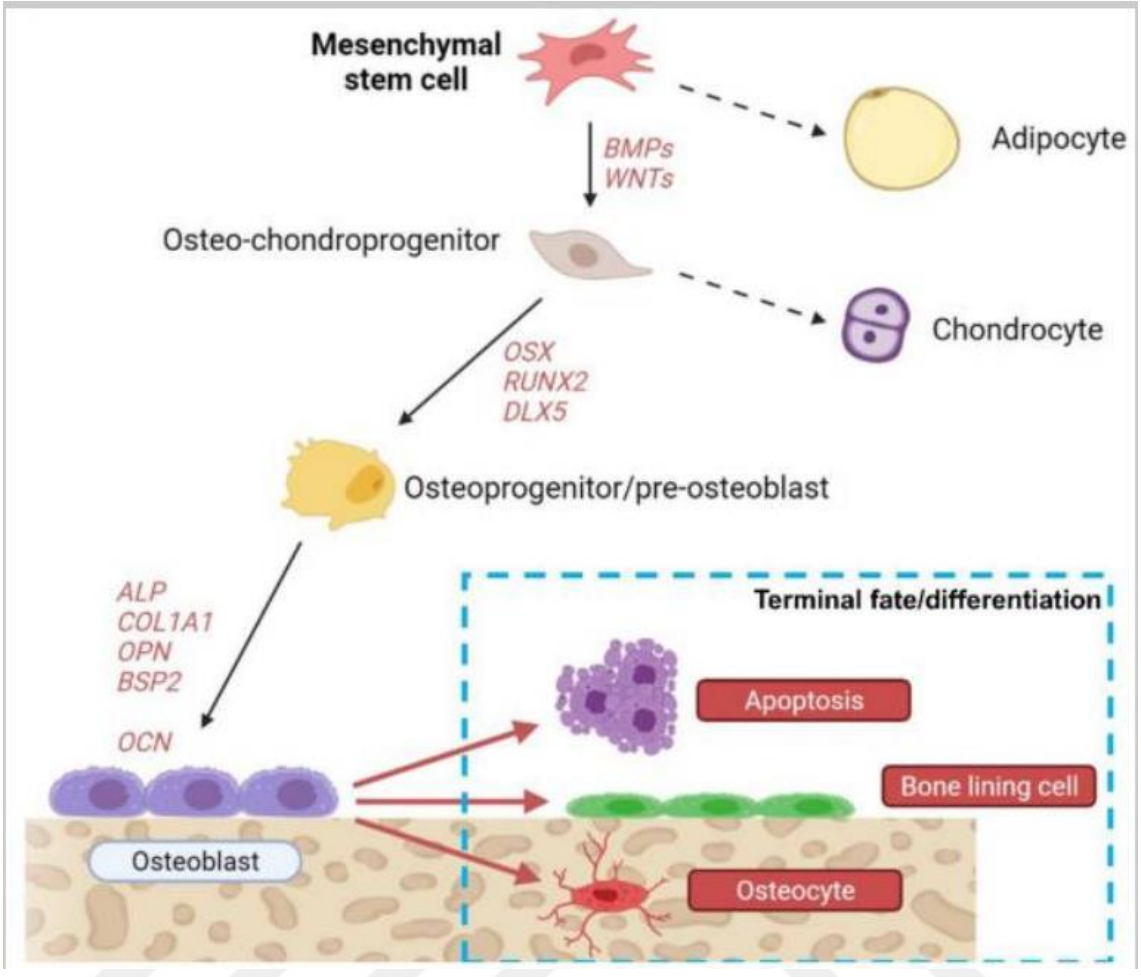

Figure 2.1. Possible differentiation fates of mesenchymal stem cells (28).

2.2.2. Osteoblasts

Osteoblasts are proliferative cells that play a crucial role in producing the organic components of the bone matrix, including type I collagen, proteoglycans, and glycoproteins. Furthermore, osteoblasts facilitate the deposition of inorganic substances into the organic matrix. The plasma membrane of osteoblasts has elevated levels of alkaline phosphatase activity, reflecting the active state of osteoblasts (22,27). Osteoblasts align along the external surfaces of the bone tissue, resulting in an epithelial-like appearance. The cells possess a cubic and prismatic morphology and a basophilic cytoplasm during active matrix synthesis. During the interval of inactivity, these cells undergo a transformation where they become flattened and the intensity of their cytoplasm's basophilia starts to diminish (22,25,27). Gap junctions exist between osteoblasts and between osteoblasts and osteocytes. Through these hyperlinks, communication is facilitated (22,27,29). Osteoblasts are polarized cells that secrete

matrix components when they come into contact with the bone matrix that has already been formed. Therefore, an immature matrix layer known as osteoid is created between the layer of osteoblasts and the pre-existing bone, but it has not yet hardened into bone tissue. The process of bone apposition, sometimes referred to as the deposition of calcium salts into the freshly created matrix, occurs gradually over time (25).

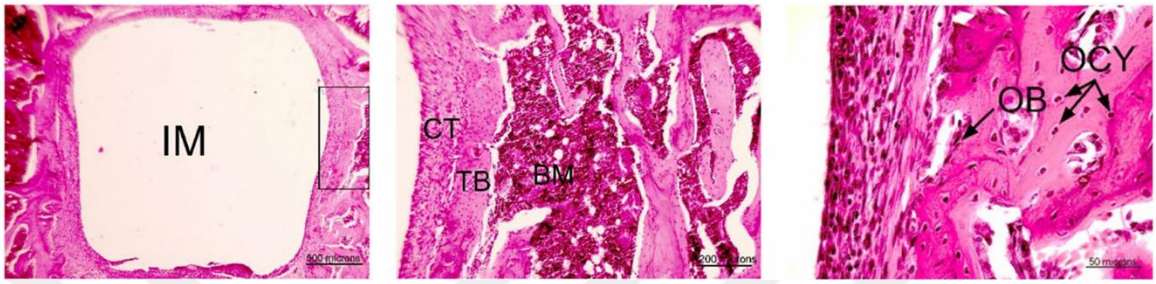

Figure 2.2. H&E images after 4weeks. IM, implant site; TB, trabecular bone; BM, bone marrow; CT, connective tissue; OCY, osteocytes; OB, osteoblast lining cells; OCL, osteoclast; RBC, red blood cell; L, lymphocytes; CHO, chondrocytes; F, fibroblasts (30).

2.2.3. Osteocytes

Osteocytes are non-dividing cells that originate from osteoblasts. Osteoblasts release bone tissue matrix in their vicinity, subsequently becoming ensnared within the tissue and undergoing a metamorphosis into osteocytes (22). Osteocytes are smaller in size compared to osteoblasts and possess a lower amount of basophilic cytoplasm (23). The osteocytes are situated within narrow gaps known as lacunae, which are found between the matrix lamellae. Each lacuna houses a single osteocyte (25). They sustain their existence by nourishing themselves through their cytoplasmic extensions that stretch within the canaliculus. Osteocytes are able to establish connections with the cells that line the periosteum and osteoblasts through cytoplasmic extensions (22,27). Osteocytes are recognized as contributing to the synthesis and resorption of bone. Furthermore, osteocytes have a crucial function in the regulation of extracellular calcium and phosphorus levels. Osteocyte loss caused by trauma, age, and apoptosis leads to bone resorption through osteoclastic activity and subsequent replacement with new bone tissue through osteoblastic activity (22,27).

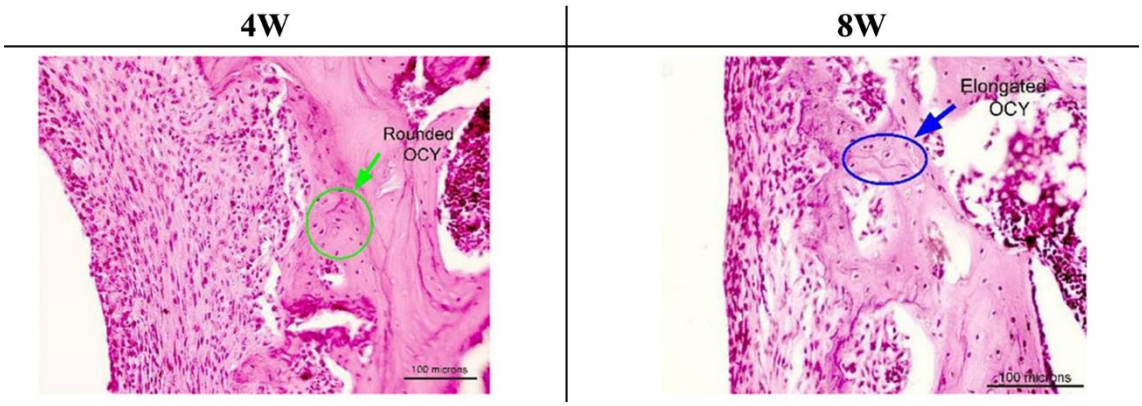

Figure 2.3. Comparison of H&E sections of peri-implant tissue in different groups at two-time points. Magnification, × 200 (30).

2.2.4. Osteoclasts

They are cells with many nuclei that come from mononuclear hemopoietic progenitor cells. The extended cell body contains a variable number of nuclei, ranging from 5 to 50 or more. The volumes of these nuclei can reach up to 200,000 cubic meters. Osteoclasts reside within the resorption cavities or Howship lacunae that develop on the surfaces of bones, and they play a crucial role in the process of bone resorption (22,25,27). Macrophage-colony stimulating factor (M-CSF) and cytokines like interleukin-6 (IL-6) and interleukin-11 (IL-11) are produced by the stromal cells in the bone marrow and are essential for the process of osteoclast differentiation. Furthermore, the establishment of osteoclast cell lineage is influenced by systemic variables such as 1,25-dihydroxy vitamin D3, parathyroid hormone, and tumor necrotizing factor (TNF) (22,27). Osteoclasts release collagenase and other enzymes that dissolve calcium salt crystals and break down collagen, while simultaneously transporting the resultant protons into subcellular compartments. Hormones and cytokines regulate the activity of osteoclasts. Osteoclasts possess receptors for calcitonin, a hormone produced by the thyroid gland, whereas osteoblasts possess receptors for parathyroid hormone. Parathyroid hormone triggers the activation of osteoblasts, which in turn release a cytokine known as osteoclast stimulating factor (25,27). Three distinct zones with varying properties can be detected in osteoclasts under electron microscopy. Osteoclasts increase their surface area by forming many folds in the sections of their cell wall that directly contact the bone. The initial section of the cell is referred to as the ruffled border. These components cling to the mineralized surface and establish the area where resorption occurs. The second region is referred to as the transparent zone, characterized by a scarcity of organelles and an abundance of actin

filaments, located directly beneath the creased border. This area facilitates the process of bone resorption. The basolateral face is the third section. It is the location where the processed food is expelled from the cell through exocytosis (19,22).

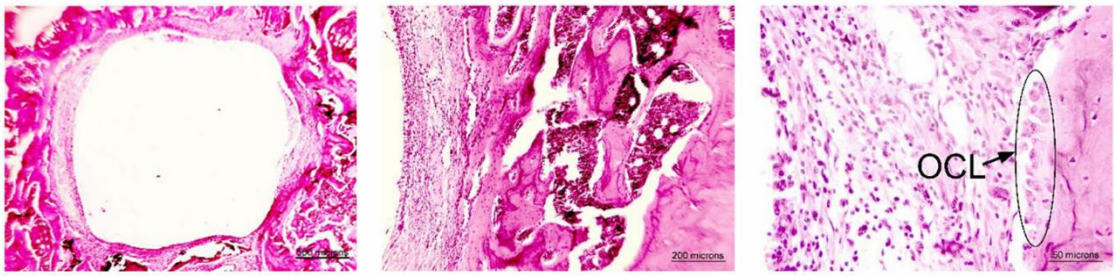

Figure 2.4. Histological H&E images of OCL, osteoclast (30).

2.2.5. Cells lining the bone surface

Inactive osteoblasts undergo a process of flattening and elongation, transforming into bone-laying cells that cover the surfaces of the bone. Endosteal cells symbolize the cells that line the inside surface of bones, whereas periosteal cells refer to the cells that line the outer surface. These cells form gap junctions with adjacent cells and osteocytes. Consequently, it is believed that they offer nourishment to osteocytes and control the influx and efflux of calcium and phosphate into the bone (22).

2.3. Periosteum and Endosteum

The bone's interior surfaces are coated with connective tissue layers known as endosteum, while the outer surfaces are coated with connective tissue layers known as periosteum (22,25,27). The periosteum is composed of two layers: the outer fibrous layer and an inner osteogenic layer. The fibrous layer is composed of collagen fibers and fibroblasts. Sharpey's fibers, which are collagen fibers in the periosteum, enter the bone matrix and securely attach the periosteum to the bone. The osteogenic layer comprises of flat cells, known as osteoprogenitor cells, which possess the ability to undergo division and differentiation in order to generate osteoblasts. Furthermore, the periosteum is absent from the area that is overlaid with joint cartilage and at the sites where tendons and muscles attach (25). The endosteum is a thin layer that lines the internal spaces of the bone. It is composed of a single layer of flat osteoprogenitor cells and a little amount of connective tissue. Thus, the endosteum is rather thin in comparison to the periosteum

(25). The primary roles of the periosteum and endosteum are to generate new osteoblasts essential for bone formation or healing and to supply nutrients to the bone tissue (23,25).

2.4. Bone Types

Upon histological examination of bone tissue, two distinct forms of bone tissue can be observed: Primary bone, also known as immature or woven bone, refers to the initial form of bone tissue that is laid down during the early stages of bone development and Secondary bone refers to a type of bone that is also known as mature or lamellar bone.

2.4.1. Primary bone tissue (woven bone)

Primary bone is the first kind of bone that emerges during the early stages of embryological development, as well as in cases of fractures and other instances of bone healing. Primary bone differs from secondary bone in terms of collagen fiber distribution. While secondary bone has a lamellar arrangement of collagen fibers, primary bone has thin collagen fibers that are randomly dispersed and oriented in various directions. Additionally, it has a lower mineral content and a higher concentration of osteocytes compared to secondary bone. Primary bone tissue is a transient tissue that is substituted by secondary bone in adulthood, with the exception of specific regions such as the articulations of flat bones in the skull, tooth sockets, and sites where tendons connect to bone (25,27).

2.4.2. Secondary bone tissue (Lamellar bone)

Adults typically have secondary bone tissue. The collagen fibers in secondary bone tissue are organized in lamellae that are either parallel to each other or grouped concentrically around a vascular canal. The lamellae that are organized in a circular fashion around the channels are referred to as Haversian lamellae. The Haversian system, commonly designated as the osteon, is defined by concentric lamellar structures surrounding a central channel known as the Haversian canal. This canal comprises vascular structures, neural elements, and loose connective tissue components. Anatomically, Haversian systems align longitudinally and are oriented parallel to the major axis of the diaphysis.The two Haversian canals are linked by Volkmann canals that traverse obliquely between them. Volkmann canals lack lamellae, unlike Haversian

canals. Osteocytes are situated in the lacunae, which can be found either between the lamellae or on the lamellae (22,25,27). The lamellae in compact bones exhibit a characteristic arrangement comprising the Haversian system, outer circumferential lamellae, inner circumferential lamellae, and interstitial lamellae. Interstitial lamellae are the remains of partially absorbed old Haversian lamellae that occupy the gaps between Haversian lamellae systems, also known as osteons. Furthermore, the bone is also covered by endosteal and periosteal lamellae, which are located on the inner and outer surfaces of the bone, respectively. The lamellae are referred to as inner circumferential lamellae and outer circumferential lamellae (22,25).

2.5. Bone Formation and Development

There are two modes in which bone development takes place: intramembranous and endochondral. In endochondral ossification, the key distinction lies in the presence of a pre-formed cartilage model between the two bone morphologies. Both types of ossification involve the initial formation of primary bone, which is subsequently replaced by secondary or lamellar bone (22,25).

2.5.1. Intramembranous bone formation (Direct ossification)

Intramembranous ossification initiates during the 8th week of gestation. Aggregations of mesenchymal cells occur in specific regions. Intramembranous ossification refers to the process of bone formation when the accumulation of cells within the mesenchymal tissue creates structures that mimic membranes (22). Mesenchymal cells undergo fast division and then differentiate into osteoprogenitor cells. Subsequently, they undergo a transformation into osteoblasts and initiate the secretion of collagen and other matrix proteins that constitute the osteoid tissue. Osteoid tissue undergoes mineralization and subsequently hardens. Mesenchymal cells in multiple distinct ossification centers persist in generating osteoblasts. As the ossification centers increase in size, they merge, resulting in the formation of spongiosa bone tissue. Subsequently, certain cancellous bones undergo a transformation into compact bone. The development of bone marrow also occurs from the mesenchymal tissue located between the trabeculae (22,25,31). Intramembranous ossification forms the frontal and parietal bones of the skull, along with some portions of the occipital, temporal, sphenoid, mandible, and maxilla.

This form of ossification also plays a role in the enlargement and thickening of compact bones (25).

2.5.2. Endochondral bone formation

Endochondral ossification transpires through the substitution of an existing cartilage model with osseous tissue. This kind of ossification is primarily observed in long bones, but it is also present in short bones. Initially, each bone serves as a provisional model of hyaline cartilage. The perichondrium encasing the cartilage converts into the periosteum enveloping the bone. Osteoprogenitor cells derived from the periosteum differentiate into osteoblasts and initiate bone synthesis. Consequently, a bone layer develops surrounding the cartilage model, and shortly thereafter, the chondrocytes in the inner and middle regions of the cartilage perish as a result of calcification. The spaces created by the disintegration of the calcified matrix coalesce to establish a structural framework for the accumulation of bone material. Osteoprogenitor cells and blood arteries infiltrate the degenerating cartilage matrix, establishing an ossification core in the forming bone. The major ossification center is initially observed in the diaphysis of long bones. The ossification center that emerges in the epiphysis at a subsequent stage is referred to as the secondary ossification center. Subsequently, osteoid tissue is synthesized and calcified inside the bone matrix. The proliferation of ossification centers leads to the complete substitution of the cartilage model with bone tissue, except the distal ends of the long bones. The enduring cartilage layer that encases the distal ends of long bones is referred to as articular cartilage (22,25,29,32).

2.6. Bone Growth and Remodeling

Bone growth transpires when a segment of pre-existing tissue undergoes destruction (resorption) concurrently with the formation of new tissue (apposition), provided that the volume of bone formation exceeds that of bone resorption. Consequently, when the bone develops, its morphology is concurrently maintained. Children's bone turnover rate is twenty times greater than that of adults.

The bone remodeling process consists of five stages.

1. Activation: This phase is characterized by the recruitment of osteoclasts to the site designated for remodeling to resorb a specified quantity of bone.

2. Resorption: This stage involves activated osteoclasts adhering to the bone surface and conducting bone resorption by the secretion of proteolytic enzymes.
3. Recycling: At this step, a cement line is established in the resorption cavity created by osteoclasts through the activation of certain mononuclear-macrophage-like cells. Subsequently, osteoblasts are guided to the resorption cavity.
4. Formation: The active cells at this stage are osteoblasts, which facilitate bone production. The activity of osteoblasts during the development stage persists for an average duration of 2 to 3 months. At this juncture, the mineralization of osteoid tissue transpires. Following the completion of mineralization, osteoblasts flatten and remodeling ceases.
5. Rest: At this stage, the bone tissue developed in the remodeling area remains dormant until the initiation of a new remodeling cycle (27).

2.7. Healing of Bone Tissue

Bone tissue is a dynamic, biologically active structure comprised of cells. The repair of the fracture line and defect site is influenced by numerous biochemical, biomechanical, cellular, hormonal, and pathological mechanisms. The processes of deposition, resorption, and remodeling in bone structure promote the repair of bone tissue. Bone healing transpires in three phases: inflammation, repair, and remodeling (33).

2.7.1. Inflammatory stage

The initial reaction to bone fractures is inflammation. Trauma to the bone tissue results in the tearing of the periosteum and nearby soft tissues, along with injury to the arteries. Hematoma arises from bleeding due to injury to blood vessels and surrounding tissues. Fibrin is formed by proteins and damaged cells as a result of this hematoma. The clot that forms subsequently obstructs the damaged vessels and halts hemorrhage. Acute inflammatory cells initially occupy the clot, followed by chronic infection cells and macrophages within a few days. Once the coagulation is organized, it is immediately replaced by granulation tissue, which occurs within 3-4 days. The hematoma supplies two critical components that are essential for bone regeneration. Initially, the hematoma establishes mechanical stability by occupying the space between the bone and soft tissue.

Secondly, it introduces embryonic osteoblast and chondrocyte cells to the fracture site, where they undergo differentiation into osteoblasts and chondroblasts (25,33).

2.7.2. Repair phase

The repair phase commences within hours post-fracture formation, although it requires 7–12 days to achieve structural typicality. Mesenchymal cells, which possess pluripotent capabilities, are crucial to the repair process. Upon differentiation, fibroblasts are the initial cells to undergo transformation, migrating into the hematoma via capillaries. These cells generate a pliable granulation tissue between the fractured segments. The cells in the central region of the fracture site differentiate into chondroblasts and chondrocytes due to diminished circulation, resulting in the formation of cartilage tissue. Fibroblasts produce collagen, chondroblasts emit collagen and glycosaminoglycans, and osteoblasts release osteoid material. This formation, comprising fibrous tissue, cartilage, and juvenile bone tissue, is referred to as callus. Increased vascularization of the originally produced soft callus enhances osteoblast activity, which regulates collagen alignment through the secretion of tropocollagen. Subsequently, a hard callus is established through the deposition of calcium ions. The period for callus development and mineralization following a fracture is approximately 4 to 16 weeks (25,33,34).

2.7.3. Remodeling phase

Bone formation is the most prolonged phase of bone recovery. This phase involves the conversion of the microscopically uneven hard callus into more uniform lamellar bone of standard strength. The process commences during the intermediate stage of repair and typically endures for 4 to 16 weeks in humans, but it may persist for several years (22,33,34).

2.8. Alveolar Bone

The segment of the jawbone encircling the tooth sockets and providing support for the teeth is referred to as the alveolar bone. The alveolar bone comprises cortical bone, which constitutes the buccal and lingual walls of the crest, the interdental and interradicular septa, as well as trabecular bone situated between these layers. The alveolar

bone interacts with the canal system and periodontal ligament, facilitating vascular and nerve conduction, and undergoes intramembranous ossification throughout fetal development (35).

The compact bone constituting the alveolar socket wall, in contact with the periodontal ligament, is rich in Sharpey's fibers and is referred to as bundle bone. The interdental and interradicular areas are primarily made up of cancellous bone. The alveolar bone's contour conforms to the shape of the tooth roots, with its height and thickness influenced by factors including tooth alignment, root angulation, and occlusal stresses. In certain regions, the bone may become significantly attenuated and vanish, leaving a segment of the root exposed. The primary determinants influencing the height, shape, and density of alveolar bone are the presence and active function of teeth. Tooth extraction significantly impacts the vertical and horizontal dimensions of the alveolar bone, potentially leading to a loss of up to 50%.This situation results in significant functional and cosmetic issues (35,36).

The healing of the alveolar bone following tooth extraction encompasses a sequential cascade of biological processes aimed at the complete regeneration and bone infill of the extraction socket. Immediately after tooth removal, the socket is filled with a blood clot, primarily composed of erythrocytes and platelets embedded within a fibrinous network. This initial clot subsequently undergoes transformation into granulation tissue, characterized by extensive vascular proliferation, which acts as the preliminary scaffold initiating new bone formation within the alveolar socket (37,38).

Both preclinical and clinical research findings demonstrate that the dimensional loss observed in the alveolar ridge subsequent to tooth extraction represents an irreversible event, involving notable reductions in ridge width and height. This resorption predominantly affects the buccal aspect of the alveolar bone, with significantly greater deterioration compared to the lingual aspect (39-41).

Subsequent to dental extraction, the alveolar bone undergoes additional resorptive changes attributable to physiological remodeling mechanisms inherent to bone tissue (42,43).

This resorptive phenomenon initiates promptly after tooth extraction, potentially resulting in a dimensional reduction of the alveolar ridge width by as much as half within the initial three-month postoperative interval (40).

Scientific investigations have demonstrated that alveolar ridge resorption occurs to a greater extent on the buccal aspect compared to the lingual side, and have emphasized the influence of several factors—including patient age—on the severity and magnitude of ridge resorption in both horizontal and vertical dimensions (43,44).

2.9. Healing of Tooth Extraction Wound

The healing process of a tooth extraction wound parallels that of a fracture and has four sequential stages.

1. Socket obstruction with clot
2. Substitution of blood clot with viable granulation tissue (day 7)
3. Gradual replacement of granulation tissue with connective tissue and juvenile periosseous tissue (day 20)
4. Bone trabeculae are inserted into the alveolar cavity on the 38th day (4,42).

In the immediate aftermath of tooth extraction, bleeding occurs, and the extraction cavity is filled with blood that contains damaged cells and proteins. These cells initiate a sequence of events that results in the formation of a fibrin network following the bleeding. Platelets, on the other hand, create a blood clot that covers the entire socket within the first 24 hours (4,45,46).. Within approximately 48 to 72 hours following dental extraction, granulation tissue initiates invasion into the blood clot, predominantly originating from the base of the extraction socket, progressively leading to the degradation of the clot structure (45,46). The epithelium proliferates around the socket and rudimentary connective tissue is observed within four days. The granulation tissue is entirely infiltrated and replaced by the thrombus after seven days (45). At the conclusion of the initial week, the vascular network is established. Two weeks later, the marginal region of the extraction cavity is covered with young connective tissue, and osteoid tissue is visible at the socket's base (45,46). Osteoid tissue commences to mineralize 3--4 weeks following extraction. The extraction cavity is initially filled with woven bone, which resorbs within

approximately one month. Subsequently, the bone is replaced with trabecular bone until it regains its original shape (4,45).

The histological and radiological examination of the healing process following tooth extraction has been conducted on a variety of laboratory animals, as well as on samples obtained from human biopsies and autopsy materials. While the fundamental characteristics of repair histogenesis are well established, the timing of new bone production may differ due to variability in the age, sex, species, and food of the experimental animals employed (47,48).

Histological investigations in animals have demonstrated that the healing of the extraction site resembles that in humans and adheres to a similar sequence, albeit at an accelerated pace (49,50).

Scientific studies evaluating the factors that impact the post-extraction wound healing process in rat models, as well as their associations with tissue regeneration, were initiated as early as 1923 (49). Euler conducted the initial radiological and histological examination investigating the sequential healing stages occurring within the alveolar socket subsequent to tooth extraction (51). Researchers study utilized dogs of identical age and size had healthy teeth and gums.

Huebsch et al . investigated the healing process after tooth extraction in male rats. This study reported that a blood clot filled the socket 7 hours post-extraction, while the periodontal membrane remained visible 14 hours later. On the fifth day post-extraction, the socket was observed to be entirely filled with connective tissue, with initial signs of bone formation emerging. By the tenth day, the epithelium had successfully closed the wound. By the 13th day, the socket exhibited significant filling with young bone tissue, and the epithelium displayed characteristics akin to the oral mucosa. By the 25th day, the socket was entirely filled with bone, and the epithelium underwent differentiation, resulting in keratinized squamous epithelium (47).

Araujo and colleagues conducted a study to histologically evaluate alveolar socket healing following tooth extraction in a canine model, spanning an observational period of eight weeks. In the first postoperative week, the extraction socket was histologically characterized by the presence of a blood clot, granulation tissue, and a provisional connective tissue matrix containing collagen fibrils, neovascularization, fibroblastic

proliferation, and limited initial bone formation. By the second postoperative week, marked bone regeneration became evident, particularly in the apical and lateral aspects of the extraction socket, where abundant newly formed bone was detected. Histological examination at this stage revealed osteoblast-rich surfaces, accompanied by developing bone marrow cavities. At four weeks post-extraction, the original bundle bone located at the crestal area was completely replaced by mature lamellar bone, substituting the initially formed woven bone.The bone surface exhibited a high density of osteoblasts alongside bone marrow spaces. By the fourth week, the bundle bone in the crestal region has been entirely replaced by crestal lamellar bone, supplanting the woven bone. The provisional matrix is located at the center of the socket, while mineralized tissue and bone marrow occupy the surrounding areas. In the eighth week, the lingual wall exhibited greater thickness compared to the buccal wall, and a broad bridge of mineralized tissue was noted between these two walls (52).

Cardaropoli et al. a study conducted in 2003 examined the healing stages of dog tooth extraction wounds over a 180-day period. This study observed that clot formation occurred in the socket on the first day post-tooth extraction, with the clot being covered by inflammatory cells, particularly neutrophilic granulocytes. By day 3, vascularized granulation tissue was replaced by clot, and by day 14, new bone formation was evident throughout the socket tissue. By day 30, the socket is nearly entirely occupied by newly formed bone. On the 90th day, the woven bone in the majority of regions was replaced by lamellar bone. The remodeling of the newly formed bone persisted until the 180th day, during which a decrease in mineralization was noted, and trabecular bone was replaced by fatty tissue (53).

Guglielmotti and Cabrini the maximum bone formation was observed on the 14th day following the extraction of all mandibular molar teeth in rats, with the socket walls and extraction socket becoming indistinguishable from the adjacent alveolar bone by the 60th day (54).

Pietrokovski et al. In 1967, researchers conducted studies on rats to examine socket healing over an 8-week duration. During the initial week, osteoblasts and immature bone tissue were identified in the central and fundus areas of the socket. In the second week, the socket exhibited young bone tissue characterized by a trabecular structure. By

the fourth and eighth weeks, the newly formed bone retained its trabecular architecture and was distinctly differentiated from the lamellar bone (55).

Numerous animal studies have extensively investigated the biological events occurring after tooth extraction, resulting in a comprehensive understanding of the mechanisms involved in alveolar socket healing.But limited research has assessed the histological aspects of socket healing following tooth extraction in human subjects. Amler et al. conducted a study that serves as an illustration of this.Also Boyne bone specimens obtained from the sockets of alveolar extraction and more recently Devlin and Sloan analyzed extraction socket biopsies obtained during resective oncological surgery (42,56,57).

In 1960, Amler et al. Analyzed the histological healing of 75 human extraction sockets over a 50-day duration. On the first day post-tooth extraction, the socket was noted to be filled with a clot. By the seventh day, the blood clot had been entirely replaced by granulation tissue, with the presence of osteoid tissue at the base of the socket. On the 20th day, granulation tissue was substituted by connective tissue, with initial mineralization observed at this stage, and bone formation commenced at the periphery and base of the extraction sockets. On the 38th day, which corresponds to the fifth week, two-thirds of the socket is occupied by newly formed trabecular bone. Epithelialization commences on the fourth day and concludes after 24 days. Amler indicated that bone regeneration progresses through all stages, starting from the socket base and periphery toward the center and apex of the socket. The study did not specify the conditions of the teeth, and tissue biopsies indicated that only single-rooted teeth were examined (42).

In a histological investigation conducted by Boyne in 1966, the healing process within extraction sockets of maxillary first premolars was evaluated in a cohort consisting of 12 human subjects over a total duration of 23 days. Histological assessments performed on days 7 and 8 indicated an absence of detectable bone regeneration within the extraction sockets. Conversely, initial osteogenesis was identified along the lateral socket margins beginning on days 9 and 10. By the 13th and 14th days post-extraction, histological analysis demonstrated that approximately one-third of the alveolar socket volume had become occupied by newly generated bone. Furthermore, by the 19th day, a considerable area of the extraction socket was substantially populated with a well-developed bone matrix (56).

Devlin and Sloan analyzed the bone biopsies collected two weeks post-extraction. Histological analysis revealed trabecular bone formation and bone marrow spaces in the socket periphery, along with the presence of osteocytes and osteoblasts at the socket edges (57).

2.10. Antioxidants

Free radicals are molecules characterized by an unpaired electron in their outermost orbit. They can arise from normal metabolic processes as well as from factors such as smoking, alcohol consumption, air pollution, certain medications, and radiation exposure. Free radicals constitute molecules characterized by inherent instability and significant reactivity, and are frequently designated in the scientific literature as reactive oxygen species (ROS) (58). Reactive oxygen species significantly contribute to the development of numerous diseases, including cancer, cardiovascular diseases, diabetes, and cerebrovascular disorders. Oxidative stress refers to the detrimental effects of free radicals that result in biological damage. To safeguard tissues from these detrimental consequences, free radicals must be neutralized. The substances that offer this benefit are termed antioxidants (59).

Antioxidants are examined in terms of enzymatic and non-enzymatic properties: Glutathione peroxidase, superoxide dismutase, catalase are examples of enzymatic antioxidants.

Non-enzymatic antioxidants, including essential minerals (selenium, zinc), various vitamins (A, C, K, and E), carotenoid compounds (such as β-carotene, lycopene, lutein, and zeaxanthin), organosulfur substances (such as allium derivatives, allyl sulfides, and indoles), antioxidants characterized by low molecular weight (e.g., glutathione, uric acid), antioxidant co-factors (including coenzyme Q), and diverse polyphenolic compounds, have been extensively investigated in scientific studies (60).

2.11. Hesperidin

A variety of botanicals and phytochemicals, naturally found in dietary sources and plant materials, have long been utilized for their therapeutic potential in managing numerous health conditions due to their accessibility and cost-effectiveness. Substantial scientific evidence indicates that many phytochemicals exert antioxidant properties,

contributing to the regulation of oxidative stress-related pathological mechanisms implicated in disorders such as cancer, cardiovascular diseases, and persistent inflammation (61-63). . Among these compounds, flavonoids have emerged as the most extensively investigated class. Flavonoids, a subset of phenolic compounds, are further categorized into anthocyanidins, flavonols, flavanones, flavanols, flavones, and isoflavones (64). Phytochemicals, especially flavonoids, are receiving growing attention for their therapeutic potential in bone health. Research indicates that flavonoids significantly influence bone formation and resorption in both cell culture and animal models, demonstrating their potential role in these processes in vitro and in vivo (65-67).

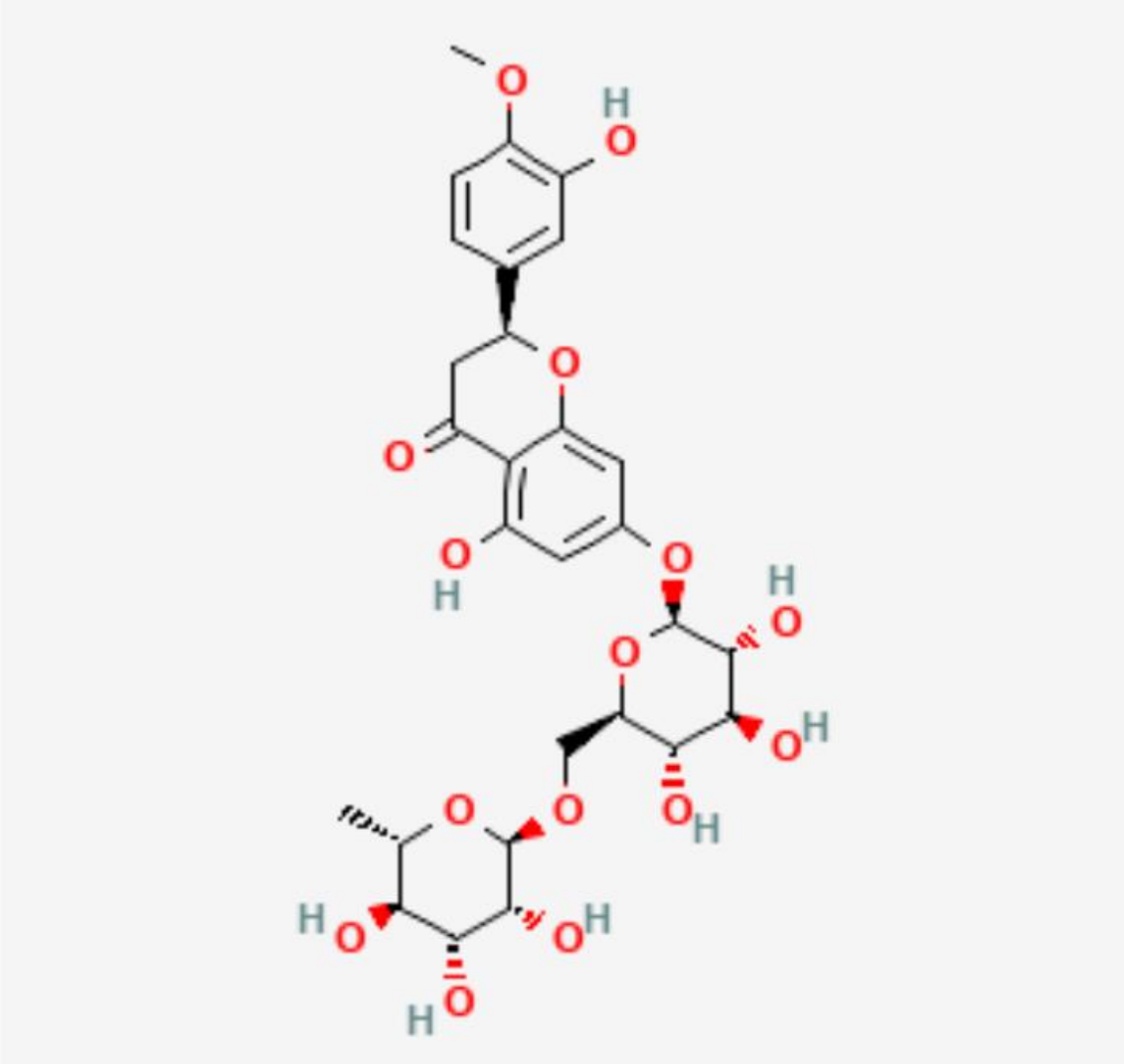

Figure 2.5. Chemical formulation of hesperidin (68).

Hesperidin serves a protective function against fungal and other microbial infections in plants. In addition to its physiological antimicrobial activity, extensive

research over several decades has identified numerous therapeutic applications for the prevention and treatment of various human disorders. These benefits are primarily attributed to its antioxidant and anti-inflammatory properties (69,70).

Hesperidin is a naturally occurring flavanone, belonging to the broader flavonoid class, and is abundantly present in numerous citrus fruits. Flavonoids derived from botanical sources typically appear as glycosides, defined structurally by their attachment to carbohydrate groups, often termed sugar residues, forming glycosidic linkages. Hesperidin is a glycoside consisting of the flavanone hesperetin (aglycone) and the disaccharide rutinose, which is formed from rhamnose linked to glucose.

2.11.1. Antioxidant activity of hesperidin

The neutralization of reactive oxygen species (ROS) is essential for preserving human health, as their overproduction leads to oxidative stress, which compromises cellular architecture and physiological functions. Oxidative stress has been documented as a key initiator of inflammatory cascades, subsequently exacerbating tissue injury through self-sustaining mechanisms that significantly contribute to the etiology of numerous critical health conditions, such as cardiovascular diseases, neurodegenerative disorders, diabetes mellitus, and various cancers. Hesperidin confers protective effects primarily through its ability to scavenge reactive oxygen species, alongside strengthening the endogenous antioxidative capacity. This protection is mediated via increased expression and enzymatic activation of endogenous antioxidants, specifically superoxide dismutase (SOD), heme oxygenase-1 (HO-1), and catalase, as well as by elevating intracellular concentrations of glutathione, a crucial antioxidant molecule within cells (71-74).

Consequently, hesperidin administration has been documented to alleviate pathological conditions that arise due to oxidative stress, thereby conferring protective benefits against adverse effects associated with clinical therapies such as radiotherapy and chemotherapeutic regimens. Moreover, preclinical studies employing animal models have revealed a substantial attenuation of therapy-induced toxicity following hesperidin treatment (75,76).

Furthermore, human peripheral blood samples obtained prior to and following the ingestion of a single oral dose of 1000 mg of Daflon (a dietary supplement containing hesperidin) exhibited significant protection against cellular irradiation damage when exposed in vitro to gamma rays (77,78).

2.11.2. Effect of hesperidin on inflammation

Oxidative stress in the body frequently correlates with systemic inflammation, which is a hallmark of numerous chronic conditions. Multiple studies demonstrate that hesperidin and hesperetin can decrease various pathologically elevated inflammatory markers (71,79-81). These bioactive agents have shown potential in attenuating the expression of pro-inflammatory cytokines, such as tumor necrosis factor-alpha (TNF-α), along with modulating pro-inflammatory mediators. Additionally, they exert regulatory effects on enzymes like inducible nitric oxide synthase (iNOS), responsible for nitric oxide (NO) synthesis, and cyclooxygenase-2 (COX-2), which facilitates the generation of inflammatory mediators including prostaglandins (72).

2.11.3. Effect of hesperidin on pain management

A diet deficient in hesperidin is correlated with pain in the extremities. Additionally, it was noted that intraperitoneal injection of this flavanone induces antinociception, characterized by reduced sensitivity to pain, which is partially mediated by μ-opioid receptors (73,74).

2.11.4. Effect of hesperidin on bone health

Recent studies conducted in vitro, in vivo, and ex vivo indicate that hesperidin may influence bone health (75,76,82). In vitro studies demonstrated that hesperidin stimulates the differentiation of osteoblasts, which are cells responsible for bone formation. A separate study demonstrated a significant increase in bone mineral density (BMD) in young rats given hesperidin. In adult rats, the enhancement of bone strength occurred without a corresponding increase in bone mineralization. In an established animal model designed to simulate postmenopausal osteoporosis induced by ovariectomy, hesperidin administration demonstrated differential protective efficacy against bone resorption based upon the age of the animals; specifically, it exhibited partial

attenuation of bone loss in mature rats, whereas in younger rats, the osteoprotective effect resulted in complete prevention of bone loss. Additionally, hesperidin supplementation may offer broader therapeutic advantages for postmenopausal women, as evidenced by experimental results indicating its dual efficacy in mitigating osteoporotic changes and simultaneously providing significant lipid-reducing properties in ovariectomized rats, both young and mature (83).

A separate study examined the role of hesperetin in mitigating osteoblast dysfunction caused by diabetic conditions. The findings indicated that hesperetin may mitigate several adverse effects associated with elevated sugar levels by enhancing collagen synthesis and reducing protein and lipid oxidation in osteoblasts (84).

2.11.5. Effect of hesperidin on infections

Hesperidin, a bioflavonoid predominantly found in citrus species, is primarily recognized for its antifungal properties; however, accumulating evidence also highlights its potential efficacy in combating viral and bacterial pathogens. A study investigated the antimicrobial potential of grapefruit seed and pulp ethanolic extracts, evaluating their inhibitory effects against a panel of 20 bacterial and 10 fungal (yeast) strains (70,85,86).

The strongest antimicrobial activity was noted in relation to *Salmonella enteritidis*, exhibiting a minimum inhibitory concentration (MIC) value of 2.06% based on the concentration of the extract employed. Conversely, for other bacterial species and yeast strains examined in the study, MIC values demonstrated variability, ranging between 4.13% and 16.5%.A recent investigation focusing on *Aeromonas hydrophila*, a pathogenic microorganism implicated in gastrointestinal and systemic infections, revealed that hesperidin possesses both antibacterial properties and immunomodulatory activity (87). Hesperidin has been shown to confer protective effects in murine models when administered prior to infection with encephalomyocarditis virus (EMCV), *Staphylococcus aureus*, or their co-infection.Additionally, separate research has demonstrated the antiviral efficacy of hesperidin against human rotavirus, a major etiological agent of pediatric diarrhea (88). In vitro analyses have demonstrated that hesperidin suppresses influenza virus replication and decreases the population of virus-infected cells (86).

2.11.6. Human studies on hesperidin

The mucus layer of the intestinal epithelium is predominantly composed of water, constituting more than 98% of its total composition. Consequently, the intestinal uptake of hesperidin is significantly limited, owing to the molecule's inherently low solubility in aqueous environments (Figure 2.6).

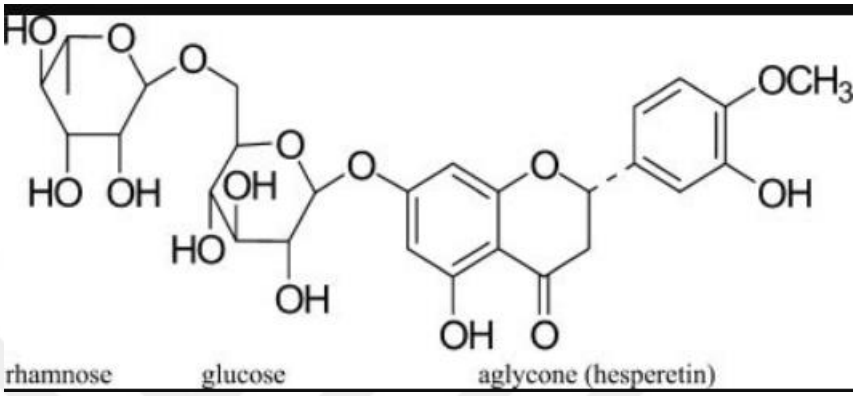

Figure 2.6. Chemical structure of hesperidin (hesperetin-7-*O*-rutinoside) (89).

Improving the aqueous solubility of hesperidin is critical for enhancing its oral bioavailability and maximizing its therapeutic potential. Enzymatic hydrolysis, which removes the rhamnose residue to generate hesperetin-7-glucoside (a hesperetin molecule conjugated solely with glucose; Fig. 2.6), has been shown to markedly improve intestinal absorption, thereby increasing systemic hesperetin levels (89).

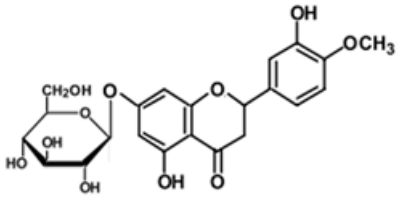

Figure 2.7. Hesperetin-7-glucoside (89).

Following administration, the peak plasma concentration of hesperetin was achieved within 36 minutes—substantially faster than the over 7-hour timeframe observed after hesperidin intake—and was approximately four times higher. Glucosyl hesperidin (G-hesperidin), which consists of hesperidin conjugated with an additional glucose unit (refer to Fig. 2.7.), demonstrates a remarkable increase in water solubility by

approximately 10,000-fold along with significantly enhanced systemic bioavailability (90).

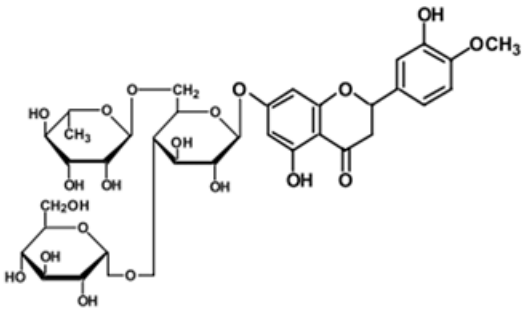

Figure 2.8. Glucosyl Hesperidin (89).

In animals administered G-hesperidin, hesperetin was detected in plasma more rapidly, with its total concentration in the bloodstream being 3.7 times greater than that observed in rats receiving hesperidin. Hesperidin methyl chalcone, a semi-synthetic compound commonly utilized in medicinal formulations, is distinguished by its open ring structure, which enhances water solubility. Additionally, the presence of multiple methyl group substitutions improves metabolic stability by redirecting metabolism towards less efficient enzymes (91,92).

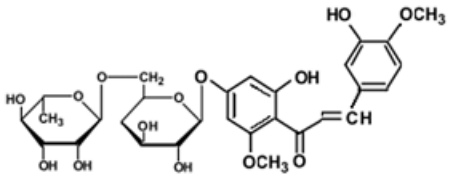

Figure 2.9. Hesperidin Methyl Chalcone (89).

2.11.7. Synergystic effect of hesperidin

Biochemical processes within the human body are highly complex and regulated, requiring the coordinated involvement of numerous molecular entities, including substrates and cofactors, to elicit specific biological outcomes. Signal transduction pathways are composed of multiple sequential components, each necessitating the involvement of distinct molecular participants. Cells utilize diverse biochemical pathways that serve as alternative mechanisms to accomplish equivalent physiological functions. Compounds participating in the same or parallel pathways may act synergistically when present simultaneously. Synergism among various agents can

enhance or support the biological actions of other compounds through mechanisms such as improving absorption or increasing the systemic availability of bioactive molecules. This cooperative interaction can reduce the required dosages while maintaining efficacy and minimizing toxicity (93).

Hesperidin exhibits synergistic interactions when combined with a range of natural substances (Table 2.1) and specific therapeutic agents (Table 2.2). It has been shown to confer cellular and tissue protection against the harmful effects of toxic agents such as arsenic, as well as to mitigate adverse reactions associated with clinically utilized drugs, including chemotherapeutic agents (Table 2.3) (93).

Table 2.1. Synergistic interactions between hesperidin/hesperetin and specific natural compounds (94-98).

Natural Compounds	**Effects**
Vitamin C	↓ hyaluronidase activity, ↑ capillary resistance
Caffeine	↓ triglycerides, ↓ hepatic lipogenesis, ↓ obesity
Diosmin	↓ capillary permeability
Naringenin and Eriodictyol	↑ antimicrobial activity

Table 2.2. Synergistic interactions between hesperidin/hesperetin and specific pharmaceuticals (73,74,99-103).

Selected Drugs	**Effects**
Benzodiazepines (diazepam, alprazolam, bromazepam, midazolam, flunitrazepam)	↑ benzodiazepines effects (↑ neuroprotection, ↓ seizures, ↓ anxiety, ↓ pain)
Ketorolac (NSAID)	↓ arthritic gout-type pain
Prednisolone (steroid drug)	↓ inflammation, ↓ allergy
Doxorubicin	↓ tumor cells resistance to doxorubicin
Methotrexate	↓ inflammatory and arthritis markers

Table 2.3. Protective effects of hesperidin and diosmetin against the toxicity of selected compounds and drugs (104-106).

Compounds/Drugs	**Effects**
Cyclophosphamide (other names: Endoxan, Cytoxan, Neosar, Procytox, Revimmune, Cycloblastin)	↑ chemoprevention, ↓ oxidative stress, ↓ genotoxicity
Sodium arsenite	↓ liver and kidneys toxicity
Carbon tetrachloride	↓ liver and kidneys toxicity

2.11.8. Safety of hesperidin

Numerous preclinical studies and clinical trials have provided robust evidence indicating that hesperidin possesses a favorable safety and tolerability profile in both animal models and human subjects. Clinical dosing recommendations for hesperidin depend significantly upon the particular therapeutic indication as well as the pharmaceutical formulation employed (refer to Human Studies). Among commercially available formulations, Daflon 500 mg is frequently prescribed, containing a combination of 450 mg diosmin and 50 mg hesperidin. Daflon 500 mg is marketed under multiple proprietary names, including Detralex, Arvenum 500, Alvenor, Capiven, Elatec, and Venitol. Comprehensive evaluations regarding the safety and tolerability of Daflon 500 mg have been extensively conducted through both experimental animal research and rigorous human clinical investigations (93).

Toxicological studies have demonstrated that hesperidin exhibits a median lethal dose (LD_{50}) value of roughly 3000 mg/kg in animal models, corresponding to approximately 180-fold greater than the customary therapeutic dosage utilized clinically. Moreover, administration of doses up to 35 times the recommended amount over a 26-week period produced no signs of toxicity. In clinical studies, individuals receiving two Daflon 500 mg tablets daily for one year experienced no significant adverse effects, with no alterations detected in hepatic or renal function, metabolic status, hematologic parameters, or blood pressure (systolic and diastolic)

Treatment of internal hemorrhoids during the final 8 weeks of pregnancy and the subsequent 4 weeks postpartum was found to be safe, with no adverse effects on pregnancy outcomes, fetal development, birth weight, or infant growth and feeding (107).

However, given the potential for interference with drug absorption, it is advisable to consult a physician before initiating hesperidin supplementation.

Preclinical studies have shown that co-administration of hesperidin with calcium channel antagonists, β-adrenergic blockers, or statins markedly influences both the peak plasma levels and overall systemic absorption of these drugs. These pharmacokinetic interactions may warrant dose modifications, frequently involving a downward adjustment to ensure therapeutic safety and efficacy (Table 2.4) (93,108,109).

Table 2.4. Influence of hesperidin on bioavailability of selected drugs (93,108-110).

Medications	**Effects**
Celiprolol (β-blocker; other names: Cardem, Selectol, Celipro, Celol, Cordiax, Dilanorm)	↓ bioavailability of celiprolol (underdosing)
Diltiazem (calcium channel blocker; other names: Cardizem, Cartia XT, Dilacor XR, Dilt-CD, Diltia XT, Diltzac, Matzim LA, Taztia XT, Tiazac)	↑ bioavailability of diltiazem (overdosing)
Verapamil (calcium channel blocker; other names: Isoptin, Verelan, Verelan PM, Calan, Bosoptin, Calaptin, Verogalid ER, Covera-HS)	↑ bioavailability of verapamil (overdosing)
Pravastatin (statin drug; other names: Pravachol, Selektine)	↑ bioavailability of pravastatin (overdosing)

2.11.9. Bioavailibility and absorption of hesperidin

The pharmacological effectiveness of orally administered hesperidin is largely dependent on its bioavailability, which is influenced by both its aqueous solubility and its ability to be absorbed through the intestinal epithelium. Despite hesperidin's limited solubility in water, its modified forms—hesperidin-7-glucoside and glucosyl hesperidin—demonstrate significantly improved solubility. This enhancement facilitates their passage through the intestinal mucosa and access to the apical membrane of enterocytes. The presence of a glucose residue may support cellular uptake through sodium-glucose co-transporter 1 (SGLT1)-mediated transport mechanisms (90).

One proposed absorption mechanism involves the enzymatic cleavage of glucosyl hesperidin into hesperidin and glucose by α-glucosidase, an enzyme situated on the brush border membrane of the small intestine, prior to its uptake by enterocytes. A portion of the released hesperidin may undergo further deglycosylation to form hesperetin, facilitated by β-glucosidase present on the brush border or produced by intestinal bacteria (90,111). Additionally, a portion of the released hesperidin is likely transported into the enterocytes without undergoing deglycosylation. An in vitro investigation using Caco-2 cell monolayers demonstrated that, in contrast to hesperidin, glucosyl hesperidin crosses the epithelial barrier via a paracellular transport route that does not require cellular energy (112).

However, the in vivo study failed to identify intact G-hesperidin in serum; however, hesperidin and its metabolites were detected in urine following G-hesperidin administration (90).

2.11.10. Cellular mechanisms of action of hesperidin

Antioxidant Mechanisms of Action: Hesperidin exerts a protective influence by enhancing the intrinsic antioxidant defense mechanisms of the body, predominantly through modulation of the extracellular signal-regulated kinase 1/2 (ERK1/2) signaling pathway. Upon activation, ERK signaling induces the nuclear localization of nuclear factor erythroid 2-related factor 2 (Nrf2), subsequently resulting in elevated expression levels of heme oxygenase-1 (HO-1) enzyme. HO-1 enzymatically mediates the catabolism of heme into multiple products, including biliverdin recognized for its potent antioxidant properties carbon monoxide, known to possess anti-inflammatory effects, and free iron. Furthermore, Nrf2 activation enhances the transcriptional upregulation of several genes involved in cellular protection, encompassing crucial antioxidant enzymes such as superoxide dismutase, catalase, glutathione reductase, and numerous phase II detoxification enzymes (64,113,114).

Anti-inflammatory Mechanisms: Hesperidin has additionally been demonstrated to possess anti-inflammatory properties through the inhibition of signaling pathways mediated by nuclear factor kappa-light-chain-enhancer of activated B cells (NF-κB). It has been shown to increase the expression of the NF-κB inhibitor protein

(NFκBIB), thereby reducing the transcription of NF-κB–regulated pro-inflammatory genes (115).

Mechanisms Supporting Bone Health: Hesperidin contributes to the preservation of bone integrity by suppressing bone resorption, an effect that may be attributed to its antioxidant capacity, stimulation of estrogen receptor pathways, and inhibition of the enzyme HMG-CoA reductase Reactive oxygen species, particularly superoxide radicals, have been shown to break down osteocalcin-a bone-specific protein-into smaller peptide fragments, ultimately compromising the structural stability of the bone matrix (86,116).

Moreover, elevated oxidative stress leads to dysfunction in osteoblasts, the cells responsible for bone formation (84).

The antioxidant properties of hesperidin may prevent the degradation of osteocalcin and the dysfunction of osteoblasts. The administration of hesperetin has been observed to significantly elevate alkaline phosphatase (ALP) activity and collagen content, while concurrently reducing oxidative stress products such as malondialdehyde (MDA) and advanced oxidation protein products (AOPP) (84).

Hesperetin is thought to exert protective effects against bone loss, in part through its interaction with estrogen receptors (87,115-118). Administration of hesperetin significantly upregulates the mRNA expression of alkaline phosphatase and the osteogenic transcription factors Runx2 and Osterix, all of which are essential for osteoblast differentiation and bone matrix synthesis. Additionally, hesperetin downregulates the expression of the receptor activator of nuclear factor kappa-B ligand (RANKL), a key molecule in osteoclastogenesis. RANKL binds to its receptor RANK on osteoclast precursors, facilitating recruitment of TNF receptor-associated factor 6 (TRAF6), which activates both the c-Jun N-terminal kinase (JNK) and NF-κB signaling cascades. These pathways are instrumental in promoting osteoclast differentiation and activation. Hesperetin has been shown to interfere with this process, thereby inhibiting osteoclast activity (119).

A third proposed mechanism by which osteoporosis may be prevented involves the inhibition of 3-hydroxy-3-methylglutaryl coenzyme A (HMG-CoA) reductase, a key regulatory enzyme in the cholesterol biosynthetic pathway (80,83). Inhibition of this

enzyme may influence bone metabolism by altering downstream cholesterol-derived metabolites. One such metabolite, 27-hydroxycholesterol (27HC), a product formed during cholesterol catabolism, has been identified as an endogenous selective estrogen receptor modulator. It has been shown to bind to estrogen receptors (ERs) and affect their transcriptional activity. This interaction can interfere with the normal protective actions of estrogens on bone tissue, ultimately attenuating their beneficial effects on bone remodeling and mineral density (114).

The 27-HC also activates liver X receptors (LXRs) in osteoblasts, which results in a decrease in osteoblast proliferation, differentiation, and activity, as well as an increase in the production of osteoclastogenic factors like TNFα and RANKL. Moreover, 27 HC, by acting on ERα, reduced the expression of the LXR inhibitor small heterodimeric partner (SHP) in osteoblasts, thus promoting unrestricted LXR activity.

Hesperetin reduces the total amount of 27 HC by inhibiting cholesterol synthesis, which affects both ER and LXR, resulting in uncoupled osteoblastogenesis and osteoclastogenesis, ultimately enhancing bone density (82,114).

2.12. Absorbable Hemostatic (Gelatin) Sponge (HS)

Hemostatic sponges were initially presented as hemostatic agents by Correll and Wise in 1945. Hemostatic sponges are composed of gelatin. The collagen in animal skin is extracted and processed through baking to create sponge. These may originate from bovines, porcines, or equines (113).

Figure 2.10. Commercially used version of Absorbable haemostatic gelatin sponge

Hemostatic substrates are devoid of hemostatic properties. It possesses a sizable chambered architecture and can absorb blood up to 45 times its own weight. It demonstrates its hemostatic effect by serving as a carrier for thrombin within the blood composition. HS, which absorbed the blood, exerted a physical surface effect and a hemostatic impact on the bleeding site. It absorbs plasma and sticks to the hemorrhaging surface. The adherence of HS to the hemorrhaging surface is contingent upon the aggregation of platelets inside its structure, situated between the sponge and the bleeding surface. Consequently, it is more efficacious in low-pressure hemorrhaging.

It is recommended for managing hemorrhagic cavities following tooth extraction. Nevertheless, hemostatic sponges experience difficulty adhering to bone surfaces after absorbing blood and may adhere to surgical instruments, causing them to detach from their intended location (120). HS is available in powder, block, and sponge forms. The surgeon has the ability to trim and shape it as needed in accordance with the bleeding area. Due to its lack of intrinsic hemostatic properties, it can be utilized by saturating it

with thrombin solution. If the hemostatic substance is applied too thinly and forced onto the hemorrhaging site, its efficacy will diminish, resulting in continued blood leakage without clot formation. Numerous investigations have been undertaken to examine tissue absorption and histological responses to HS implantation. Light and Prentice's study demonstrated that tissue reaction commenced on the sixth day post-HS placement, with leukocytes initially infiltrating the area, followed by the predominance of lymphocytes and macrophages by the twelfth day. Complete absorption of the material was noted on the twentieth and forty-fifth days. It was noted that this inflammatory response was comparable to the response observed during clot resorption (121).

Despite being derived from animal skin collagen, it does not exhibit antigenicity. The lack of antigenicity is attributed to the absence of aromatic radicals that can induce anaphylactoid reactions. Nonetheless, infrequent allergic reactions associated with HS have been documented (122).

HS may elevate the risk of postoperative infection. Studies indicate that it triggers infection development due to a foreign tissue reaction when implanted in the tissues (122).

In contrast to other hemostatic agents, HS does not impede bone healing (123). HS, primarily utilized in cancellous bone bleeding, absorbs blood from the surrounding environment, facilitating the development of hemostatic activity in the affected area. Enhanced hemostatic activity fosters an optimal environment for bone healing (120).

3. MATERIALS AND METHOD

This study was conducted at Yeditepe University Experimental Animals Research and Application Center (YUDETAM) with the approval of Yeditepe University Experimental Animals Local Ethics Committee (2014/A-65). In the study, 48 male Sprague Dawley rats, 3-5 months old, weighing between 250-300 g, were used as experimental animals. Before the experimental procedure, rats were kept in a 12-hour dark and 12-hour light environment at 21°C and ad libitum.

In this study, we used 56 animals and divided them into 4 groups and 2 different times. After tooth extraction, we divided them into groups as inflammation, epithelialization, connective tissue formation, and new bone formation and scored them. After 56 Sprague Dawley rats had their teeth extracted, they were sacrificed at the end of the specified times, their jaw sections were separated, placed in tissue fixative (10% formalin) and delivered to Yeditepe University, Faculty of Medicine, Department of Pathology. Haematoxylin-eosin and Masson trichrome staining methods were used to observe bone healing, epithelialization, and connective tissue formation.

Rats were divided into four groups, each consisting of 6 rats, using simple random sampling method: Control, spongestan, spongestan+local hesperidin, and systemic hesperidin groups. After the extraction of the lower left first molars, each main group was divided into 2 subgroups, each consisting of 6 subjects, depending on the sacrification period. Additionally, the animals were weighed daily and the dosage of the drugs was adjusted accordingly.

The main groups and subgroups determined were planned as follows.

1. Control Group: The group in which the lower left first molars of the rats were extracted and placebo solution was given from the day of extraction to the day of sacrifice and the healing of the extraction socket was monitored (n=12).
    1.1. 28th Day Group: The group that was sacrificed 28 days after tooth extraction, after giving placebo solution and monitoring the healing of the extraction socket (n=6).

1.2. 56th Day Group: The group that was sacrificed 56 days after tooth extraction, after giving placebo solution and monitoring the healing of the extraction socket (n=6).

2. Spongostan Group: This group consisted of rats (n=12) in which Spongostan was applied directly to the tooth extraction socket following the removal of the lower left first molar. The post-extraction healing process of the socket was subsequently monitored throughout the experimental period.
   2.1. 28th Day Group: The group that was sacrificed on the 28th day after tooth extraction, by placing spongestan in the extraction socket and monitoring the healing of the extraction socket (n=6)
   2.2. 56th DAY GROUP: The group that was sacrificed on the 56th day after tooth extraction, by placing spongestan in the extraction socket and monitoring the healing of the extraction socket (n=6)

3. Local Hesperidin (HSP) Group: The group in which the extraction socket healing was monitored by applying vortexed hesperidin solution impregnated with spongestan to the extraction socket after the lower left first molar tooth of the rats was extracted (n=12)
   3.1. 28th Day Group: The group of rats that were administered local hesperidin after tooth extraction and sacrificed on the 28th day after the extraction socket healing was monitored (n=6)
   3.2. Day 56 Group: The group of rats that were administered local hesperidin after tooth extraction and sacrificed on the 56th day after the extraction socket healing was monitored (n=6)

4. Local Hesperidin and Systemic Hesperidin Group: The group in which the extraction socket was monitored by applying vortexed hesperidin solution impregnated with spongestan and hesperidin via gavage after the lower left first molar tooth of the rats was extracted (n=12)
   4.1. 28th Day Group: The group in which local hesperidin and systemic hesperidin were administered after tooth extraction and the extraction socket healing was monitored and the rats were sacrificed on the 28th day (n=6)

4.2. 56th Day Group: The group in which local hesperidin and systemic hesperidin were administered after tooth extraction and the extraction socket healing was monitored and the rats were sacrificed on the 28th day (n=6)

3.1. Preparation, Dosage and Route of Administration of Hesperidin

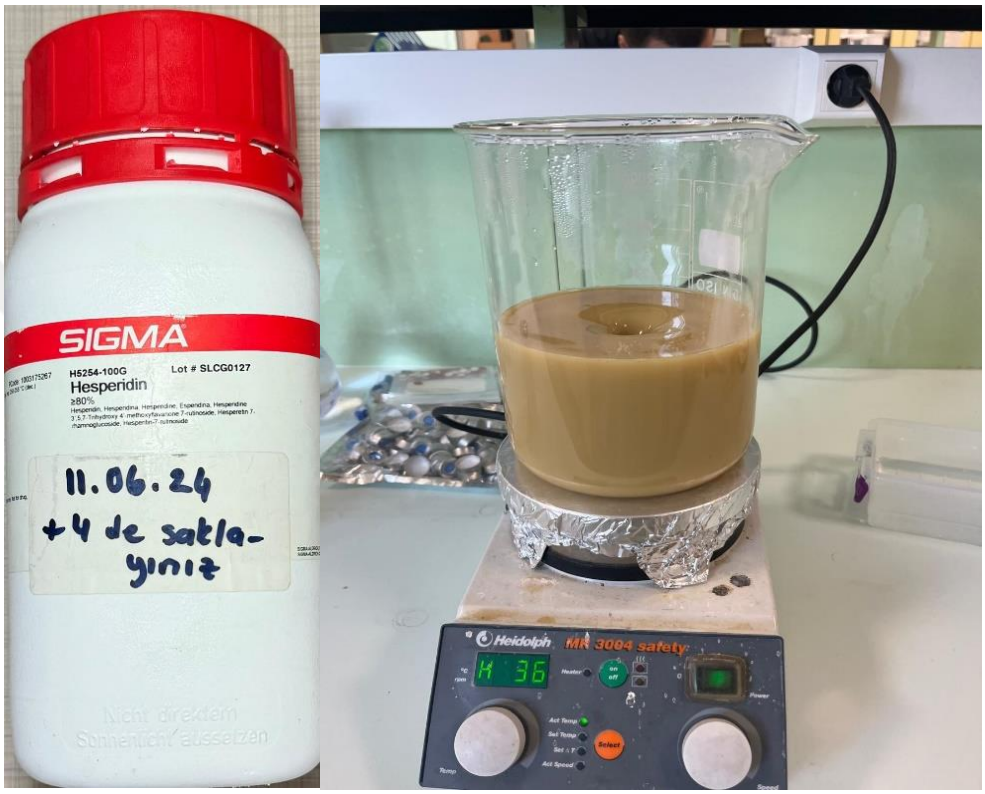

Figure 3.1. Commercial form of Hesperidin (Sigma-Aldrich H5254 Hesperidin ≥80%) and liquid form prepared in a magnetic stirrer

The Hesperidin we used in our study was obtained from the brand Sigma-Aldrich (H5254 ≥80% 100 G).

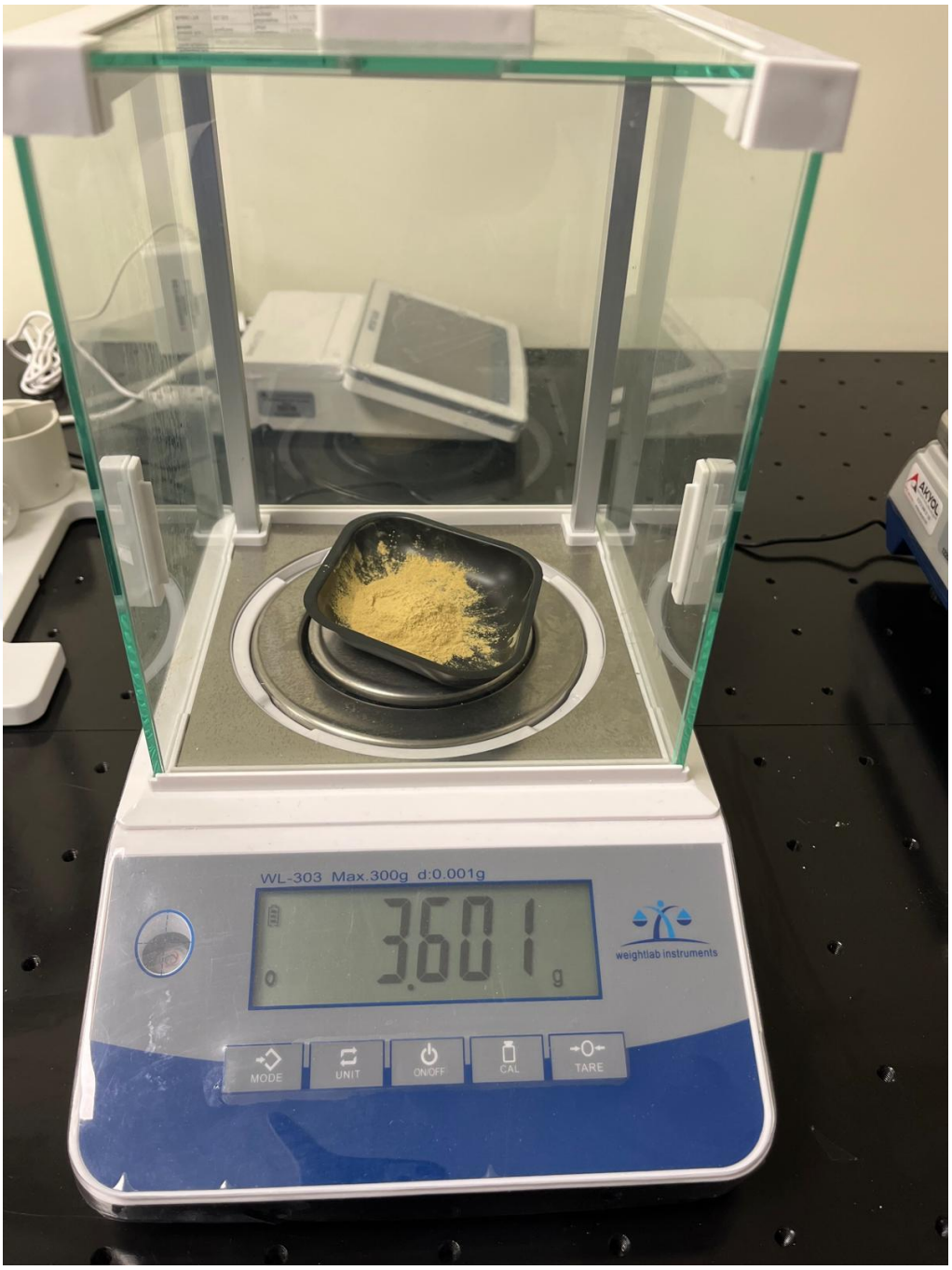

Figure 3.2. Weighing powdered hesperidin

The dosage of Hesperidin we applied to the experimental animals was 100 mg/kg. While preparing 100 mg/kg hesperidin,we used Carboxymethylcellulose obtained from Sigma-Aldrich (C5678 Carboxymethylcellulose sodium salt low viscosity 2.5 kg) as a solvent. 0.5% CMC solution was prepared with dissolving at distilled water.

Figure 3.3. Prepared and labeled falcon tubes

100mg/kg hesperidin solution was obtained by dissolving hesperidin with 0.5% CMC solution on a magnetic stirrer. The prepared solution was stored in the +4 degree refrigerator.

Figure 3.4. After mixing Hesperidin with CMC (carboxymethyl cellulose) and placing it in falcon tubes, labeling and sequential preparation for 28 days

Figure 3.5. Falcon tubes prepared to be vortexed one per day and containing hesperidin and its solution ready to be placed in the refrigerator

The resulting solution was applied locally to the sponge group by dipping it in the sponge, and was applied to the 28 and 56 day groups by gavage in 1.5 ml solutions per animal, day by day until their sacrifice, by removing it from the +4 refrigerator and vortexing.

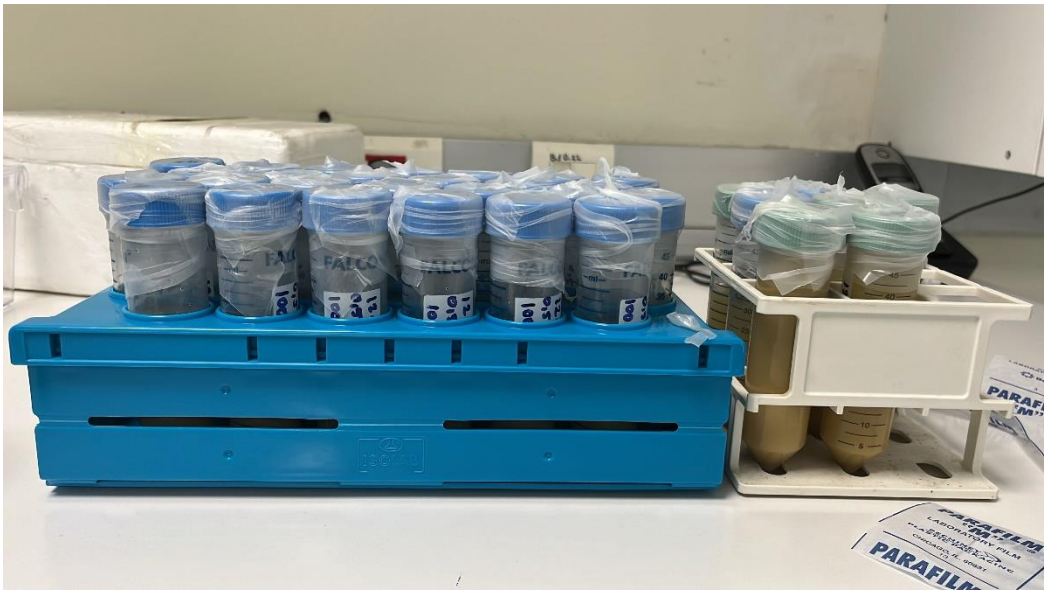

Figure 3.6. Preperated Hesperidin solutions before putting +4 C refrigerator

3.2. Tooth extraction method

On the first day of the experiment, all subjects were injected intramuscularly with ketamine hydrochloride ((10% Alfamine, Alfasan, Netherlands) 50 mg/kg and xylazine hydrochloride ((2% Alfazyne, Alfasan, Netherlands) 5 mg/kg for anesthesia, in compliance with the rules of asepsis and antisepsis (Fig. 3.3).

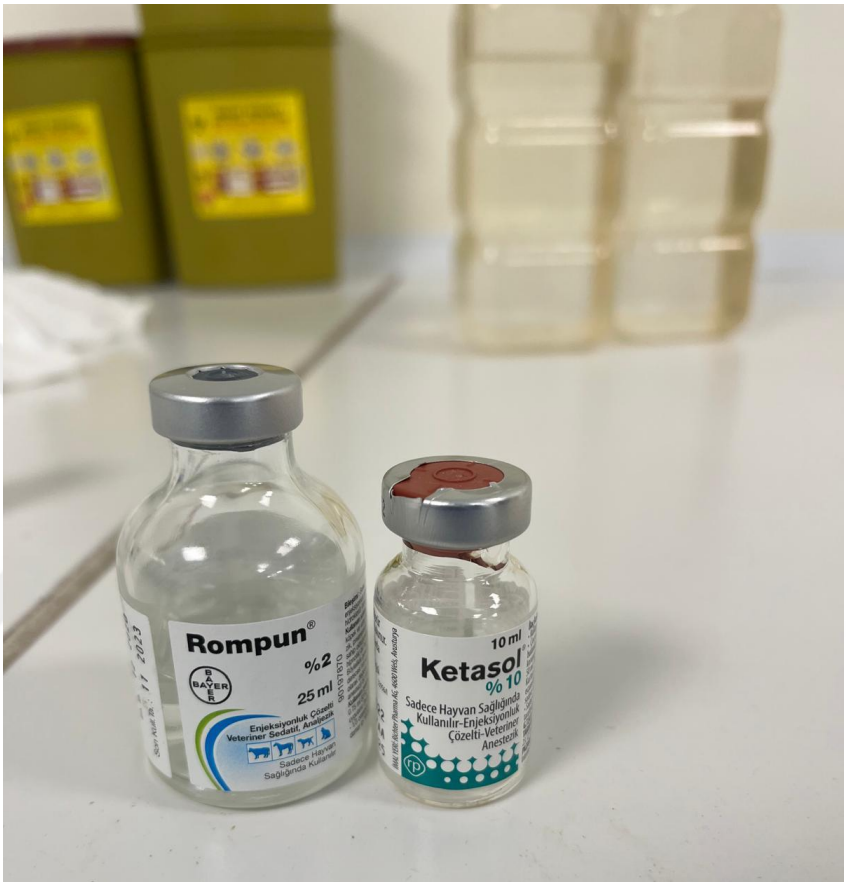

Figure 3.7. Ketamine hydrochloride (10% Ketasol, Richter Farma, Germany) and xylazine hydrochloride (2% Rompun, Bayer, Germany)

Figure 3.8. Image of an anesthetized rat before tooth extraction

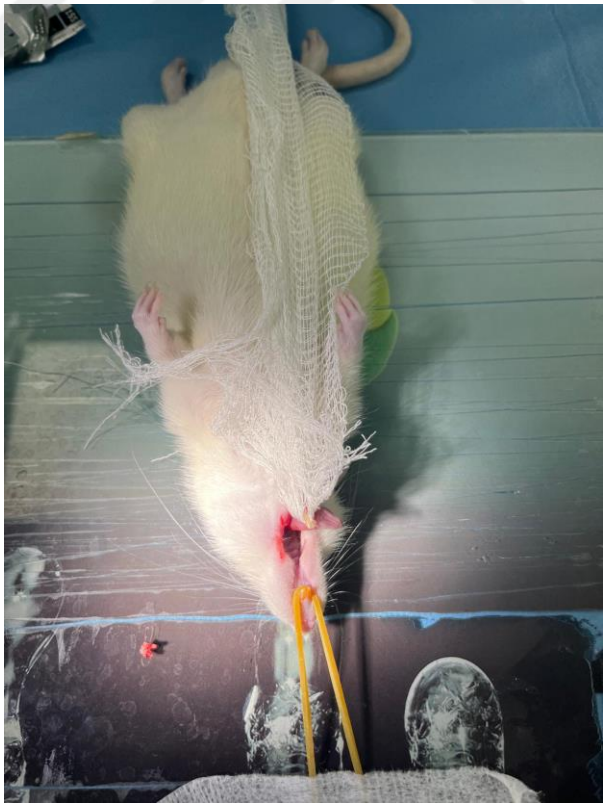

Figure 3.9. Extraction wound and extracted tooth after extraction of lower left first molars

Figure 3.10. Image of the extracted tooth before fixation with formalin

Figure 3.11. Rats that have been anesthetized and have had their teeth extracted are placed in cages after the procedure.

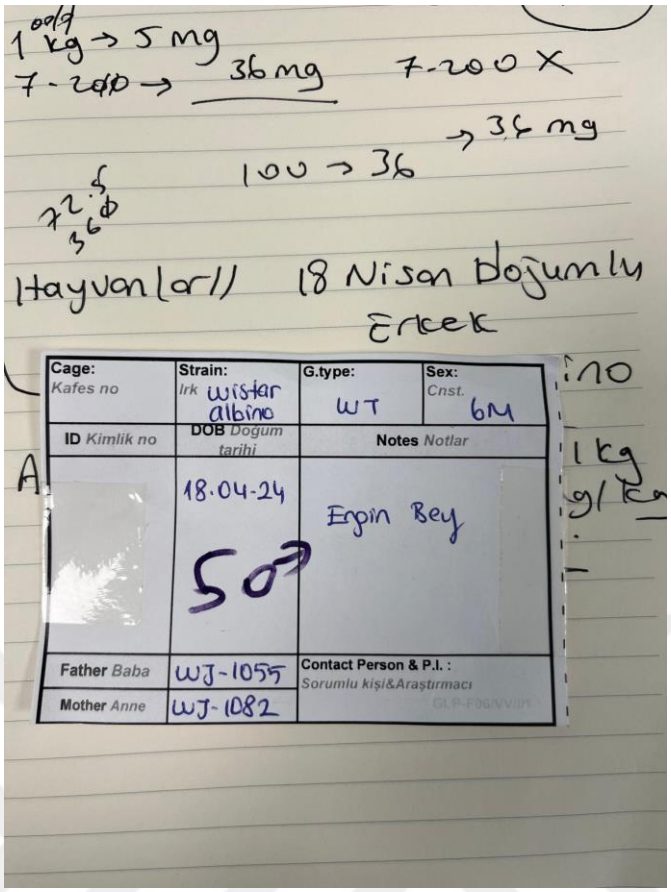

Figure 3.12. Identity forms prepared for rats before they were placed in cages

Figure 3.13. A place where experimental animals are kept for the required periods of time and where humidity, temperature and other ideal conditions are provided.

Figure 3.14. Mice sacrificed in a closed box with isoflurane

Figure 3.15. The state of a rat that has been sacrificed and its mandible removed and placed in a 10% formalin container

After the tongue and cheek of the rat were retracted with the tools in the sterile surgical kit, the lower left first molars of the subjects were extracted by applying luxation with the help of a curved hemostat and a blunt scalpel (Fig. 3.6). Sterile tamponade was applied to ensure hemostasis. No antibiotics were administered to the rats after the extraction and the animals were fed with appropriate food throughout the experiment(Fig. 3.7). Animals were sacrificed by administering isoflurane in a closed environment on the 28th and 56th days according to their groups. After the left mandibles of the rats were removed, the materials were placed in 10% buffered formalin.

3.3. Histological Evaluation

The tissue samples were sent to the Department of Pathology, Yeditepe University Faculty of Medicine for histological examination. The bone tissue samples were fixed in 10% neutral buffered formaldehyde for 72 hours at room temperature. Following the fixation process, bone tissue samples underwent decalcification in a 10% formic acid solution, with the solution being replaced every two days for a duration of 10 days. Following the completion of the decalcification process, the bone tissue samples were washed in running tap water, subjected to a series of increasing ethanol concentrations (50%-99%), and processed through xylene series before being embedded in paraffin blocks after infiltration with molten paraffin at 62 °C. Sections measuring 6 μm in thickness were obtained from paraffin blocks onto slides utilizing a microtome (Leica DFC280). Sections were stained using Hematoxylin-Eosin (H-E) and Masson trichrome methods. Inflammatory cell infiltration, epithelialization, connective tissue formation, and bone tissue formation in tooth socket areas were assessed semiquantitatively across all sections (Table 3.1).

Table 3.1. Scoring of histological findings

Score	Inflammation	Ephithelization	Connective tissue	New bone formation
0	not present	not present	not present	not present
1	mild-focal areas	ends of surface area, epithelization of 1/3 of the surface	up to 1-20% of socket area	up to 1-20% of socket area
2	moderate-local areas	epithelization of 2/3 of the surface	up to 21-40% of socket area	up to 21-40% of socket area
3	severe-diffuse	epithelization of all of the surface	greater than 40% of socket area	greater than 40% of socket area

3.4. Statistical Evaluation

In the current investigation, statistical evaluations were performed using the Number Cruncher Statistical System (NCSS) 2007 software package (Utah, USA). In addition to employing standard descriptive statistics such as mean, standard deviation, median, and interquartile range, the normality of data distributions was assessed via the Shapiro-Wilk normality test. For analyses involving group comparisons in which variables exhibited non-normal distributions, the Kruskal-Wallis test was utilized. When significant differences emerged, subsequent pairwise comparisons among subgroups were performed using Dunn's multiple comparison test. Comparisons between two independent groups were conducted using the Mann-Whitney U test. Throughout the statistical analysis, a significance level of $p<0.05$ was considered as the criterion for determining statistical significance.

4. FINDINGS

4.1. Histological Findings

The scores presented in Table 3.1 were utilized in the assessment of histological findings in this study.

4.1.1. Histological findings of the sacrificed groups on day 28

Table 4.1. Histological findings of the sacrificed groups on day 28

	sample	inflammation	epithelialization	connective tissue	bone
spongestan 28. day	1	1	1	2	1
spongestan 28. day	2	1	1	2	0
spongestan 28. day	3	1	1	2	1
spongestan 28. day	4	2	0	2	1
spongestan 28. day	5	2	1	2	1
spongestan 28. day	6	2	1	2	0
local hesp 28. day	1	1	1	2	0
local hesp 28. day	2	2	0	3	1
local hesp 28. day	3	1	1	3	0
local hesp 28. day	4	1	1	2	0
local hesp 28. day	5	1	0	1	0
local hesp 28. day	6	1	1	2	1
local+gavage 28. day	1	2	0	3	0
local+gavage 28. day	2	1	0	3	0
local+gavage 28. day	3	1	1	2	0
local+gavage 28. day	4	2	0	2	0
local+gavage 28. day	5	1	1	2	1
local+gavage 28. day	6	2	1	2	0
control group 28. day	1	2	0	2	0
control group 28. day	2	2	1	2	0
control group 28. day	3	2	0	1	0
control group 28. day	4	2	1	2	0
control group 28. day	5	1	0	1	0
control group 28. day	6	2	0	2	0

- **Spongestan 28. day:**

In sections stained with hematoxylin and eosin, fibrous connective tissue areas were observed in the area of 21-40% of the tooth socket area (Figure 4.1). In some of the sections, inflammation was observed in mild focal areas, while in others, inflammation was observed in moderate local areas. While no epithelialization area was observed in one section, in other sections, there were epithelialization areas at the ends of the surface

area, on 1/3 of the surface. While no new bone formation was observed in two sections, new bone formation areas were observed in the area of 1-20% of the socket area in the other sections (Figure 4.2).

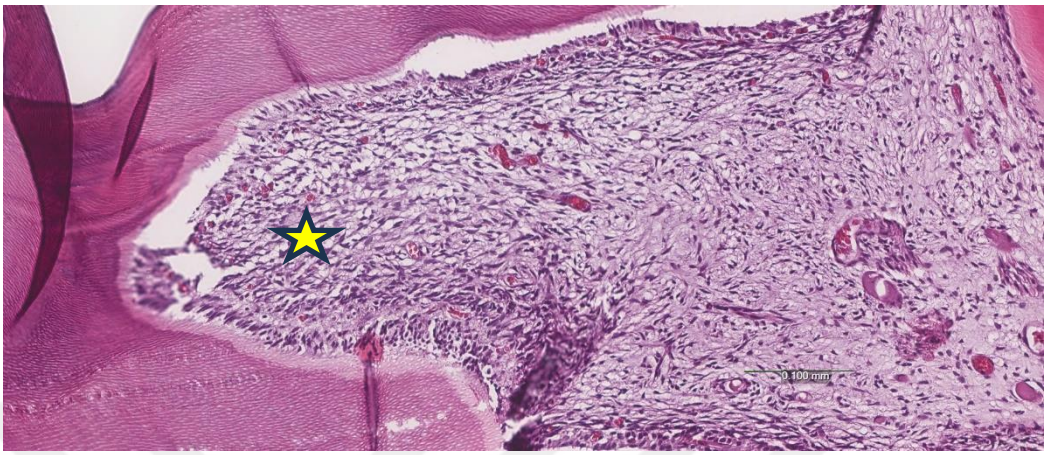

Figure 4.1. Fibrous connective tissue areas (star) on day 28 of Spongestan

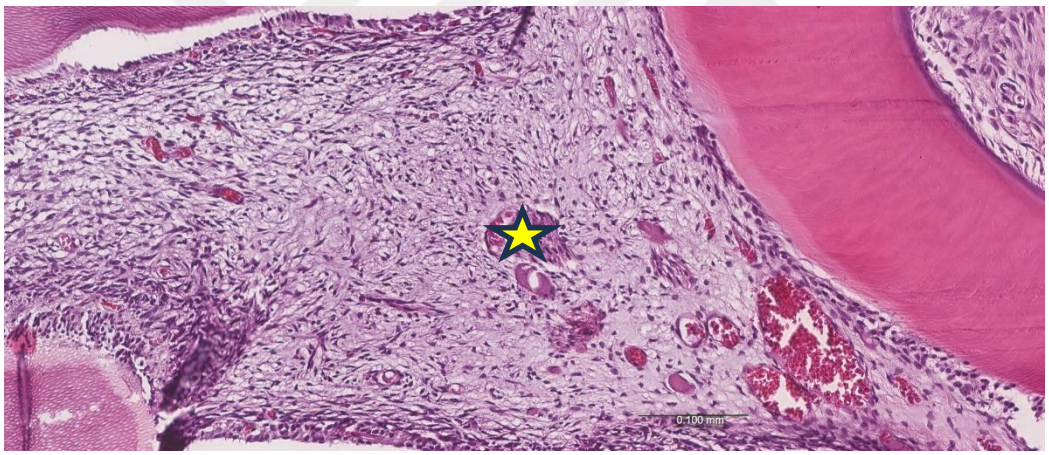

Figure 4.2. Areas of bone formation on day 28 of Sponges (star)

- **Local hesperidin 28. day:**

In some of the sections stained with hematoxylin and eosin, fibrous connective tissue areas were observed in an area of up to 21-40% of the tooth socket area, while in others, fibrous connective tissue was observed in an area greater than 40% of the socket area, and in only one of the sections, fibrous connective tissue areas were observed in an area of up to 1-20% of the socket area (Figure 4.3). Inflammation was observed in mild-focal areas in the sections. While no epithelialization was observed in some of the sections, in some there were epithelialization areas at the ends of the surface area, on 1/3 of the surface. In two of the sections, new bone formation areas were observed in the area

of 1-20% of the socket area, while no bone formation areas were observed in the other sections (Figure 4.4).

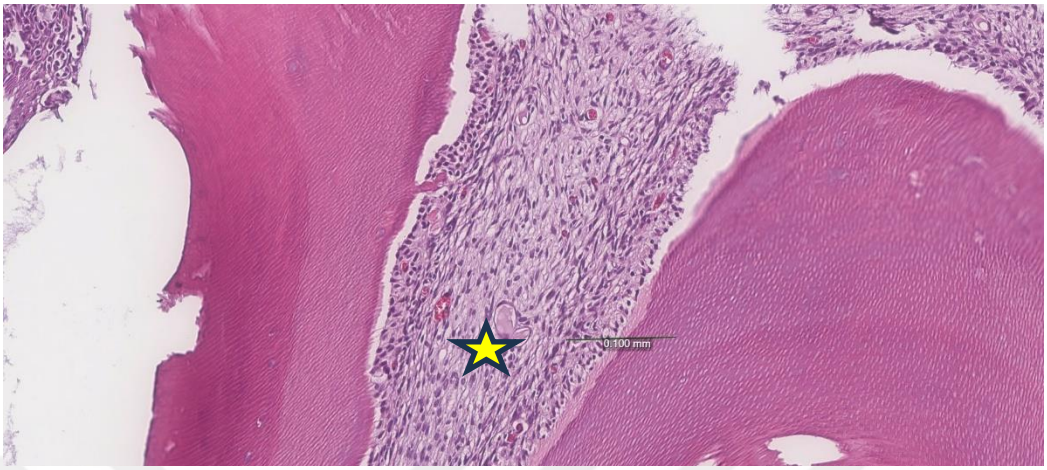

Figure 4.3. Local hesperidin 28th day fibrous connective tissue areas (star)

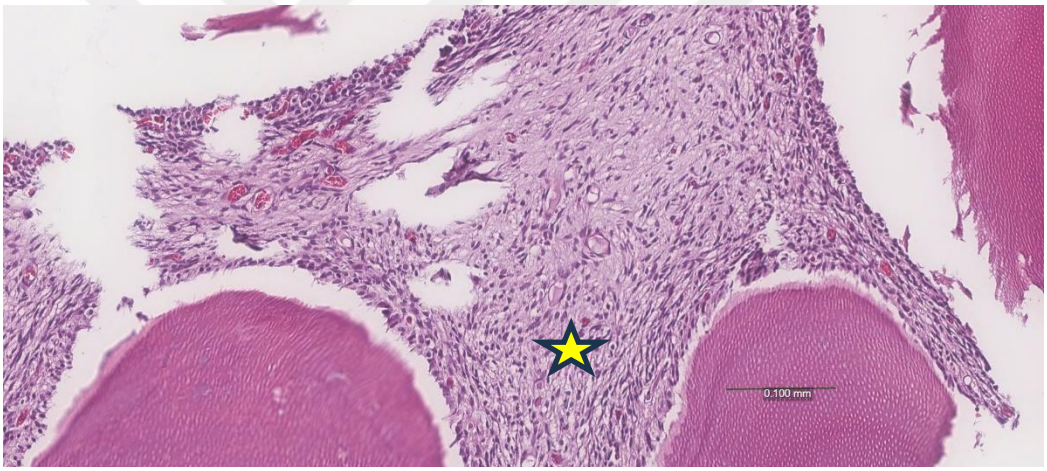

Figure 4.4. Local hesperidin 28th day focal bone formation areas (star)

- **Local hesperidin and gavage 28. day:**

In several of the histological sections prepared with hematoxylin and eosin staining, regions of fibrous connective tissue were found to occupy between 21% and 40% of the total extraction socket area. In contrast, other sections demonstrated a more extensive presence of fibrous connective tissue, covering more than 40% of the socket area. (Figure 4.5). In some of the sections, inflammation was observed in mild focal areas, while in others, inflammation was observed in moderate local areas. While no epithelialization was observed in some of the sections, in some, there were epithelialization areas at the ends of the surface area, on 1/3 of the surface. While new

bone formation areas were observed in the area of 1-20% of the socket area in one of the sections, no bone formation areas were observed in the other sections (Figure 4.6).

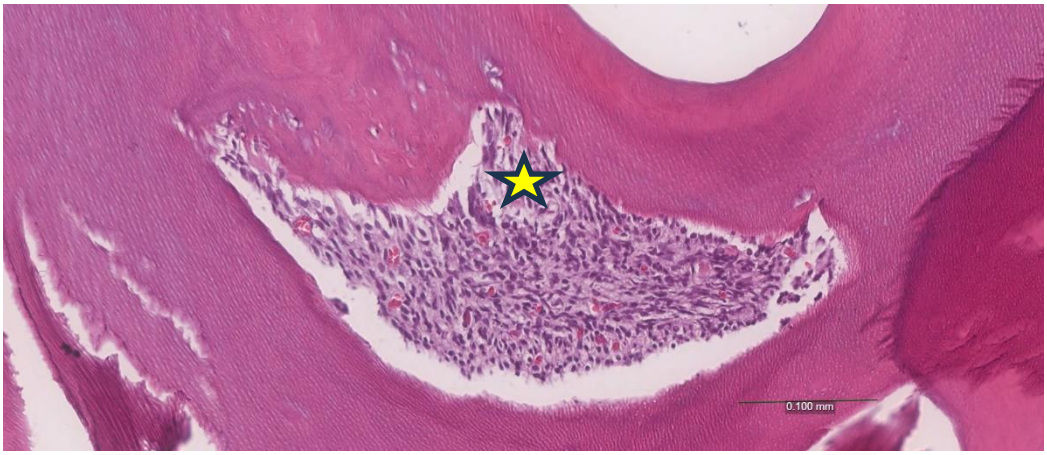

Figure 4.5. Local hesperidin gavage 28th day fibrous connective tissue area (star)

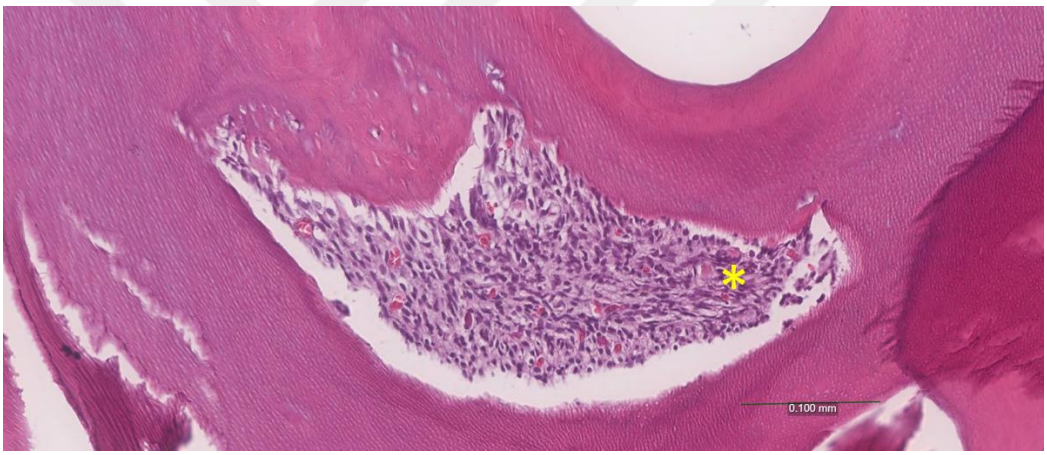

Figure 4.6. Focal bone formation areas on day 28 of local hesperidin gavage

• **Control group 28. day:**

In certain sections stained with hematoxylin and eosin, fibrous connective tissue was identified in 21-40% of the tooth socket area, whereas in other sections, it was present in more than 40% of the socket area. While inflammation was observed in mild focal areas in one of the sections, inflammation was observed in moderate local areas in the other sections (Figure 4.7). In two of the sections, epithelialization areas were observed at the ends of the surface area, on 1/3 of the surface, while no epithelialization area was observed in the remaining sections. New bone formation was not observed in the sections.

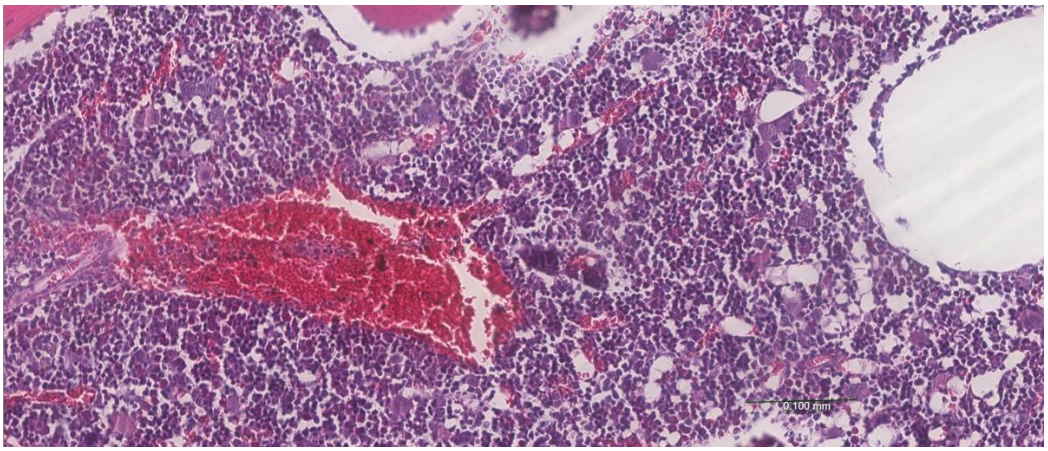

Figure 4.7. Control day 28 widespread inflammatory cells

4.1.2. Histological findings of the sacrificed groups on day 56

Table 4.2. Histological findings of the sacrificed groups on day 56

	sample	inflammation	epithelialization	connective tissue	bone
spongestan 56. day	1	1	2	2	2
spongestan 56. day	2	1	2	2	2
spongestan 56. day	3	0	1	2	2
spongestan 56. day	4	1	2	3	1
spongestan 56. day	5	1	1	3	1
spongestan 56. day	6	1	2	2	0
local hesp 56. day	1	2	1	1	0
local hesp 56. day	2	1	1	2	1
local hesp 56. day	3	1	1	2	1
local hesp 56. day	4	0	1	2	0
local hesp 56. day	5	1	1	2	1
local hesp 56. day	6	1	1	3	2
gavage 56. day	1	1	2	2	1
gavage 56. day	2	0	2	2	1
gavage 56. day	3	0	2	2	2
gavage 56. day	4	1	2	3	2
gavage 56. day	5	0	1	2	1
gavage 56. day	6	1	2	2	2
control 56. day	1	1	1	3	2
control 56. day	2	1	1	2	1
control 56. day	3	necrosis	necrosis	necrosis	Necrosis
control 56. day	4	0	2	2	2
control 56. day	5	1	1	1	1
control 56. day	6	1	2	2	2

*: new bone formation

- **Spongestan group 56. day:**

In some of the sections stained with hematoxylin and eosin, fibrous connective tissue areas were observed in an area of up to 21-40% of the tooth socket area, while in others, fibrous connective tissue was observed in an area greater than 40% of the socket area (Figure 4.8). In one of the sections, no inflammation was observed, while in the other sections, inflammation was observed in mild-focal areas. In two of the evaluated sections, epithelial coverage was detected at the terminal regions of the socket surface, encompassing approximately one-third of the total surface area. In the remaining sections, epithelialization was observed to extend over two-thirds of the surface. Regarding bone regeneration, three sections exhibited new bone formation occupying 21–40% of the socket area, while two sections demonstrated bone formation within a range of 1–20%. Notably, one section revealed an absence of newly formed bone tissue (Figure 4.9).

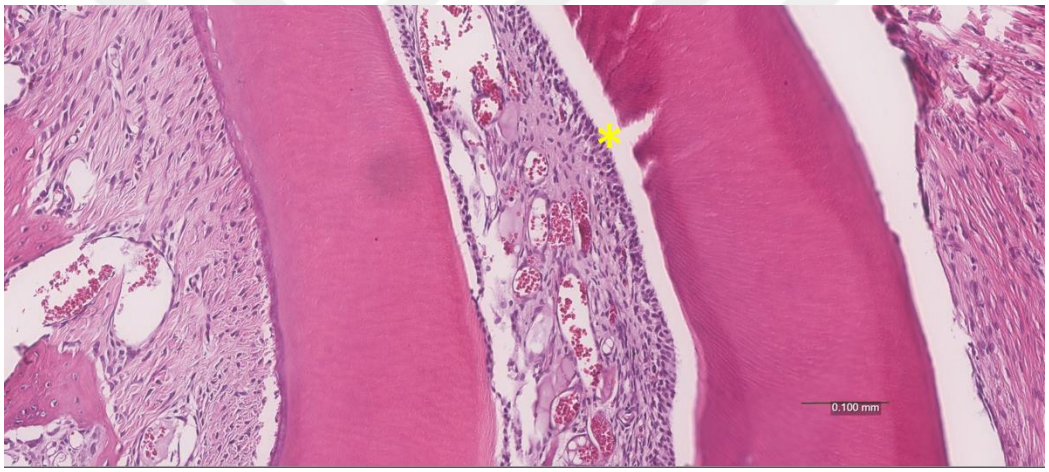

Figure 4.8. Spongostan epithelialization areas on day 56 (star)

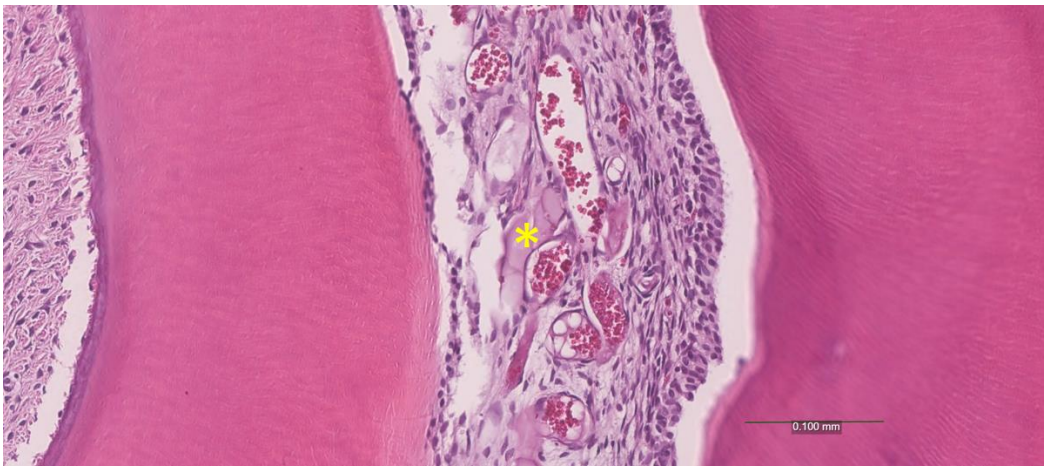

Figure 4.9. Areas of bone formation on day 56 of Sponges (star)

- **Local hesperidin group 56. day:**

In one of the sections stained with hematoxylin and eosin, a fibrous connective tissue area of 1-20% of the socket area was observed, while in one section, a fibrous connective tissue area greater than 40% of the socket area was observed, and in the remaining sections, a fibrous connective tissue area of 21-40% of the socket area was observed (Figure 4.10). In one of the sections, moderate local inflammation was observed, in one section no inflammation was observed and in the remaining sections mild focal inflammation was observed (Figure 4.11). In the sections, epithelialization areas were observed at the ends of the surface area, on 1/3 of the surface. In one of the sections, new bone formation was observed up to 21-40% of the socket area, while in two of them, bone formation was observed up to 1-20% of the socket area, and in two sections, no new bone formation was observed (Figure 4.12).

Figure 4.10. Local hesperidin 56th day fibrous connective tissue areas (star)

Figure 4.11. Local hesperidin mild inflammation areas on day 56

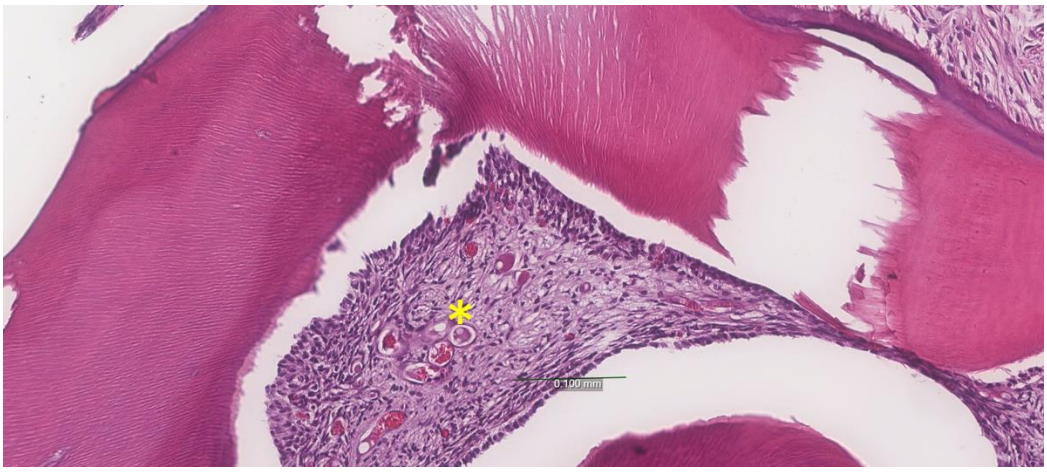

Figure 4.12. Local hesperidin 56th day bone formation areas

- **Local hesperidin and gavage group 56. day:**

In one of the sections stained with hematoxylin and eosin, fibrous connective tissue was observed in an area greater than 40% of the tooth socket area, while in the other sections, fibrous connective tissue areas were observed in an area of 21-40% of the tooth socket area (Figure 4.13). While no inflammation area was observed in half of the sections, inflammation was observed in mild-focal areas in half of them. In one section, epithelialization areas were observed on 1/3 of the surface at the ends of the surface area, while epithelialization was observed on 2/3 of the surface in the remaining sections. In half of the sections, new bone formation was observed in the area of 1-20% of the socket area, while in the other half, new bone formation was observed in the area of 21-40% of the socket area (Figure 4.14).

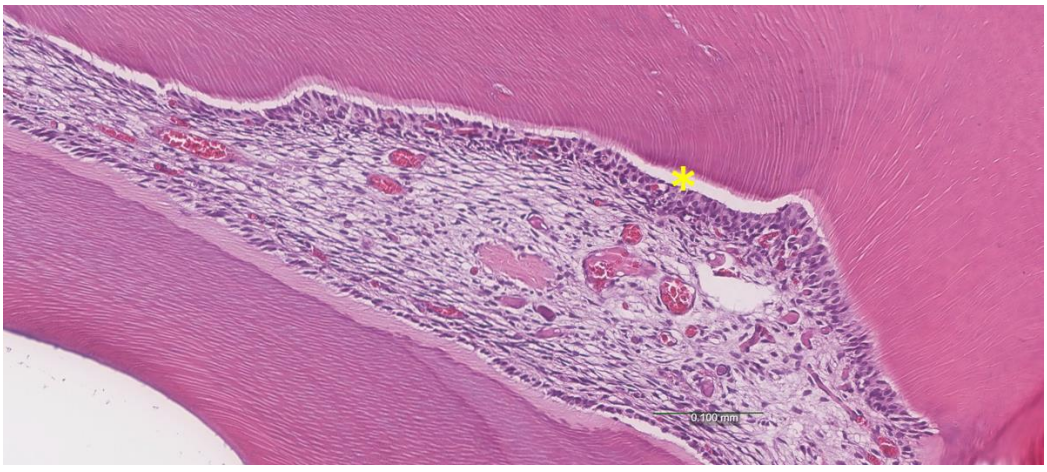

Figure 4.13. Local hesperidin gavage 56th day epithelialization area (star)

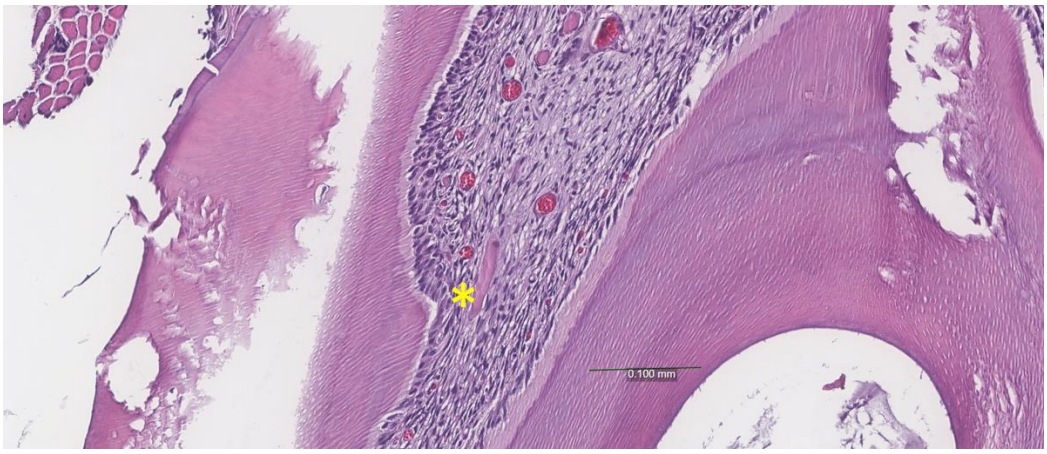

Figure 4.14. Areas of new bone formation (star) on day 56 of local hesperidin gavage

- **Control 56. day:**

In one of the sections stained with hematoxylin and eosin and trichrome, fibrous connective tissue was observed in an area greater than 40% of the tooth socket area, while in one of the sections, fibrous connective tissue area was observed in 1-20% of the socket area (Figure 4.15, 4.16). One section was necrosed (Figure 4.17) and in the remaining three sections, fibrous connective tissue areas were observed in an area of 21-40% of the tooth socket area. While no inflammation was observed in one of the sections, one section was necrosed and in the other sections, inflammation was observed in mild-focal areas. In two sections, epithelialization was observed on 2/3 of the surface, while one section was necrosed and in the other sections, epithelialization areas were observed on 1/3 of the surface at the ends of the surface area. While new bone formation was observed in the area of 1-20% of the socket area in two sections, one section was necrotic and in the remaining sections, new bone formation was observed in the area of 21-40% of the socket area (Figure 4.18).

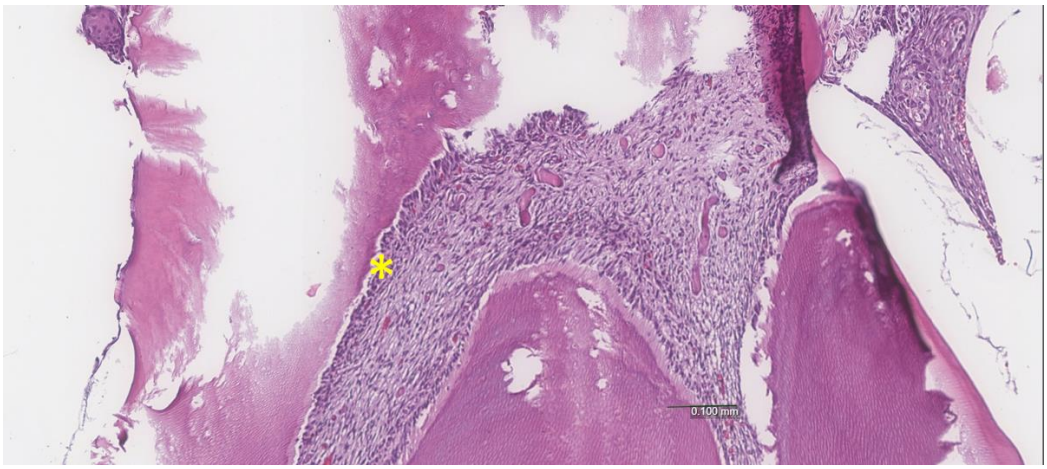

Figure 4.15. Control 56th day epithelialization area (star)

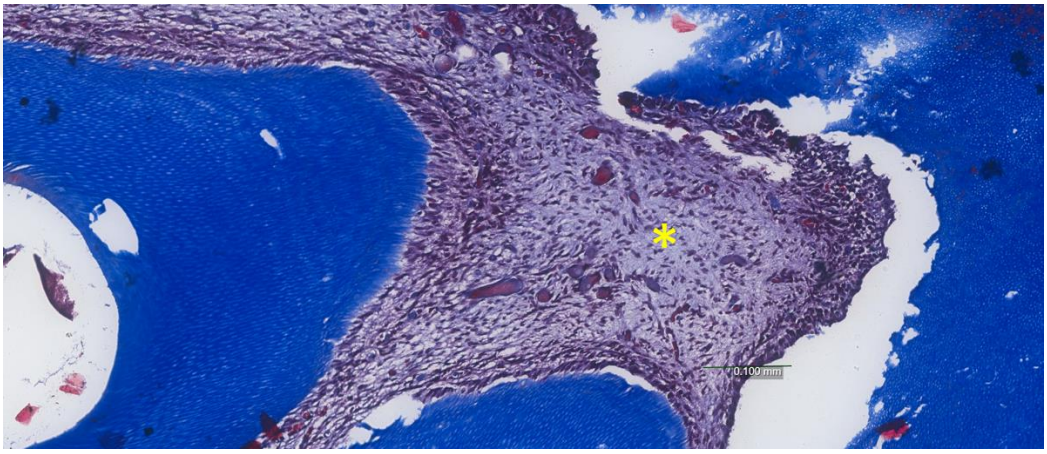

Figure 4.16. Control 56th day fibrous connective tissue areas-MTC (star)

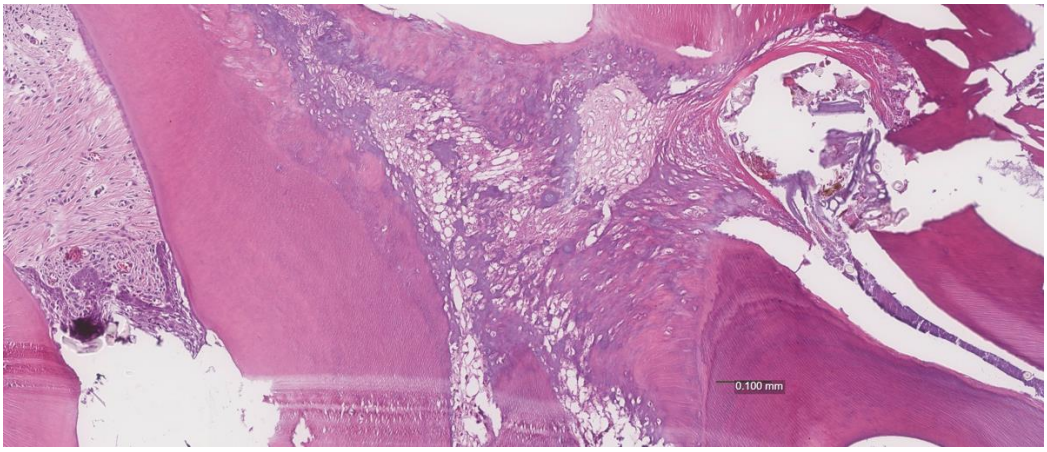

Figure 4.17. Control 56th day necrosis areas

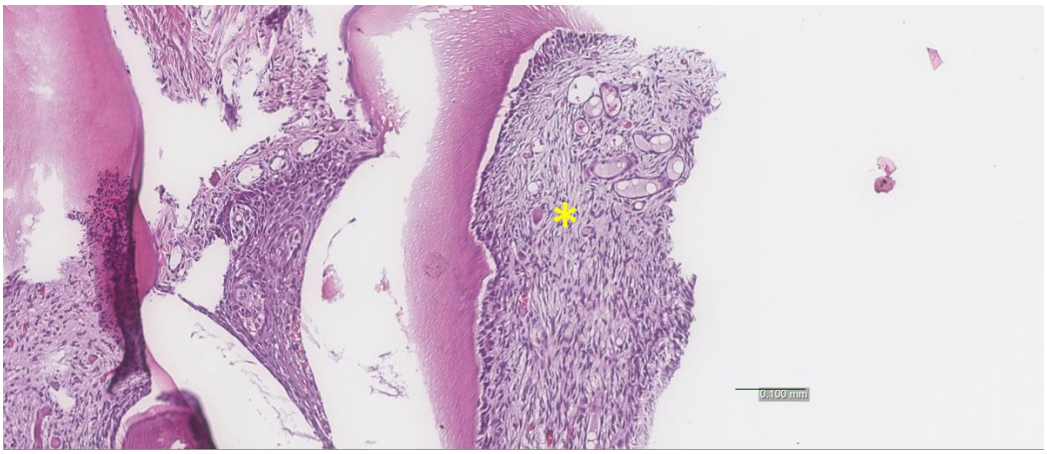

Figure 4.18. Control, 56th day, new bone formation areas (star)

4.1.3. Statistical evaluation of histological findings

The evaluation of each group, both internally and in comparison with other groups, regarding inflammation, epithelialization, connective tissue, and new bone formation yielded the results presented in Table 4.3.

Table 4.3. İnflammation

İnflammation		**Control Group**	**Spongostan Group**	**Local HESP Group**	**Local H Gavaj Group**	**p***
28.Day	**Ave±SS**	1,83±0,41	1,5±0,55	1,17±0,41	1,5±0,55	0,164
	Median (IQR)	2 (1,75-2)	1,5 (1-2)	1 (1-1,25)	1,5 (1-2)	
56.Day	**Ave±SS**	0,8±0,45	0,83±0,41	1±0,63	0,50±0,55	0,424
	Median (IQR)	1 (05-1)	1 (0,75-1)	1 (0,75-1,25)	0,5 (0-1)	
	p	**0,009**	**0,043**	**0,598**	**0,019**	

*Kruskal Wallis Test †Mann Whitney U test

On day 56, the control group exhibited a statistically significant reduction in mean inflammation scores compared to those recorded on day 28, with a p-value of 0.009, indicating a notable decrease in inflammatory response over time.

The 56th Day Inflammation score averages of the Spongestan group were found to be statistically significantly lower than the 28th Day Inflammation score averages (p=0.043).

No statistically significant difference was observed between the mean inflammation scores of the local HESP group on Day 28 and Day 56 (p=0.598).

The mean inflammation scores of the Local H Gavage group on the 56th day were found to be statistically significantly lower than the mean inflammation scores on the 28th day (p=0.019).

No statistically significant difference was observed between the 28th Day Inflammation score averages of the Control, Spongostan, Local HESP Group and Local H Gavage Groups (p=0.164).

No statistically significant difference was observed between the 56th Day Inflammation score averages of the Control, Spongostan, Local HESAP Group and Local H Gavage Groups (p=0.424).

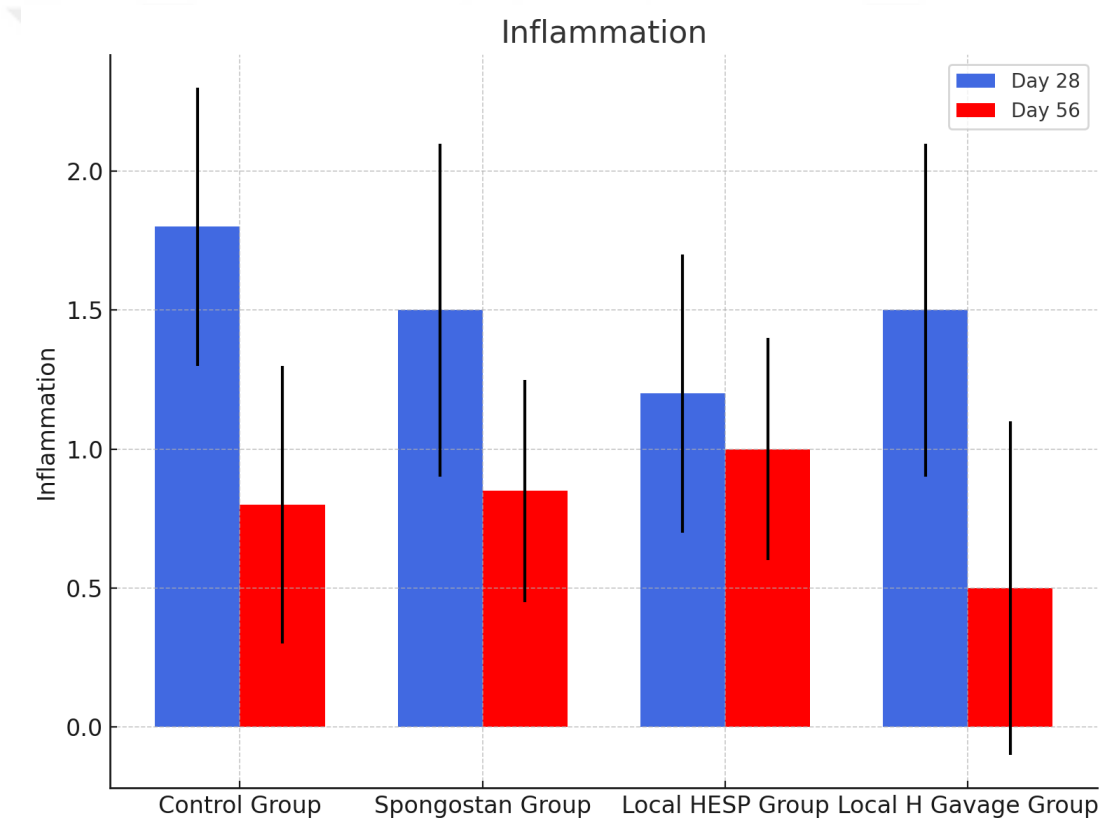

Graph 4.1. İnflammation

Table 4.4. Epitelization

Epitelization		Control Group	Spongostan Group	Local HESP Group	Local H Gavage Group	p*
28.Day	**Ave±SS**	0,33±0,52	0,83±0,41	0,67±0,52	0,5±0,55	0,350
	Median (IQR)	0 (0-1)	1 (0,75-1)	1 (0-1)	0,5 (0-1)	
56.Day	**Ave±SS**	1,4±0,55	1,67±0,52	1±0	1,83±0,41	0,028
	Median (IQR)	1 (1-2)	2 (1-2)	1 (1-1)	2 (1,75-2)	
	p	**0,016**	**0,019**	0,138	**0,005**	

*Kruskal Wallis Test †Mann Whitney U test

Table 4.5. Dunn's multiple comparison test

Dunn's multiple comparison test	56.Day
Control Group / Spongostan Group	0,537
Control Group / Local HESP Group	0,102
Control Group / Local H Gavage Group	0,156
Spongostan Group / Local HESP Group	**0,019**
Spongeotan Group / Local H Gavage Group	0,523
Local HESP Group / Local H Gavage Group	**0,005**

The 56th Day Epithelialization score average of the control group was found to be statistically significantly higher than the 28th Day Epithelialization score average (p=0.016).

The 56th Day Epithelialization score average of the Spongestan group was found to be statistically significantly higher than the 28th Day Epithelialization score average (p=0.019).

No statistically significant difference was observed between the mean epithelialization scores of the local HESP group on Day 28 and Day 56 (p=0.138).

The 56th Day Epithelialization score average of the Local H Gavage group was found to be statistically significantly higher than the 28th Day Epithelialization score average (p=0.005).

No statistically significant difference was observed between the 28th Day Epithelialization score averages of the Control, Spongostan, Local HESAP Group and Local H Gavage Groups (p=0.350).

A statistically significant difference was observed between the 56th Day Epithelialization score averages of the Control, Spongostan, Local HESAP Group and Local H Gavage Groups (p=0.028).

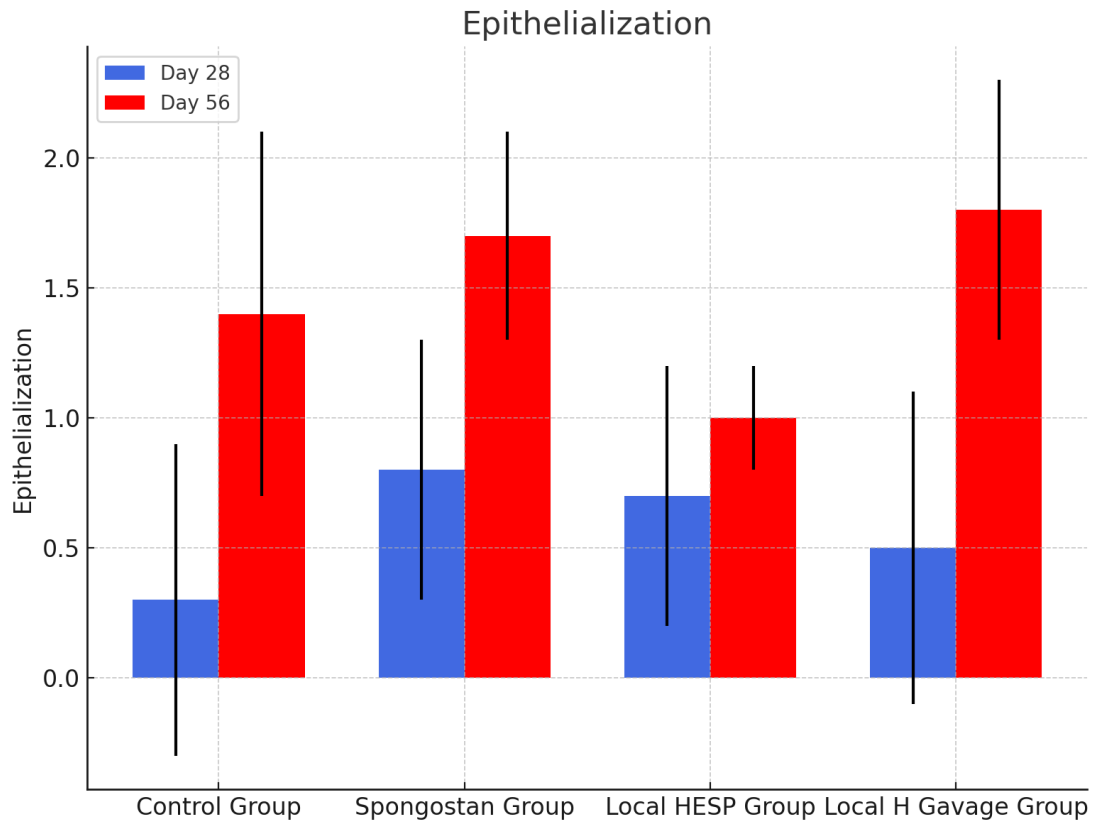

Graph 4.2. Epitelization

Table 4.6. Connective tissue

Connective Tissue		**Control Group**	**Spongostan Group**	**Local HESP Group**	**Local H Gavage Group**	**p***
28.Day	**Ave±SS**	1,67±0,52	2±0	2,17±0,75	2,33±0,52	0,185
	Median (IQR)	2 (1-2)	2 (2-2)	2 (1,75-3)	2 (2-3)	
56.Day	**Ave±SS**	2±0,71	2,33±0,52	2±0,63	2,17±0,41	0,714
	Median (IQR)	2 (1,5-2,5)	2 (2-3)	2 (1,75-2,25)	2 (2-2,25)	
	p	**0,009**	**0,043**	**0,598**	**0,019**	

*Kruskal Wallis Test †Mann Whitney U test

No statistically significant difference was observed between the 28th day and 56th day Connective Tissue score averages of the control group (p=0.392).

No statistically significant difference was observed between the 28th day and 56th day Connective Tissue score averages of the Spongestan group (p=0.138).

No statistically significant difference was observed between the 28th day and 56th day Connective Tissue score averages of the local HESP group (p=0.652).

No statistically significant difference was observed between the 28th day and 56th day Connective Tissue score averages of the Local H Gavage group (p=0.523).

No statistically significant difference was observed between the 28th Day Connective Tissue score averages of the Control, Spongostan, Local HESP Group and Local H+Gavage Groups (p=0.185).

No statistically significant difference was observed between the 56th Day Connective Tissue score averages of the Control, Spongostan, Local HESP Group and Local H+Gavage Groups (p=0.714).

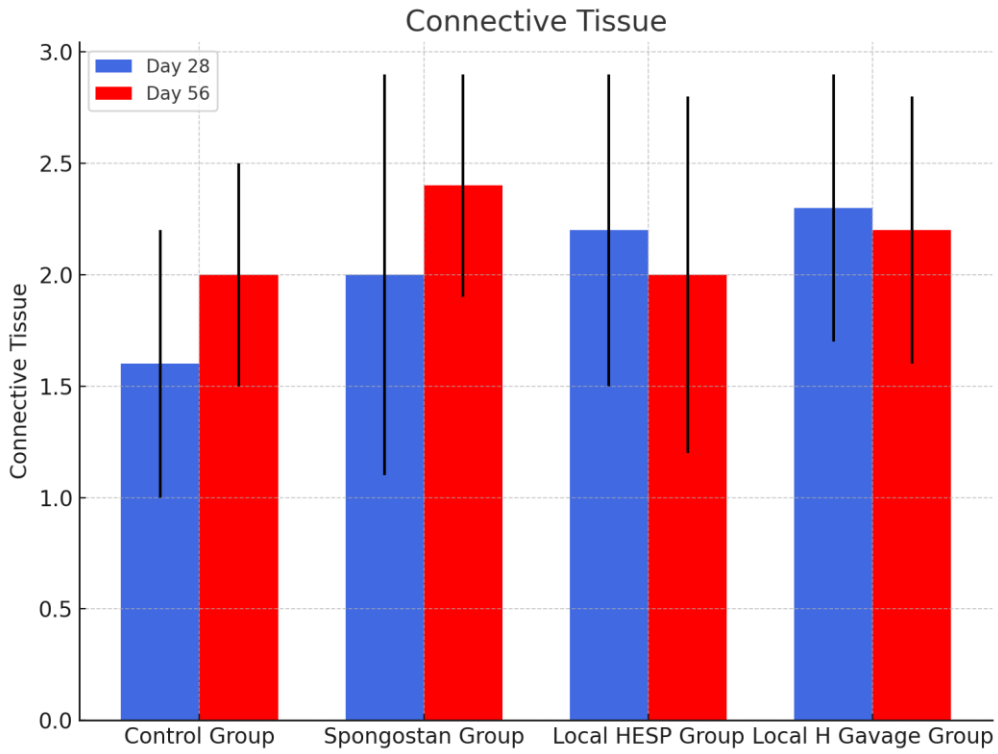

Graph 4.3. Connective tissue

Table 4.7. New bone formation

New bone formation		Control Group	Spongostan Group	Local HESP Group	Local H Gavage Group	p*
28.Day	**Ave±SS**	0±0	0,67±0,52	0,33±0,52	0,17±0,41	0,08
	Median (IQR)	1 (0-0)	1 (0-1)	0 (0-1)	0 (0-0,25)	
56.Day	**Ave±SS**	1,6±0,55	1,33±0,82	0,83±0,75	1,5±0,55	0,297
	Median (IQR)	2 (1-2)	1,5 (0,75-2)	1 (0-1,25)	1,5 (1-2)	
	p	**0,002**	**0,118**	**0,212**	**0,005**	

*Kruskal Wallis Test †Mann Whitney U test

The 56th Day New Bone Formation mean score of the control group was found to be statistically significantly higher than the 28th Day New Bone Formation mean score (p=0.002).

No statistically significant difference was observed between the 28th Day and 56th Day New Bone Formation score averages of the Spongestan group (p=0.118).

No statistically significant difference was observed between the mean New Bone Formation scores of the local HESP group on Day 28 and Day 56 (p = 0.212).

The 56th Day New Bone Formation mean score of the Local H Gavage group was found to be statistically significantly higher than the 28th Day New Bone Formation mean score (p=0.005).

No statistically significant difference was observed between the 28th Day New Bone Formation score averages of the Control, Spongostan, Local HESAP Group and Local H Gavage Groups (p=0.08).

No statistically significant difference was observed between the 56th Day New Bone Formation score averages of the Control, Spongostan, Local HESAP Group and Local H Gavage Groups (p=0.297).

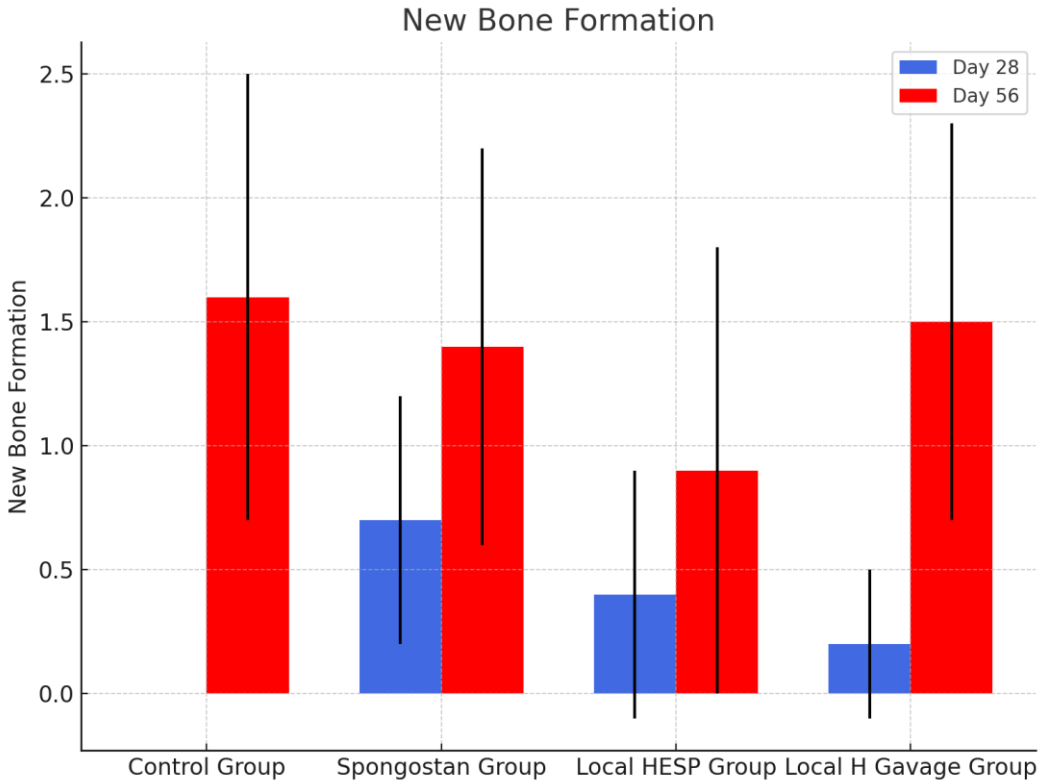

Graph 4.4. New bone formation

5. DISCUSSION

The process of wound healing following tooth extraction has been extensively studied over the years, with a wide range of investigations examining the effects of different pharmacological agents, systemic conditions, and healing durations. In the present study, our primary focus was on post-extraction bone and soft tissue healing. Specifically, we aimed to evaluate both normal and prolonged bone regeneration, along with the assessment of connective tissue development, epithelialization, and the degree of inflammation during the healing process.

Korany et al. conducted a study to evaluate socket healing in rats exposed to gamma radiation following diode laser application. Their findings indicated that low-level laser therapy (LLLT) using a GaAlAs diode laser device effectively promoted bone regeneration and mineral deposition in extraction sockets previously subjected to ionizing radiation. The study involved thirty male Swiss albino rats, which were sacrificed at various time points to allow for histological assessment of the healing process (124).

Toshiki Yoneda et conducted a study examining the use of coenzyme Q10 (rCoQ10) to accelerate soft tissue healing following tooth extraction in a rat model. Their results demonstrated that the topical administration of rCoQ10 effectively enhanced soft tissue regeneration in the coronal region of the alveolar socket. However, the influence of rCoQ10 on the underlying bone remodeling process was found to be minimal in the experimental rats (125).

This study examined the effects of systemic and local applications of hesperidin on healing following tooth extraction, utilizing spongestan for local application.

Todorović et al. investigated the impact of nanoliposome-encapsulated coenzyme Q10 (CoQ10) on the wound healing process following tooth extraction. Their findings provided clear evidence that the encapsulation of CoQ10 within nanoliposomes significantly enhances its biological efficacy, leading to a marked acceleration in post-extraction wound healing (126).

This study by Todorovic et al aimed to investigate the effects of hesperidin at appropriate dosages by making comparisons with coenzyme Q10 as summarized in the

relevant literature. Bioflavonoids have gained interest as materials to be studied after tooth extraction (126). We aimed to use hesperidin, a bioflavonoid that has been previously investigated for its effects on healing both in vivo and in vitro.

Hesperidin is a plant flavanone, a subclass of flavonoids, primarily and abundantly present in citrus fruits (65). In nature, the majority of flavonoids are conjugated with a sugar moiety and are referred to as glycosides. Hesperidin is a glycoside consisting of the flavanone hesperetin (aglycone) and the disaccharide rutinose (a combination of rhamnose and glucose) (75).

The name "hesperidin" originates from the term "hesperidium," which refers to the type of fruit borne by citrus species such as lemons, limes, oranges, and tangerines—recognized as the primary natural sources of this flavonoid. Among these, the highest concentrations of hesperidin are found in the outer peel. Notably, tangerine peels are particularly rich in hesperidin, comprising approximately 5–10% of their dry weight (127).

Hesperidin, a naturally occurring flavonoid, has undergone pharmacological evaluation for its potential as an anti-cancer and anti-inflammatory drug due to its antioxidant properties (128).

Recent research has extensively examined the effects of hesperidin on bone healing, indicating potential positive outcomes, particularly over the past two decades.

In their research, Habazuit et al investigated the effects of hesperidin and narengenin on bones (66).

The study demonstrated that consistent daily administration of hesperidin over a three-month period led to significant enhancements in femoral bone quality. This was evidenced by notable increases in both total and site-specific bone mineral density (BMD), ranging from 9.7% to 12.3% ($p<0.05$), as well as a 24.3% improvement in trabecular bone volume fraction at the femoral site when compared to the control group. Additionally, when analyzing its anti-inflammatory potential—used here as a comparative benchmark—it was observed that both hesperidin and naringenin markedly reduced the expression levels of key inflammatory mediators. Specifically, interleukin-6

(IL-6) levels were diminished by 81.0–87.9%, while nitric oxide (NO) production decreased by 34.7–39.5% relative to control values (40).

The objective of this study is to evaluate the impact of inflammation on bone tissue over both short-term and long-term periods. Unlike prior research, this investigation specifically concentrated on the physiological bone remodeling cycle and aimed to identify any alterations that may occur over extended durations.

Consistent with the aforementioned results, previous research conducted by Chiba et al. revealed that administration of 0.5% hesperidin for a duration of two months in ovariectomized mice at 2 months of age resulted in attenuation of trabecular bone loss and preservation of trabecular thickness within the femoral metaphysis. Additionally, the number of osteoclasts was notably diminished in comparison to the control animals that underwent sham surgical procedures (76).

Hesperidin required dissolution in the intestines for effective absorption; therefore 100mg/kg hesperidin which dissolved at 0.5% solution of hesperidin was prepared and vortexed prior to each gavage. Hesperidin exhibits moderate solubility in water; however, our findings indicate that dissolving it in carboxy methyl cellulose (CMC) enhances its effectiveness, leading to the application of hesperidin in this manner.

Due to the inherently low aqueous solubility of hesperidin and the presence of its rutinose glycoside structure, its absorption following oral ingestion necessitates prior transit into the colonic environment. Within the colon, hesperidin undergoes enzymatic biotransformation mediated by resident intestinal microbiota, which catalyze the hydrolytic cleavage of the glycosidic linkage, liberating hesperetin, the corresponding aglycone form. Following its microbial cleavage, hesperetin becomes available for intestinal absorption into the systemic bloodstream or may alternatively undergo further metabolic transformation (129).

Before reaching the systemic circulation, hesperetin—once absorbed in the intestinal or colonic epithelium—undergoes further metabolic processing within these gastrointestinal tissues as well as in the liver. These transformations are essential steps in its bioconversion and systemic bioavailability (127,129). For this reason, we chose to administer via gavage. Additionally, while dividing into groups, we wanted to investigate whether local application was effective in addition to systemic application, and one of the

groups we created was local application, and the other was administering hesperidin via gavage at the required daily dose in addition to local application. We have found that previous studies have found that spongostan and similar bone scaffold materials have effects on bone healing (130).

Vordemvenne et al. reported that Spongostan possesses a well-defined nanotopographical structure, characterized by pore sizes measuring approximately 32.97 ± 1.41 nm, which facilitates the osteogenic differentiation of stem cells. The study concluded that these specific micropores permit the infiltration of endogenous stem cells into the Spongostan matrix in vivo, where the nanotopographical features serve as biological cues that promote their differentiation along the osteogenic lineage (130).

Furthermore, the authors noted in their study that this property facilitates the migration of endogenous stem cells and promotes their osteogenic differentiation within the Spongostan matrix. These findings indicate that Spongostan does not exert a detrimental effect on bone regeneration; rather, it appears to contribute positively to the overall healing process (130). In this study, all parameters were parallel between the control group and the spongostan group and no statistically significant difference was observed.

In a clinical study conducted by Jia and colleagues, entitled "Safety and Effectiveness of a Drug-Loaded Haemostatic Sponge in Chronic Rhinosinusitis," the authors assessed the therapeutic performance of a drug-loaded haemostatic sponge (DLHS). In total, 49 patients were enrolled and randomly allocated into two separate intervention groups. Participants assigned to Group A (n = 25) received placement of a DLHS composed of 1 mg budesonide combined with 0.67 mg sodium hyaluronate directly within the sinus cavity. Conversely, patients assigned to Group B (n = 24) underwent treatment with a Nasopore device following endoscopic sinus surgery (ESS).The postoperative healing process was monitored through endoscopic examinations conducted over a 12-week period, during which outcomes were assessed using the discharge, inflammation, and polyps/edema (DIP) endoscopic scoring system. All participants completed standardized assessments to evaluate sinonasal symptoms, utilizing the Chinese version of the Sino-Nasal Outcome Test-22 (SNOT-22) and the Visual Analogue Scale (VAS). In Group A, serum cortisol levels were monitored at baseline (preoperatively) and subsequently on postoperative days 1, 3, 7, and 14 (131).

Upon comparative assessment of Groups A and B at the two-week postoperative evaluation, researchers observed no statistically meaningful differences regarding either objective clinical assessments or subjective symptom evaluations. Nevertheless, at subsequent follow-up intervals of 6 and 12 weeks, Group A exhibited notably reduced mean visual analogue scale (VAS) scores specific to rhinorrhea, lower discharge-inflammation-polyps/edema (DIP) scores indicative of diminished edema, and a decreased frequency of nasal adhesion formation compared with Group B. Conversely, between-group comparisons at the same intervals (6 and 12 weeks) revealed no statistically significant differences in Sino-Nasal Outcome Test-22 (SNOT-22) scores or in dysosmia-related VAS ratings. Additionally, throughout the entire observation duration, the average serum cortisol levels recorded in Group A remained consistently within normal physiological limits without any significant variations observed. These observations substantiate the therapeutic efficacy and favorable safety profile of the novel biodegradable drug-loaded haemostatic sponge (DLHS), highlighting its potential appropriateness for therapeutic application in individuals diagnosed with chronic rhinosinusitis (CRS). The findings further suggest that the DLHS exerts beneficial effects by locally delivering therapeutic agents, thereby diminishing inflammation and mitigating nasal adhesion development, without eliciting measurable systemic exposure to corticosteroids (131).

In our research, we normally use spongostan for endogenous healing in bone regeneration. In order to keep the hesperidin of this scaffold structure for a while and to spread it over time if hesperidin has a local effect, we applied it to the tooth extraction sockets impregnated with spongestan. For local application, we applied vortexed hesperidin impregnated with spongostan. In order to neutralize the effect of spongostan alone on bone healing, we created a separate experimental group and applied only spongostan to a separate group after tooth extraction.

Apaydın Yıldırım and colleagues conducted an experimental study to assess the effects of Coenzyme Q10 (CoQ10) and Hesperidin (HESP) on total antioxidant status (TAS) and total oxidant status (TOS) in a rat model of lower extremity ischemia-reperfusion (IR) injury. The study utilized 28 male Sprague-Dawley rats, each weighing between 200–250 grams, which were randomly assigned to four groups: Control (C), Ischemia-Reperfusion (IR), IR+CoQ10, and IR+HESP. Prior to the induction of

ischemia, the IR+CoQ10 group received 0.5 mL of CoQ10 at a dose of 10 mg/kg via gastric gavage, administered three times at 8-hour intervals. Similarly, the IR+HESP group was administered 0.5 mL of Hesperidin at a dose of 100 mg/kg, also delivered by gavage at the same frequency and intervals. With the exception of the control group, all animals underwent ischemia induced by applying a tourniquet to the left lower limb under anesthesia, maintained for 2 hours, followed by 2 hours of reperfusion. At the end of the experimental period, blood samples were collected under anesthesia to evaluate TAS and TOS levels. The IR group demonstrated a significant increase in TOS levels compared to all other groups. However, treatment with either CoQ10 or Hesperidin markedly reduced TOS values relative to the IR group. Additionally, administration of these antioxidants during the ischemic process led to a statistically significant elevation in TAS levels compared to the untreated IR group. The findings suggest that both CoQ10 and Hesperidin confer protective effects against oxidative stress by lowering oxidant levels and enhancing antioxidant capacity in this ischemia-reperfusion injury model (132).

Inspired by this and similar articles, we administered 0.5 mL of 0.25% CMC to rats via gastric gavage and continued this once a day until they were sacrificed.

The impact of hesperidin on healing has been examined in multiple domains. The neuroprotective effect of hesperidin (HSP) at varying doses against oxidative damage in experimental spinal cord injury in rats was assessed histopathologically and biochemically. It was concluded that high-dose HSP may confer a neuroprotective effect, positively influencing the reduction of neuron loss and mild degeneration in spinal cord injury (133).

Furthermore, the impact of combined diosmin and hesperidin therapy on serum lipid profiles and the oxidative-antioxidative balance was evaluated in rats fed a high-cholesterol diet, alongside the investigation of hesperidin's individual oxidative effects. In this model, administration of the diosmin-hesperidin combination resulted in a significant increase in high-density lipoprotein (HDL) cholesterol levels, while other lipid parameters remained largely unaffected. The treatment also produced favorable modifications in the oxidative-antioxidative system, as evidenced by a marked elevation in the enzymatic activities of glutathione peroxidase (GPX) and superoxide dismutase (SOD), indicating enhanced antioxidant defense mechanisms (134).

Furthermore, Bolat and colleagues investigated the protective role of hesperidin against toxic effects induced by bisphenol A (BPA). In their study, the authors analyzed hesperidin's influence on BPA-mediated neurotoxicity, various biochemical markers, and histopathological changes occurring within cerebral tissues. Their findings demonstrated that hesperidin administration effectively attenuated oxidative stress, metabolic disturbances, and inflammatory responses elicited by BPA exposure. The protective efficacy of hesperidin was further evidenced by its capacity to significantly lower lipid peroxidation levels and elevate the activity of intrinsic antioxidant enzymes, thereby reducing BPA-induced tissue injury (135).

Bolat et al. designed an experimental study comprising four groups, each containing 13 rats. The active substances were administered via intragastric gavage over a 14-day period. In the co-treatment group, bisphenol A (BPA) was administered one hour after hesperidin (HESP). The experimental groups were organized as follows: the Control group received 1 mL of olive oil daily for 14 days; the HESP group was administered hesperidin at a dose of 50 mg/kg for the same duration; the BPA group received BPA dissolved in olive oil at a dosage of 100 mg/kg for 14 days; and the BPA+HESP group was treated with 100 mg/kg of BPA and 50 mg/kg of HESP intragastrically for 14 days, with BPA given one hour following HESP. Based on histopathological assessments, the study demonstrated that hesperidin exerted a neuroprotective effect by reducing BPA-induced damage in brain tissue (135).

Studies examining the effects of hesperidin on bone healing have been conducted on rats, revealing its antiresorptive and anti-inflammatory properties. The osteoblastic effects have been investigated, suggesting an influence on cells involved in bone formation. The research findings do not yield a definitive conclusion; however, the prevalence of articles reporting negative results is minimal.

A significant study conducted by Kim et al. demonstrated that dietary administration of hesperetin to both 6-month-old and 24-month-old rats resulted in modulation of nuclear factor kappa B (NF-κB) activity within renal tissue. This observation is particularly noteworthy, as NF-κB plays a central role not only in inflammatory signaling but also in the regulation of osteoclast proliferation and differentiation. These findings suggest a potential antiresorptive effect of hesperetin, likely mediated through its influence on NF-κB signaling pathways (112).

Horcajada-Molteni et al. demonstrated that rutin, the principal flavonol found in onions, effectively attenuated trabecular bone deterioration caused by ovariectomy (OVX) in rats through mechanisms involving a decrease in bone resorptive activity and an enhancement of osteoblast function. In their experiment, young (3-month-old) and mature (6-month-old) female Wistar rats were assigned to groups receiving either a standard casein-based diet alone or one supplemented with 0.5% hesperidin (Hp), with each group comprising ten animals. This dietary regimen was maintained consistently for a duration of 90 days. The investigators observed a partial prevention of OVX-induced bone degradation in older rats administered Hp, while younger rats receiving Hp exhibited complete inhibition of such bone loss. Notably, hesperidin administration did not alter plasma osteocalcin levels at either age; however, it significantly reduced the urinary excretion of deoxypyridinoline, indicative of decreased bone resorptive activity. Intriguingly, intact younger rats fed with Hp showed a marked elevation in bone mineral density (BMD). Indeed, the BMD measurements in 6-month-old Hp-supplemented sham-operated rats reached levels comparable to untreated sham-operated adult rats at 9 months of age, suggesting an accelerated rate of bone accrual in younger animals. Conversely, adult intact rats given hesperidin exhibited no additional improvement in BMD, yet demonstrated enhanced bone strength parameters. Collectively, the researchers concluded that hesperidin supplementation conferred protective effects against ovariectomy-induced bone loss in both age groups without inducing uterine stimulation, accompanied by beneficial lipid profile modulation. Moreover, the researchers underscored that their unanticipated findings—specifically, the marked enhancement of bone mineral density (BMD) observed in younger rats with intact physiology and the significantly improved femoral mechanical strength noted in adult rats—necessitate additional extensive investigation to elucidate the underlying mechanisms and clinical implications fully (136).

Miguez et al. presented initial findings establishing a correlation between the osteogenic effects of hesperidin demonstrated in vitro and its bone regeneration capabilities confirmed through corresponding in vivo experimental analyses. Their findings particularly highlighted the measurable influence of hesperidin on enhancing collagen matrix organization and mineralization quality. Furthermore, they underscored hesperidin's role in regulating bone regeneration processes mediated by bone morphogenetic proteins (BMPs) (67).

Xue and colleagues conducted an investigation focusing on the role of hesperetin in modulating mesenchymal stem cell (MSC) proliferation as well as their differentiation towards the osteogenic lineage, including associated cellular mechanisms under controlled in vitro conditions. Furthermore, their complementary in vivo experiments demonstrated that gelatin sponge scaffolds incorporating hesperetin significantly promoted and supported the healing process of bone fractures (137).

Furthermore, it was said that the inexpensive cost of hesperetin may facilitate its utilization as an osteogenic factor for clinical applications (137).

Chiba and colleagues reported that treatment with hesperidin (Hes), α-glucosyl hesperidin (aG-Hes), or statin markedly alleviated bone loss induced by orchiectomy (ORX) in a mouse model. These interventions notably improved essential histomorphometric indices, specifically augmenting bone volume fraction (BV/TV) and trabecular number (Tb.N), as well as significantly reducing the number of osteoclasts per bone surface (N.Oc/BS). Based on these observations, the authors proposed that hesperidin might offer superior protective effects against osteoporosis linked to age-related hypogonadism in males when contrasted with osteoporosis occurring post-menopause in females (75).

Chiba and colleagues investigated hesperidin's efficacy in protecting against bone loss using an ovariectomized (OVX) mouse model, widely accepted for the study of postmenopausal osteoporosis. The experiment involved forty female ddY mice aged 8 weeks, randomly allocated into five groups: (1) a sham-operated control group fed with a standard diet (AIN-93G); (2) an OVX group receiving the same standard diet; (3) an OVX+HesA group provided with a diet containing 0.5 g/100 g hesperidin; (4) an OVX+HesB group supplied with a diet including 0.7 g/100 g α-glucosyl hesperidin; and (5) an OVX+17β-estradiol (E2) group, receiving the control diet accompanied by a daily infusion of 0.03 μg E2 administered via a mini-osmotic pump. At the conclusion of the 4-week study period, all animals were euthanized, and immediate collection of blood samples, femoral bones, uterine tissues, and hepatic tissues was conducted for subsequent analysis (75).

Administration of hesperidin did not produce significant changes in uterine weight measurements. In mice subjected to ovariectomy (OVX), there was a statistically

significant reduction in femoral bone mineral density (BMD) relative to the control group undergoing sham surgical procedures ($P < 0.05$).However, this bone density decrease was effectively counteracted by dietary supplementation with hesperidin or α-glucosylhesperidin. Additionally, hesperidin-supplemented and 17β-estradiol (E2)-treated groups exhibited significantly elevated femoral concentrations of calcium (Ca), phosphorus (P), and zinc (Zn) relative to OVX mice on the control diet. Quantitative histomorphometric analysis demonstrated notable reductions in trabecular bone volume as well as trabecular thickness within the distal metaphyseal region of the femur following ovariectomy, with these differences achieving statistical significance ($P < 0.05$). Nevertheless, administration of α-glucosylhesperidin effectively counteracted this ovariectomy-induced bone loss. Additionally, hesperidin treatment resulted in a substantial reduction of osteoclast population in the femoral metaphysis of ovariectomized mice, a finding closely paralleling the established effects observed with 17β-estradiol (E2).Significant reductions in serum and hepatic lipid concentrations were observed in groups receiving dietary hesperidin compared to OVX mice fed the standard control diet ($P < 0.05$). Collectively, these findings underscore the potential efficacy of citrus flavonoids, particularly hesperidin, in mitigating lifestyle-associated disorders by exerting beneficial effects on skeletal health and lipid metabolism (76).

Moreover, Chiba et al. reported that dietary supplementation with hesperidin effectively decreased cholesterol concentrations in both serum and hepatic tissues, in addition to attenuating osteoporotic changes by reducing osteoclast populations in ovariectomized (OVX) mice. They proposed that subsequent research should investigate the influence of flavonoid compounds, particularly hesperidin, on bone metabolism in women with osteoporosis, thereby providing essential insights into the therapeutic efficacy of hesperidin in human populations (75).

Kuzu et al. established that co-treatment with hesperidin exhibited protective effects on both tissues, contingent upon the dosage, by diminishing oxidative stress and apoptosis, enhancing antioxidant enzyme activities, and mitigating inflammation. They conclude that, with these characteristics, hesperidin may be regarded as a therapeutic alternative for mitigating sodium arsenite toxicity in cardiac and cerebral tissues (138).

Trzeciakiewicz and colleagues demonstrated that hesperetin glucuronide has the capacity to influence osteoblast differentiation at concentrations corresponding to nutritional and physiological conditions. Additionally, their findings suggest that hesperetin-7-glucoside (Hp7G) may mediate its effects on osteoblast activity predominantly via activation of the transcription factors Runx2 and Osterix, although the precise molecular pathways underlying these interactions remain incompletely characterized (65).

If we look at the limitations of this research, we can say that the fact that there was no group in which we applied only gavage in the group separation caused us to not be able to clearly reveal the difference with local application. Despite the possible negative effects of local application, no statistically significant difference was found in the recovery parameters in local + gavage application. Perhaps if only one gavage group was examined, statistically significant positive results could have been observed due to the absorption of hesperidin from the intestine. In addition, the fact that the catalyst is unknown and carboxymethylcellulose is used as a solvent when applying hesperidin locally may be a factor that creates a difference in the effect of hesperidin.

The objective of the present investigation is to evaluate the influence of hesperidin administration on the process of alveolar bone regeneration subsequent to dental extraction using a rat experimental model.

6. CONCLUSION

In this study, we used 56 animals and divided them into 4 groups and 2 different times. After tooth extraction, we divided them into groups and scored them as inflammation, epithelialization, connective tissue formation, and new bone formation. After 56 Sprague Dawley rat teeth were extracted, they were sacrificed at the end of the specified time periods, their jaw sections were separated, placed in tissue fixative (10% formalin) and delivered for histochemical analysis. Haematoxylin-eosin and Masson trichrome bp patch methods were used to observe bone healing, epithelialization and connective tissue formation. According to the results of the research, no difference was observed between the groups and timing in terms of connective tissue formation and it was observed that connective tissue formed within the expected period. We observed connective tissue epithelialization and necrosis in inflammation only in 1 subject in the +control group, which was waited for 56 days.

In the control group, as expected, the degree of inflammation was detected in moderate local areas in the group sacrificed on the 28th day, while it was detected in mild focal areas in the control groups on the 56th day.

In the group given local Hesperidin and regular hesperidin with Gavage, the degree of inflammation on the 56th day was mild focal, while the inflammation seen on the 28th day was observed to be moderate locally, and it was seen that the healing progressed as expected.

In the control group, the inflammation was either absent or only seen on the surface of the 1/3 of the surface area at the ends, while in the control group, the epithelialization score was observed to increase and rise in the subjects sacrificed on the 56th day. In the control group, the epithelialization was generally observed at the ends of the surface area and covering 2/3 of it on the 56th day, with the only difference being necrosis in 1 subject in the 56th day group.

New bone formation was examined with Masson trichrome stain in control and other rats, and as expected in healing, new bone formation was found to be higher in rats sacrificed on the 56th day than in the control group rats sacrificed on the 28th day. (p: 0.004)

When the new bone formation of rats that were followed up by local hesperidin application only on the day of extraction and only spongestan application after tooth extraction was examined on the 28th and 56th days, it was determined that no progress was observed, that is, no significant new bone formation in the intervening 28 days.

However, it was observed that new bone formation increased in rats given hesperidin by gavage every day throughout the experimental period along with local hesperidin application, when the group sacrificed on the 28th day was compared with the group sacrificed on the 56th day. (p:0.011)

In the histochemical analysis results revealed in long-term inflammation, epithelization, and new bone formation levels are negatively affected in local hesperidin group. Whereas the local hesperidin+gavage group showed parallel results with control and spongestan group in short term. This study showed; hesperidin's systemic administration by gavage can enhance healing in both soft and hard tissue whereas local application slowdowns healing.More research is needed to reach a definitive conclusion.

As a result, we think that the effect of hesperidin may change over time and that when used for a longer period of time, it may reduce the negative effects caused by the traumatic situation of tooth extraction. However, more research is needed to reach a definitive conclusion.

7. REFERENCES

1. Kuroshima S, Kovacic BL, Kozloff KM, McCauley LK, Yamashita J. Intra-oral PTH administration promotes tooth extraction socket healing. *J Dent Res*. Jun 2013;92(6):553-9. doi:10.1177/0022034513487558
2. Farina R, Trombelli L. Wound healing of extraction sockets. *Endodontic Topics*. 2011;25:16-43.
3. Jaafar N, Nor GM. The prevalence of post-extraction complications in an outpatient dental clinic in Kuala Lumpur Malaysia--a retrospective survey. *Singapore Dent J*. Feb 2000;23(1):24-8.
4. Ozkan A, Bayar GR, Altug HA, et al. The effect of cigarette smoking on the healing of extraction sockets: an immunohistochemical study. *J Craniofac Surg*. Jul 2014;25(4):e397-402. doi:10.1097/SCS.0b013e31829ae609
5. Ansari N, Sims NA. The cells of bone and their interactions. *Bone Regulators and Osteoporosis Therapy*. 2020:1-25.
6. Salhotra A, Shah HN, Levi B, Longaker MT. Mechanisms of bone development and repair. *Nature reviews Molecular cell biology*. 2020;21(11):696-711.
7. Kim J-M, Lin C, Stavre Z, Greenblatt MB, Shim J-H. Osteoblast-osteoclast communication and bone homeostasis. *Cells*. 2020;9(9):2073.
8. Welch AA, Hardcastle AC. The effects of flavonoids on bone. *Current osteoporosis reports*. 2014;12:205-210.
9. Lane JM, Russell L, Khan SN. Osteoporosis. *Clinical Orthopaedics and Related Research®*. 2000;372:139-150.
10. Shim J-h, Stavre Z, Gravallese EM. Bone loss in rheumatoid arthritis: basic mechanisms and clinical implications. *Calcified tissue international*. 2018;102(5):533-546.
11. Baldwin P, Li DJ, Auston DA, Mir HS, Yoon RS, Koval KJ. Autograft, allograft, and bone graft substitutes: clinical evidence and indications for use in the setting of orthopaedic trauma surgery. *Journal of orthopaedic trauma*. 2019;33(4):203-213.
12. Dimitriou R, Jones E, McGonagle D, Giannoudis PV. Bone regeneration: current concepts and future directions. *BMC medicine*. 2011;9:1-10.

13. Nogueira DMB, Figadoli ALdF, Alcantara PL, et al. Biological Behavior of Xenogenic Scaffolds in Alcohol-Induced Rats: Histomorphometric and Picrosirius Red Staining Analysis. *Polymers*. 2022;14(3):584.

14. Pandini FE, Kubo FMM, Plepis AMdG, et al. In vivo study of nasal bone reconstruction with collagen, elastin and chitosan membranes in abstainer and alcoholic rats. *Polymers*. 2022;14(1):188.

15. Fiorillo L, Cervino G, Galindo-Moreno P, Herford AS, Spagnuolo G, Cicciù M. Growth factors in oral tissue engineering: new perspectives and current therapeutic options. *BioMed Research International*. 2021;2021(1):8840598.

16. Weaver CM, Alekel DL, Ward WE, Ronis MJ. Flavonoid intake and bone health. *Journal of nutrition in gerontology and geriatrics*. 2012;31(3):239-253.

17. Latos-Brozio M, Masek A. The effect of natural additives on the composting properties of aliphatic polyesters. *Polymers*. 2020;12(9):1856.

18. Masek A, Latos-Brozio M. The effect of substances of plant origin on the thermal and thermo-oxidative ageing of aliphatic polyesters (PLA, PHA). *Polymers*. 2018;10(11):1252.

19. Mescher A. *Junqueira's Basic Histology Text & Atlas (14th ed.)*. 2016.

20. N. S. Genel histoloji. *İstanbul: İÜ Basımevi ve Film*

Merkezi: 100-19. 1985;

21. Oryan A, Moshiri A, Alidadi S. Current concerns regarding healing of bone defects. *Hard Tissue*. 02/26 2013;2:13. doi:10.13172/2050-2303-2-2-374

22. Eşrefoğlu M. Genel Histoloji 1. Baskı. Malatya,. *Medipress Matbaacılık*

Yayıncılık Ltd. 2009;169-88

23. Cormack D. Essential Histology, 2th ed. United States of America,. *Lippincott Williams and Wilkins,*. 2001;179-206

24. JCJ Webb JT. A review of fracture healing. *Current Orthopaedics*. 2000, 14;457-63.

25. LC Junqueira JC. Basic Histology, 10th ed. New York. *McGraw Hill Professional Publishing,*. 2003;141-159

26. HW Hollinshead CR. Textbook of Anatomy, 4th ed. Philadelphia. *Harper & Row Publishing,*. 1985;24-30

27. Çay HF SN. Kemik yapısı ve kemik döngüsü üzerine bir derleme. *Fiziksel Tıp*. 2002, 5;177-84

28. Ponzetti M, Rucci N. Osteoblast Differentiation and Signaling: Established Concepts and Emerging Topics. *Int J Mol Sci*. Jun 22 2021;22(13)doi:10.3390/ijms22136651

29. Shapiro F. Bone development and its relation to fracture repair. The role of mesenchymal osteoblasts and surface osteoblasts. *Eur Cell Mater*. Apr 1 2008;15:53-76. doi:10.22203/ecm.v015a05

30. Bahraminasab M, Arab S, Safari M, Talebi A, Kavakebian F, Doostmohammadi N. In vivo performance of Al(2)O(3)-Ti bone implants in the rat femur. *J Orthop Surg Res*. Jan 22 2021;16(1):79. doi:10.1186/s13018-021-02226-7

31. Çay HF SN. Kemik yapısı ve kemik döngüsü üzerine bir derleme. *Fiziksel Tıp*. 2002, 5;177-84

32. Eroschenko V. Di Fiore's Atlas of Histology with Functional Correlations. 01/01 2012;

33. Kalfas IH. Principles of bone healing. *Neurosurg Focus*. Apr 15 2001;10(4):E1. doi:10.3171/foc.2001.10.4.2

34. Kiliçoğlu S. Mikroskobi Düzeyinde Kırık İyileşmesi. *Ankara Üniversitesi Tıp Fakültesi Mecmuası*. 02/01 2002;55doi:10.1501/Tipfak_0000000021

35. Evren C, Çinar F, Sarikaya S, Alpay A, Bektas S. Ankaferd "Blood Stopper"in Tükrük Bezi Kanamasında Etkinliği Effectiveness of Ankaferd Blood Stopper on Salivary Gland Bleeding. *J Kartal*. 01/01 2012;1:1-5. doi:10.5505/jkartaltr.2012.50479

36. Saffar JL, Lasfargues JJ, Cherruau M. Alveolar bone and the alveolar process: the socket that is never stable. *Periodontol 2000*. Feb 1997;13:76-90. doi:10.1111/j.1600-0757.1997.tb00096.x

37. Kawasaki K, Shimizu N. Effects of low-energy laser irradiation on bone remodeling during experimental tooth movement in rats. *Lasers Surg Med*. 2000;26(3):282-91. doi:10.1002/(sici)1096-9101(2000)26:3<282::aid-lsm6>3.0.co;2-x

38. Pagni G, Pellegrini G, Giannobile WV, Rasperini G. Postextraction alveolar ridge preservation: biological basis and treatments. *Int J Dent*. 2012;2012:151030. doi:10.1155/2012/151030

39. Araújo MG, Lindhe J. Ridge alterations following tooth extraction with and without flap elevation: an experimental study in the dog. *Clin Oral Implants Res*. Jun 2009;20(6):545-9. doi:10.1111/j.1600-0501.2008.01703.x

40. Schropp L, Wenzel A, Kostopoulos L, Karring T. Bone healing and soft tissue contour changes following single-tooth extraction: a clinical and radiographic 12-month prospective study. *Int J Periodontics Restorative Dent*. Aug 2003;23(4):313-23.

41. Avila-Ortiz G, Elangovan S, Kramer KW, Blanchette D, Dawson DV. Effect of alveolar ridge preservation after tooth extraction: a systematic review and meta-analysis. *J Dent Res*. Oct 2014;93(10):950-8. doi:10.1177/0022034514541127

42. Amler MH, Johnson PL, Salman I. Histological and histochemical investigation of human alveolar socket healing in undisturbed extraction wounds. *J Am Dent Assoc*. Jul 1960;61:32-44. doi:10.14219/jada.archive.1960.0152

43. Horváth A, Mardas N, Mezzomo LA, Needleman IG, Donos N. Alveolar ridge preservation. A systematic review. *Clin Oral Investig*. Mar 2013;17(2):341-63. doi:10.1007/s00784-012-0758-5

44. Albrektsson T, Brånemark PI, Hansson HA, Lindström J. Osseointegrated titanium implants. Requirements for ensuring a long-lasting, direct bone-to-implant anchorage in man. *Acta Orthop Scand*. 1981;52(2):155-70. doi:10.3109/17453678108991776

45. Çakır M, Karaca İ. İMPLANT UYGULAMALARI İÇİN KRET KORUMA TEKNİKLERİ. Ridge preservation tehchniques for implant therapy. *Atatürk Üniversitesi Diş Hekimliği Fakültesi Dergisi*. May 2015;25(1):107-118. doi:10.17567/dfd.27854

46. Irinakis T. Rationale for socket preservation after extraction of a single-rooted tooth when planning for future implant placement. *J Can Dent Assoc*. Dec 2006;72(10):917-22.

47. Huebsch RF, Coleman RD, Frandsen AM, Becks H. The healing process following molar extraction. I. Normal male rats (long-evans strain). *Oral Surg Oral Med Oral Pathol*. Aug 1952;5(8):864-76. doi:10.1016/0030-4220(52)90316-2

48. Schulte WC. Effect of an osteogenic extract on the healing of extraction wounds. *J Dent Res*. Jul-Aug 1967;46(4):656-60. doi:10.1177/00220345670460040401

49. Bodner L, Kaffe I, Cohen Z, Dayan D. Long-term effect of desalivation on extraction wound healing: a densitometric study in rats. *Dentomaxillofac Radiol*. Nov 1993;22(4):195-8. doi:10.1259/dmfr.22.4.8181646

50. Elsubeihi ES, Heersche JN. Quantitative assessment of post-extraction healing and alveolar ridge remodelling of the mandible in female rats. *Arch Oral Biol*. May 2004;49(5):401-12. doi:10.1016/j.archoralbio.2003.12.003

51. H E. Die Heilung Von Extraktionswunden; Eine Tierexperimentelle

Studie (Healing of Extraction Wounds; An Experimental Study). *Deutsche Monat f Zahn-heilk*. 1923;4:687

52. Araújo MG, Lindhe J. Dimensional ridge alterations following tooth extraction. An experimental study in the dog. *J Clin Periodontol*. Feb 2005;32(2):212-8. doi:10.1111/j.1600-051X.2005.00642.x

53. Cardaropoli G, Araújo M, Lindhe J. Dynamics of bone tissue formation in tooth extraction sites. An experimental study in dogs. *J Clin Periodontol*. Sep 2003;30(9):809-18. doi:10.1034/j.1600-051x.2003.00366.x

54. Guglielmotti MB, Cabrini RL. Alveolar wound healing and ridge remodeling after tooth extraction in the rat: a histologic, radiographic, and histometric study. *J Oral Maxillofac Surg*. May 1985;43(5):359-64. doi:10.1016/0278-2391(85)90257-5

55. Pietrokovski J, Massler M. Ridge remodeling after tooth extraction in rats. *J Dent Res*. Jan-Feb 1967;46(1):222-31. doi:10.1177/00220345670460011501

56. Boyne PJ. Osseous repair of the postextraction alveolus in man. *Oral Surg Oral Med Oral Pathol*. Jun 1966;21(6):805-13. doi:10.1016/0030-4220(66)90104-6

57. Devlin H, Sloan P. Early bone healing events in the human extraction socket. *Int J Oral Maxillofac Surg*. Dec 2002;31(6):641-5. doi:10.1054/ijom.2002.0292

58. Fang YZ, Yang S, Wu G. Free radicals, antioxidants, and nutrition. *Nutrition*. Oct 2002;18(10):872-9. doi:10.1016/s0899-9007(02)00916-4

59. Rock CL, Jacob RA, Bowen PE. Update on the biological characteristics of the antioxidant micronutrients: vitamin C, vitamin E, and the carotenoids. *J Am Diet Assoc*. Jul 1996;96(7):693-702; quiz 703-4. doi:10.1016/s0002-8223(96)00190-3

60. Yılmaz İ, Üniversitesi İ, Fakültesi E, Dalı F, Malatya. Antioksidan İçeren Bazı Gıdalar ve Oksidatif Stres. 08/01 2010;

61. Bagchi D, Sen CK, Ray SD, et al. Molecular mechanisms of cardioprotection by a novel grape seed proanthocyanidin extract. *Mutation Research/Fundamental and Molecular Mechanisms of Mutagenesis*. 2003/02/01/ 2003;523-524:87-97. doi:https://doi.org/10.1016/S0027-5107(02)00324-X

62. Jain M, Parmar HS. Evaluation of antioxidative and anti-inflammatory potential of hesperidin and naringin on the rat air pouch model of inflammation. *Inflamm Res*. May 2011;60(5):483-91. doi:10.1007/s00011-010-0295-0

63. Neto CC. Cranberry and its phytochemicals: a review of in vitro anticancer studies. *J Nutr*. Jan 2007;137(1 Suppl):186s-193s. doi:10.1093/jn/137.1.186S

64. Chen CY, Blumberg JB. Phytochemical composition of nuts. *Asia Pac J Clin Nutr*. 2008;17 Suppl 1:329-32.

65. Trzeciakiewicz A, Habauzit V, Mercier S, et al. Molecular mechanism of hesperetin-7-O-glucuronide, the main circulating metabolite of hesperidin, involved in osteoblast differentiation. *J Agric Food Chem*. Jan 13 2010;58(1):668-75. doi:10.1021/jf902680n

66. Habauzit V, Sacco SM, Gil-Izquierdo A, et al. Differential effects of two citrus flavanones on bone quality in senescent male rats in relation to their bioavailability and metabolism. *Bone*. Nov 2011;49(5):1108-16. doi:10.1016/j.bone.2011.07.030

67. Miguez PA, Tuin SA, Robinson AG, et al. Hesperidin Promotes Osteogenesis and Modulates Collagen Matrix Organization and Mineralization In Vitro and In Vivo. *International Journal of Molecular Sciences*. 2021;22(6):3223.

68. Kim YJ, & Uyama, H. *Flavonoids: Chemistry, Biochemistry and Applications*. 2005.

69. del Río JA, Gómez P, Baidez AG, Arcas MC, Botía JM, Ortuño A. Changes in the levels of polymethoxyflavones and flavanones as part of the defense mechanism of Citrus sinensis (cv. Valencia Late) fruits against Phytophthora citrophthora. *J Agric Food Chem*. Apr 7 2004;52(7):1913-7. doi:10.1021/jf035038k

70. Marín L, Miguélez EM, Villar CJ, Lombó F. Bioavailability of dietary polyphenols and gut microbiota metabolism: antimicrobial properties. *Biomed Res Int*. 2015;2015:905215. doi:10.1155/2015/905215

71. Roohbakhsh A, Parhiz H, Soltani F, Rezaee R, Iranshahi M. Neuropharmacological properties and pharmacokinetics of the citrus flavonoids hesperidin and hesperetin--a mini-review. *Life Sci*. Sep 15 2014;113(1-2):1-6. doi:10.1016/j.lfs.2014.07.029

72. Yang HL, Chen SC, Senthil Kumar KJ, et al. Antioxidant and anti-inflammatory potential of hesperetin metabolites obtained from hesperetin-administered rat serum: an ex vivo approach. *J Agric Food Chem*. Jan 11 2012;60(1):522-32. doi:10.1021/jf2040675

73. Loscalzo LM, Yow TT, Wasowski C, Chebib M, Marder M. Hesperidin induces antinociceptive effect in mice and its aglycone, hesperetin, binds to μ-opioid receptor and inhibits GIRK1/2 currents. *Pharmacol Biochem Behav*. Sep 2011;99(3):333-41. doi:10.1016/j.pbb.2011.05.018

74. Martínez AL, González-Trujano ME, Chávez M, Pellicer F, Moreno J, López-Muñoz FJ. Hesperidin produces antinociceptive response and synergistic interaction with

ketorolac in an arthritic gout-type pain in rats. *Pharmacol Biochem Behav*. Feb 2011;97(4):683-9. doi:10.1016/j.pbb.2010.11.010

75. Chiba H, Uehara M, Wu J, et al. Hesperidin, a citrus flavonoid, inhibits bone loss and decreases serum and hepatic lipids in ovariectomized mice. *J Nutr*. Jun 2003;133(6):1892-7. doi:10.1093/jn/133.6.1892

76. Chiba H, Kim H, Matsumoto A, et al. Hesperidin prevents androgen deficiency-induced bone loss in male mice. *Phytother Res*. Feb 2014;28(2):289-95. doi:10.1002/ptr.5001

77. Hosseinimehr SJ, Ahmadi A, Mahmoudzadeh A, Mohamadifar S. Radioprotective effects of Daflon against genotoxicity induced by gamma irradiation in human cultured lymphocytes. *Environ Mol Mutagen*. Dec 2009;50(9):749-52. doi:10.1002/em.20499

78. Kalpana KB, Devipriya N, Srinivasan M, Menon VP. Investigation of the radioprotective efficacy of hesperidin against gamma-radiation induced cellular damage in cultured human peripheral blood lymphocytes. *Mutat Res*. May 31 2009;676(1-2):54-61. doi:10.1016/j.mrgentox.2009.03.005

79. Fathy S, Abdel-Hamid F, Agwa S, El-Diasty S. The Anti-Proliferative Effect of Hesperidin on Hepatocarcinoma Cells HepG2. *Egyptian Academic Journal of Biological Sciences C, Physiology and Molecular Biology*. 12/01 2014;6:75-83. doi:10.21608/eajbsc.2014.16033

80. Agrawal YO, Sharma PK, Shrivastava B, et al. Hesperidin produces cardioprotective activity via PPAR-γ pathway in ischemic heart disease model in diabetic rats. *PLoS One*. 2014;9(11):e111212. doi:10.1371/journal.pone.0111212

81. Parhiz H, Roohbakhsh A, Soltani F, Rezaee R, Iranshahi M. Antioxidant and anti-inflammatory properties of the citrus flavonoids hesperidin and hesperetin: an updated review of their molecular mechanisms and experimental models. *Phytother Res*. Mar 2015;29(3):323-31. doi:10.1002/ptr.5256

82. Trzeciakiewicz A, Habauzit V, Mercier S, et al. Hesperetin stimulates differentiation of primary rat osteoblasts involving the BMP signalling pathway. *J Nutr Biochem*. May 2010;21(5):424-31. doi:10.1016/j.jnutbio.2009.01.017

83. Horcajada MN, Habauzit V, Trzeciakiewicz A, et al. Hesperidin inhibits ovariectomized-induced osteopenia and shows differential effects on bone mass and strength in young and adult intact rats. *J Appl Physiol (1985)*. Mar 2008;104(3):648-54. doi:10.1152/japplphysiol.00441.2007

84. Choi EM, Kim YH. Hesperetin attenuates the highly reducing sugar-triggered inhibition of osteoblast differentiation. *Cell Biol Toxicol*. Jun 2008;24(3):225-31. doi:10.1007/s10565-007-9031-0

85. Cvetnić Z, Vladimir-Knezević S. Antimicrobial activity of grapefruit seed and pulp ethanolic extract. *Acta Pharm*. Sep 2004;54(3):243-50.

86. Saha RK, Takahashi T, Suzuki T. Glucosyl hesperidin prevents influenza a virus replication in vitro by inhibition of viral sialidase. *Biol Pharm Bull*. Jul 2009;32(7):1188-92. doi:10.1248/bpb.32.1188

87. Abuelsaad AS, Mohamed I, Allam G, Al-Solumani AA. Antimicrobial and immunomodulating activities of hesperidin and ellagic acid against diarrheic Aeromonas hydrophila in a murine model. *Life Sci*. Nov 6 2013;93(20):714-22. doi:10.1016/j.lfs.2013.09.019

88. Bae EA, Han MJ, Lee M, Kim DH. In vitro inhibitory effect of some flavonoids on rotavirus infectivity. *Biol Pharm Bull*. Sep 2000;23(9):1122-4. doi:10.1248/bpb.23.1122

89. Nielsen IL, Chee WS, Poulsen L, et al. Bioavailability is improved by enzymatic modification of the citrus flavonoid hesperidin in humans: a randomized, double-blind, crossover trial. *J Nutr*. Feb 2006;136(2):404-8. doi:10.1093/jn/136.2.404

90. Yamada M, Tanabe F, Arai N, et al. Bioavailability of glucosyl hesperidin in rats. *Biosci Biotechnol Biochem*. Jun 2006;70(6):1386-94. doi:10.1271/bbb.50657

91. Chanal JL, Cousse H, Sicart MT, Bonnaud B, Marignan R. Absorption and elimination of (14C) hesperidin methylchalcone in the rat. *Eur J Drug Metab Pharmacokinet*. 1981;6(3):171-7. doi:10.1007/bf03189486

92. Walle T. Methylation of dietary flavones greatly improves their hepatic metabolic stability and intestinal absorption. *Mol Pharm*. Nov-Dec 2007;4(6):826-32. doi:10.1021/mp700071d

93. Cho YA, Choi DH, Choi JS. Effect of hesperidin on the oral pharmacokinetics of diltiazem and its main metabolite, desacetyldiltiazem, in rats. *J Pharm Pharmacol*. Jun 2009;61(6):825-9. doi:10.1211/jpp.61.06.0017

94. Beiler JM, Martin GJ. Inhibitory action of vitamin P compounds on hyaluronidase. *J Biol Chem*. Dec 1947;171(2):507-11.

95. Beiler JM, Martin GJ. Inhibition of hyaluronidase action by derivatives of hesperidin. *J Biol Chem*. May 1948;174(1):31-5.

96. Ohara T, Muroyama K, Yamamoto Y, Murosaki S. A combination of glucosyl hesperidin and caffeine exhibits an anti-obesity effect by inhibition of hepatic lipogenesis in mice. *Phytother Res*. Feb 2015;29(2):310-6. doi:10.1002/ptr.5258

97. Paysant J, Sansilvestri-Morel P, Bouskela E, Verbeuren TJ. Different flavonoids present in the micronized purified flavonoid fraction (Daflon 500 mg) contribute to its anti-hyperpermeability effect in the hamster cheek pouch microcirculation. *Int Angiol*. Feb 2008;27(1):81-5.

98. Mandalari G, Bennett RN, Bisignano G, et al. Antimicrobial activity of flavonoids extracted from bergamot (Citrus bergamia Risso) peel, a byproduct of the essential oil industry. *J Appl Microbiol*. Dec 2007;103(6):2056-64. doi:10.1111/j.1365-2672.2007.03456.x

99. Fernández SP, Wasowski C, Paladini AC, Marder M. Synergistic interaction between hesperidin, a natural flavonoid, and diazepam. *Eur J Pharmacol*. Apr 11 2005;512(2-3):189-98. doi:10.1016/j.ejphar.2005.02.039

100. Kumar A, Lalitha S, Mishra J. Hesperidin potentiates the neuroprotective effects of diazepam and gabapentin against pentylenetetrazole-induced convulsions in mice: Possible behavioral, biochemical and mitochondrial alterations. *Indian J Pharmacol*. May-Jun 2014;46(3):309-15. doi:10.4103/0253-7613.132180

101. Fujita T, Shiura T, Masuda M, et al. Anti-allergic effect of a combination of Citrus unshiu unripe fruits extract and prednisolone on picryl chloride-induced contact dermatitis in mice. *J Nat Med*. Apr 2008;62(2):202-6. doi:10.1007/s11418-007-0208-x

102. Febriansah R, Putri DD, Sarmoko, Nurulita NA, Meiyanto E, Nugroho AE. Hesperidin as a preventive resistance agent in MCF-7 breast cancer cells line resistance to doxorubicin. *Asian Pac J Trop Biomed*. Mar 2014;4(3):228-33. doi:10.1016/s2221-1691(14)60236-7

103. Rovenský J, Svík K, Rovenská E, Stvrtinová V, Stancíková M. Effects of purified micronized flavonoid fraction (Detralex) on prophylactic treatment of adjuvant arthritis with methotrexate in rats. *Isr Med Assoc J*. May 2008;10(5):377-80.

104. Ahmadi A, Hosseinimehr SJ, Naghshvar F, Hajir E, Ghahremani M. Chemoprotective effects of hesperidin against genotoxicity induced by cyclophosphamide in mice bone marrow cells. *Arch Pharm Res*. Jun 2008;31(6):794-7. doi:10.1007/s12272-001-1228-z

105. das Neves RN, Carvalho F, Carvalho M, et al. Protective activity of hesperidin and lipoic acid against sodium arsenite acute toxicity in mice. *Toxicol Pathol*. Sep-Oct 2004;32(5):527-35. doi:10.1080/01926230490502566

106. Tirkey N, Pilkhwal S, Kuhad A, Chopra K. Hesperidin, a citrus bioflavonoid, decreases the oxidative stress produced by carbon tetrachloride in rat liver and kidney. *BMC Pharmacol*. Jan 31 2005;5:2. doi:10.1186/1471-2210-5-2

107. Buckshee K, Takkar D, Aggarwal N. Micronized flavonoid therapy in internal hemorrhoids of pregnancy. *Int J Gynaecol Obstet*. May 1997;57(2):145-51. doi:10.1016/s0020-7292(97)02889-0

108. Piao YJ, Choi JS. Enhanced bioavailability of verapamil after oral administration with hesperidin in rats. *Arch Pharm Res*. Apr 2008;31(4):518-22. doi:10.1007/s12272-001-1187-4

109. Uesawa Y, Mohri K. Hesperidin in orange juice reduces the absorption of celiprolol in rats. *Biopharm Drug Dispos*. Apr 2008;29(3):185-8. doi:10.1002/bdd.603

110. Watanabe M, Matsumoto N, Takeba Y, et al. Orange juice and its component, hesperidin, decrease the expression of multidrug resistance-associated protein 2 in rat small intestine and liver. *J Biomed Biotechnol*. 2011;2011:502057. doi:10.1155/2011/502057

111. Németh K, Plumb GW, Berrin JG, et al. Deglycosylation by small intestinal epithelial cell beta-glucosidases is a critical step in the absorption and metabolism of dietary flavonoid glycosides in humans. *Eur J Nutr*. Jan 2003;42(1):29-42. doi:10.1007/s00394-003-0397-3

112. Kim M, Kometani T, Okada S, Shimuzu M. Permeation of hesperidin glycosides across Caco-2 cell monolayers via the paracellular pathway. *Biosci Biotechnol Biochem*. Dec 1999;63(12):2183-8. doi:10.1271/bbb.63.2183

113. Sabel M, Stummer W. The use of local agents: Surgicel and Surgifoam. *Eur Spine J*. Oct 2004;13 Suppl 1(Suppl 1):S97-101. doi:10.1007/s00586-004-0735-z

114. Nelson ER, DuSell CD, Wang X, et al. The oxysterol, 27-hydroxycholesterol, links cholesterol metabolism to bone homeostasis through its actions on the estrogen and liver X receptors. *Endocrinology*. Dec 2011;152(12):4691-705. doi:10.1210/en.2011-1298

115. Liu L, Xu DM, Cheng YY. Distinct effects of naringenin and hesperetin on nitric oxide production from endothelial cells. *J Agric Food Chem*. Feb 13 2008;56(3):824-9. doi:10.1021/jf0723007

116. Key LL, Jr., Wolf WC, Gundberg CM, Ries WL. Superoxide and bone resorption. *Bone*. Jul-Aug 1994;15(4):431-6. doi:10.1016/8756-3282(94)90821-4

117. Pradeep K, Park SH, Ko KC. Hesperidin a flavanoglycone protects against gamma-irradiation induced hepatocellular damage and oxidative stress in Sprague-Dawley rats. *Eur J Pharmacol*. Jun 10 2008;587(1-3):273-80. doi:10.1016/j.ejphar.2008.03.052

118. Hwang SL, Yen GC. Effect of hesperetin against oxidative stress via ER- and TrkA-mediated actions in PC12 cells. *J Agric Food Chem*. May 25 2011;59(10):5779-85. doi:10.1021/jf104632a

119. Matsumoto Y, Otsuka F, Takano-Narazaki M, et al. Estrogen facilitates osteoblast differentiation by upregulating bone morphogenetic protein-4 signaling. *Steroids*. May 2013;78(5):513-20. doi:10.1016/j.steroids.2013.02.011

120. Schonauer C, Tessitore E, Barbagallo G, Albanese V, Moraci A. The use of local agents: bone wax, gelatin, collagen, oxidized cellulose. *Eur Spine J*. Oct 2004;13 Suppl 1(Suppl 1):S89-96. doi:10.1007/s00586-004-0727-z

121. Arand AG, Sawaya R. Intraoperative chemical hemostasis in neurosurgery. *Neurosurgery*. Feb 1986;18(2):223-33. doi:10.1227/00006123-198602000-00022

122. Tomizawa Y. Clinical benefits and risk analysis of topical hemostats: a review. *J Artif Organs*. 2005;8(3):137-42. doi:10.1007/s10047-005-0296-x

123. Harris WH, Crothers OD, Moyen BJ, Bourne RB. Topical hemostatic agents for bone bleeding in humans. A quantitative comparison of gelatin paste, gelatin sponge plus bovine thrombin, and microfibrillar collagen. *J Bone Joint Surg Am*. Jun 1978;60(4):454-6.

124. Korany NS, Mehanni SS, Hakam HM, El-Maghraby EM. Evaluation of socket healing in irradiated rats after diode laser exposure (histological and morphometric studies). *Arch Oral Biol*. Jul 2012;57(7):884-91. doi:10.1016/j.archoralbio.2012.01.009

125. Yoneda T, Tomofuji T, Kawabata Y, et al. Application of coenzyme Q10 for accelerating soft tissue wound healing after tooth extraction in rats. *Nutrients*. Dec 10 2014;6(12):5756-69. doi:10.3390/nu6125756

126. Todorovic K, Jovanovic G, Todorovic A, et al. Effects of coenzyme Q(10) encapsulated in nanoliposomes on wound healing processes after tooth extraction. *J Dent Sci*. Jun 2018;13(2):103-108. doi:10.1016/j.jds.2017.10.004

127. Liu EH, Zhao P, Duan L, et al. Simultaneous determination of six bioactive flavonoids in Citri Reticulatae Pericarpium by rapid resolution liquid chromatography

coupled with triple quadrupole electrospray tandem mass spectrometry. *Food Chem*. Dec 15 2013;141(4):3977-83. doi:10.1016/j.foodchem.2013.06.077

128. Emim JADS, Oliveira AB, Lapa AJ. Pharmacological evaluation of the anti-inflammatory activity of a citrus bioflavonoid, hesperidin, and the isoflavonoids, duartin and claussequinone, in rats and mice. *Journal of pharmacy and Pharmacology*. 1994;46(2):118-122.

129. Jin MJ, Kim U, Kim IS, et al. Effects of gut microflora on pharmacokinetics of hesperidin: a study on non-antibiotic and pseudo-germ-free rats. *J Toxicol Environ Health A*. 2010;73(21-22):1441-50. doi:10.1080/15287394.2010.511549

130. Vordemvenne T, Wähnert D, Koettnitz J, et al. Bone Regeneration: A Novel Osteoinductive Function of Spongostan by the Interplay between Its Nano- and Microtopography. *Cells*. 2020;9(3):654.

131. Jia X, Meng J, Wang J, Wang W, Wu D, Xu M. Safety and effectiveness of a drug-loaded haemostatic sponge in chronic rhinosinusitis: a randomized, controlled, double-blind study. *Scientific Reports*. 2024/09/20 2024;14(1):21968. doi:10.1038/s41598-024-64669-2

132. B. AY. Koenzim Q10 ve Hesperidinin Ratlarda Alt Ekstremite İskemi-Reperfüzyon Hasarında TAS ve TOS Düzeylerine Etkisi. *Koenzim Q10 ve Hesperidinin Ratlarda Alt Ekstremite İskemi-Reperfüzyon Hasarında TAS ve TOS Düzeylerine Etkisi*. 2022;2:90-95.

133. Keskin E, Aydin HA. Ratlarda deneysel spinal kord yaralanmasında Hesperidin'in nöroprotektif etkisi. Neuroprotective effect of Hesperidin on experimental spinal cord injury in rats. *Pamukkale Medical Journal*. July 2022;15(3):451-459. doi:10.31362/patd.1057660

134. Davut Ö Z, Metin K, Harun Ç I, İsmail T. The effect of diosmin-hesperidin combination treatment on the lipid profile and oxidative-antioxidative system in high-cholesterol diet-fed rats. *Türk Göğüs Kalp Damar Cerrahisi Dergisi*. 2011;19(1):55-61.

135. Burak Batuhan L, Fikret Ç E. Investigation of the Effects of Hesperidin on Bisphenol-A Induced Neurotoxicity in Rats. *Veterinary sciences and practices (Online)*. 2024;19(1):17-24.

136. Horcajada-Molteni MN, Crespy V, Coxam V, Davicco MJ, Rémésy C, Barlet JP. Rutin Inhibits Ovariectomy-Induced Osteopenia in Rats. *Journal of Bone and Mineral Research*. 2009;15(11):2251-2258. doi:10.1359/jbmr.2000.15.11.2251

137. Xue D, Chen E, Zhang W, et al. The role of hesperetin on osteogenesis of human mesenchymal stem cells and its function in bone regeneration. *Oncotarget*. Mar 28 2017;8(13):21031-21043. doi:10.18632/oncotarget.15473

138. Kuzu M, Kandemir FM, Yıldırım S, Çağlayan C, Küçükler S. Attenuation of sodium arsenite-induced cardiotoxicity and neurotoxicity with the antioxidant, anti-inflammatory, and antiapoptotic effects of hesperidin. *Environ Sci Pollut Res Int*. Mar 2021;28(9):10818-10831. doi:10.1007/s11356-020-11327-5

8. CURRICULUM VITAE

Personal Informations

Name	Engin Emre	**Surname**	Selçuk

Education

Degree	Department	The name of the Institution Graduated From	Graduation year
Doctorate	Oral and maxillofacial surgery	Yeditepe university Faculty of Dentistry	2025
University	Dentıstry	Yeditepe unıversity	2018
High school	-	Tokat Anatolian high school	2012

Languages	Grades (#)
English	70,00000

All the grades must be listed if there is more than one (KPDS, ÜDS, TOEFL; EELTS vs),

Computer Skills

Program	Level
Microsoft Office	Good

***Excellent , good, average or basic**

Others (Projects / Certificates / Rewards)

Publication	